A Notch-dependent transcriptional mechanism controls expression of temporal patterning factors in *Drosophila* medulla

Alokananda Ray[1] and Xin Li[1,2]

1. Department of Cell and Developmental Biology, University of Illinois at Urbana-Champaign, Urbana- IL 61801

2. Corresponding author, email: lixin@illinois.edu

Abstract

Temporal patterning is an important mechanism for generating a great diversity of neuron subtypes from a seemingly homogenous progenitor pool in both vertebrates and invertebrates. *Drosophila* neuroblasts are temporally patterned by sequentially expressed Temporal Transcription Factors (TTFs). These TTFs are proposed to form a transcriptional cascade based on mutant phenotypes, although direct transcriptional regulation between TTFs has not been verified in most cases. Furthermore, it is not known how the temporal transitions are coupled with the generation of the appropriate number of neurons at each stage. We use neuroblasts of the *Drosophila* optic lobe medulla to address these questions and show that the expression of TTFs Sloppy-paired 1/ 2 (Slp1/2) is directly regulated at the transcriptional level by two other TTFs and the cell-cycle dependent Notch signaling through two *cis*-regulatory elements. We also show that supplying constitutively active Notch can rescue the delayed transition into the Slp stage in cell cycle arrested neuroblasts. Our findings reveal a novel Notch-pathway

20 dependent mechanism through which the cell cycle progression regulates the timing of a
21 temporal transition within a TTF transcriptional cascade.

22

23 Introduction

24 The generation of a great diversity of neurons from a small pool of neural progenitors is critical
25 for constructing functional nervous systems. This is partially achieved by integration of
26 temporal patterning and spatial patterning of neural progenitors [reviewed in [1-4]]. Temporal
27 patterning of neural progenitors refers to the generation of differently fated progeny in a birth-
28 order-dependent manner, and this is observed in both invertebrates and vertebrates [reviewed
29 in [5-7]]. The central nervous system in *Drosophila melanogaster* has been an excellent model to
30 study temporal patterning. Neural progenitors called neuroblasts (NBs) have been shown to
31 sequentially express series of temporal transcription factors (TTFs), which are each required to
32 specify subsets of neuron fates [reviewed in [8,9]]. For example, neuroblasts in the embryonic
33 ventral nerve cord (VNC) are temporally patterned by a TTF cascade Hunchback (Hb), Kruppel
34 (Kr), Nubbin/Pdm2 (Pdm), Castor (Cas) and Grainy head (Grh) [10-13], while *Drosophila* optic lobe
35 medulla neuroblasts utilize a different TTF cascade composed of Homothorax (Hth), SoxNeuro
36 (SoxN), Doublesex-Mab related 99B (Dmrt99B), Odd paired (Opa), Eyeless (Ey), Earmuff (Erm),
37 Homeobrain (Hbn), Sloppy-paired (Slp1,Slp2), Scarecrow (Scro), Dichaete (D), BarH1/2, Tailless
38 (Tll), and Glial cell missing (Gcm) [14-19]. In these TTF cascades, cross-regulations were identified
39 among TTF genes based on loss and gain of function phenotypes, and they were proposed to
40 form transcriptional cascades [11-13,18,20] that can in theory self-propagate [21]. However, with a few

41 exceptions [22], the *cis*-regulatory elements of these TTF genes haven't been characterized. Thus,
42 it is not known whether these cross-regulations are indeed direct transcriptional regulations.
43 Moreover, in the embryonic TTF cascade, although mis-expression of one TTF is sufficient to
44 activate the next TTF and repress the "next plus one" TTF, loss of one TTF often does not block
45 temporal progression, but only causes the corresponding fates to be skipped [11]. In the medulla
46 TTF cascade, one TTF is required but not sufficient to promote the TTF cascade progression [18].
47 These studies suggest that additional mechanisms besides cross-regulations among TTFs might
48 function to regulate TTF progression.
49
50 As the neural progenitors go through the TTF cascade, they need to generate a certain number
51 of postmitotic progeny at each temporal stage. Therefore, it has been questioned whether cell
52 cycle progression is required for the TTF cascade progression. In the embryonic VNC TTF
53 cascade, cytokinesis is required for the first transition (Hb to Kr) and acts by promoting the
54 nuclear export of seven-up (*svp)* mRNA encoding a switching factor, but all later temporal
55 transitions progress normally in G2-arrested neuroblasts [11,23,24]. In larval VNC NBs, timely
56 transition from the Imp /Castor/Chinmo to Syncrip/Broad stage also requires cell cycle
57 progression [25]. These results suggest that the requirement of cell-cycle progression varies
58 depending on the specific temporal transition. In the vertebrate cortex, the temporal transition
59 from generating deep layer neurons to generating upper layer neurons is not affected by
60 blocking cell cycle progression when constitutively active Notch signaling is provided to
61 maintain the un-differentiated status of cortical neural progenitors [26]. However, it is possible
62 that Notch signaling, which is normally dependent on the asymmetric cell division of neural

63 progenitors, may have rescued the possible phenotype caused by the arrest of cell cycle
64 progression.
65 Notch signaling plays pleiotropic roles in neurogenesis and neural development in both
66 vertebrates and invertebrates [reviewed in [27]]. Upon binding to a ligand from a neighboring
67 cell, the Notch receptor is cleaved to release the Notch intracellular domain (NICD), which then
68 enters the nucleus and associates with the DNA-binding protein CSL (CBF1/RBPjκ/Su(H)/Lag-1).
69 The NICD-CSL then recruits the transcriptional coactivator Mastermind (MAM) to activate
70 transcription of Notch target genes, mainly the bHLH transcriptional repressors of the HES
71 (hairy and enhancer of split) /HEY families [reviewed in [28-30]]. *Drosophila* NBs divide
72 asymmetrically multiple times and at each division generate a self-renewed neuroblast and a
73 more differentiated progeny, that is either an intermediate progenitor [Ganglion Mother Cell
74 (GMC) for type I NBs, or Intermediate Neural Progenitor (INP) for type II NBs], or a postmitotic
75 progeny (type 0 NBs) [reviewed in [31]]. During the asymmetric division of Drosophila
76 neuroblasts, Numb, a negative regulator of Notch signaling, is asymmetrically localized to the
77 intermediate progenitor, resulting in unidirectional Delta-Notch signaling from the intermediate
78 progenitor to the neuroblast [32-35]. Ectopic activation of Notch signaling in the progeny causes
79 them to revert into neuroblasts and over-proliferate, while inhibition of Notch signaling in type
80 II NBs eliminates the whole lineage [36-39]. In contrast, in most type I NB lineages, loss of N
81 signaling does not affect neuroblast maintenance, and it was shown that E(spl) complex
82 proteins and Deadpan act redundantly to maintain the un-differentiated state (stemness) of
83 neuroblasts by repressing differentiation genes [39-41]. Notch signaling is also involved in
84 controlling the daughter cell proliferation modes specifically the type I to type 0 switch in

85 embryonic VNC NBs [42,43]. Work in the vertebrate central nervous system suggests that during
86 the asymmetric division of neural progenitors, the more differentiated progeny expresses Delta
87 and activates Notch signaling in the sister cell to maintain the neural progenitor fate [reviewed
88 in [27]]. In addition, Notch signaling shows cell-cycle-dependent activation and the expression of
89 the Notch target Hes genes oscillates during the cell cycle in neural progenitors [reviewed in [44]].
90 Although Notch signaling has been shown to play many important roles in neural lineage
91 development, whether Notch signaling also has a role in temporal transitions between TTFs has
92 not been investigated.
93
94 Here, we use *Drosophila* medulla neuroblasts to address these questions. In the larval optic
95 lobe, a neurogenesis wave spreads in a medial to lateral direction to sequentially convert
96 neuroepithelial cells into medulla neuroblasts. As a result, medulla neuroblasts of different
97 ages are orderly aligned on the lateral to medial spatial axis with the youngest on the lateral
98 side (Fig. 1A). Medulla neuroblasts divide asymmetrically multiple times to self-renew and to
99 generate a series of GMCs. At the same time, they transit through the TTF sequence (Fig. 1A).
100 Among the TTFs, Slp1 and Slp2 are two homologous fork-head family transcription factors
101 expressed in the same temporal pattern in medulla neuroblasts (Fig. 1B-B'''). We have chosen
102 the Ey to Slp1/2 transition as a focal point because in the earliest studies that reported
103 temporal patterning of medulla neuroblasts, Slp was the first medulla TTF whose regulatory
104 relationship with the previous TTF Ey was clearly understood from genetic studies: Slp
105 expression is activated by Ey and Slp in turn represses Ey expression[15,18]. In this work, we
106 identified two *cis*-regulatory enhancer elements that regulate the temporal expression pattern

107 of Slp1/2, and showed that the previous TTF Ey, another TTF Scro, and the Notch signaling
108 pathway directly regulate the transcription of *slp* through these enhancers. Slp1/2 expression is
109 delayed when N signaling is lost or when cell cycle progression is blocked which also causes loss
110 of N signaling. Furthermore, we show that supplying transcriptionally active Notch can rescue
111 the timely Ey to Slp transition in cell-cycle arrested neuroblasts. Thus, our work demonstrates
112 that cell cycle-dependent Notch signaling cooperates with TTFs to promote the progression of
113 the TTF transcriptional cascade.
114

115 ## Results

116 **The expression of Slp1 and Slp2 in medulla neuroblasts is regulated at the transcriptional**
117 **level by the coordinated function of two enhancers.**

118 The observed distribution of temporal patterning transcription factors may be regulated at
119 either the transcriptional or post-transcriptional level. The protein expression pattern of TTFs is
120 not necessarily the same as that of their mRNA transcripts. A case in point is the expression
121 pattern of the SoxN protein recently reported to function alongside Dmrt99B and Hth to specify
122 identities of early-born neurons in the medulla; while mRNA transcripts of the *soxN* gene are
123 widely distributed in neuroblasts, the SoxN protein is only expressed in the youngest
124 neuroblasts, suggesting that post-transcriptional mechanisms are at work to confine the actual
125 domain of SoxN protein expression [16]. To examine whether the expression of Slp1/2 in medulla
126 neuroblasts is regulated at transcription, we observed the distribution of *slp1* and *slp2* mRNA
127 transcripts by fluorescence *in situ*-hybridization (Fig. 1C-D''''). The observed patterns of *slp1*

128 and *slp2* mRNA expression closely parallel the expression of Slp1 and Slp2 proteins (Fig. 1B-
129 D''''), and are also corroborated by scRNA-seq data [16], indicating that the expression of *slp1* and
130 *slp2* is directly regulated at transcription.

131 We then sought to identify transcriptional enhancers that enabled the expression of the *slp1*
132 *and slp2* genes in the characteristic pattern observed in medulla neuroblasts. We examined
133 patterns of GFP expression driven by putative enhancer elements [45-47] (available from the
134 Janelia FlyLight image database https://flweb.janelia.org/cgi-bin/flew.cgi), in *Drosophila* third
135 instar larval brains. We identified the *GMR35H02 Gal4* line as containing a candidate enhancer
136 driving Slp1/2 expression in medulla neuroblasts (Fig. 2A). We then verified the expression of
137 *UAS-GFP* driven by *GMR35H02*-Gal4 and found that, indeed the GFP expression in medulla
138 neuroblasts was initiated at the same time as endogenous Slp1 and Slp2 (Figure 2—figure
139 supplement 1 A-A'''').

140 Subsequently, we looked for conserved sequences within the GMR35H02 fragment to narrow
141 down the sequence element containing the potential active enhancer of Slp1/2 expression.
142 Previous cross-taxa comparative studies have indicated that in many cases, circuits regulating
143 critical patterning processes are conserved across vast evolutionary distances [48-51]. Therefore,
144 we reasoned that enhancers of genes essential for temporal patterning might be conserved at
145 least across various related *Drosophila* species. We compared using Evoprinter [52] the sequence
146 within *GMR35H02* DNA element across twelve *Drosophila* species. This comparison revealed
147 three broadly conserved segments within *GMR35H02* of sizes 2.1 kbp (R2.2), 973 bp (M1), and
148 1.5 kbp (L1.5) (Figure 2A shows their relative positions within the GMR35H02 sequence). For
149 the first iteration of enhancer bashing experiments, we cloned these three sequences into

150 pJR12 vector that expresses an eGFP reporter gene from a basal *hsp70* promoter [53] and made
151 transgenic flies (See primers in Supplementary Table1). All DNA constructs containing the
152 enhancer fragments were inserted at the same genomic landing site by ϕC31 transgenesis, to
153 minimize variation due to genomic position differences and to ensure direct comparability
154 between different reporters. The transgenic line containing the 1.5 kbp enhancer fragment
155 named SlpL1.5 expressed GFP in the same pattern observed for *GMR35H02-Gal4* (Figure 2—
156 figure supplement 1B-B"), indicating that the active enhancer of *slp1* and *slp2* genes in
157 *GMR35H02* is located within this smaller 1584 bp sequence. We then searched for smaller
158 conserved DNA segments within this 1584 bp sequence by Evoprinter and identified three even
159 smaller conserved sequences of sizes 220 bp, 592 bp, and 123 bp, respectively, that we named
160 Slpf1 (220 bp), Slpf2 (592 bp) and Slpf3(123 bp)(Fig. 2A). As earlier, we cloned these three
161 smaller DNA elements into the pJR12 vector and generated transgenic flies expressing the GFP
162 reporters from an identical chromosomal location. Transgenic flies containing the 220bp
163 fragment (Slpf1) expressed GFP very similar to the *GMR35H02-Gal4* line we had earlier
164 observed, while the other two did not show any expression (Fig. 2 B-B’’’) (Figure 2—figure
165 supplement 1C-E"), indicating that we had narrowed down the active enhancer within the
166 *GMR35H02* sequence to a 220bp element.

167 However, the deletion of this element by CRISPR-Cas9 failed to eliminate the expression of Slp1
168 and Slp2 in neuroblasts (Figure 2—figure supplement 2A-A’’’), though it noticeably reduced the
169 expression domain of Slp1 (Figure 2—figure supplement 2C). Given that the expression of
170 developmentally regulated genes is often controlled by multiple enhancers [54,55] and that
171 enhancer redundancy is important for achieving robust developmental outcomes [54,56,57], this

172 indicated that other enhancers might act redundantly with this 220 bp enhancer to regulate
173 Slp1/2 expression in medulla neuroblasts. To find other enhancers of *slp* expression, we
174 scanned through the REDfly database[58,59] – a curated repository of enhancers reported for
175 *Drosophila melanogaster* genes. An earlier study had conducted an exhaustive analysis of a 30
176 kbp genomic region surrounding the *slp* transcription units to understand better the regulatory
177 networks underlying *slp* expression during embryonic segmentation and to identify *cis*-
178 regulatory elements driving slp1 /2 expressions at parasegment boundary formation [55]. In this
179 study, segments of regulatory DNA within 30 kbp of *slp1* and *slp2* transcription start sites,
180 averaging 2kbp in size, were incorporated in a *lacZ* reporter coupled to an *even-skipped*
181 promoter, and patterns of lacZ expression were then observed in transgenic flies (Fig. 2A, Table
182 1). We obtained transgenic lines used in this study (kind gifts from Dr. Miki Fujioka and Dr.
183 James B. Jaynes) and then tested by antibody staining whether the expression of *lacZ* driven by
184 these enhancers colocalized with endogenous Slp1 and Slp2 proteins in the medulla (Figure 2—
185 figure supplement 3). Through this screen we identified a second regulatory segment
186 corresponding to the REDfly enhancer d5778 (Fig. 2A) that drove GFP expression in medulla
187 neuroblasts within the endogenous Slp1/2 expression domain (Figure 2—figure supplement 3Q-
188 Q''). Since the overlapping d6383 did not express GFP in medulla neuroblasts (Figure 2—figure
189 supplement 3R-R''), we narrowed down the active enhancer's location to an 850 bp segment
190 within the d5778 enhancer (Fig. 2C-C'''). Reporter expression driven by this second enhancer
191 (hereafter referred to as d5778 850bp enhancer) is initiated at a slightly later time compared to
192 the first identified enhancer, and it is in older Slp expressing neuroblasts and also in glial cells at
193 the junction of the medulla and the central brain. To confirm that the d5778 850bp driven

194 reporter is expressed in medulla neuroblasts, we used *dpn*-Gal4 to drive *UAS-GFP-RNAi* in
195 neuroblasts, and this eliminated GFP expression in medulla neuroblasts. In contrast, GFP
196 expression in neuroblasts is not affected when we use *repo*-Gal4 to drive *UAS-GFP-RNAi* in glia
197 (Figure 2—figure supplement 4). Our analysis of the REDfly enhancers that could potentially
198 regulate expression of Slp1/2 in the medulla also revealed that the 220 bp enhancer segment
199 identified earlier is contained within another REDfly enhancer named u8772 (Fig. 2A). Thus, we
200 refer to the first identified enhancer hereafter as u8772 220bp. As in the case of the u8772
201 220bp enhancer deletion, sole deletion of the d5778 enhancer by CRISPR-Cas9 did not abolish
202 Slp1/2 expression (Figure 2—figure supplement 2B-B’’’, C), suggesting that these two enhancers
203 function redundantly and may make additive contributions to attaining the observed levels of
204 Slp1 and Slp2 expression.

205 To test whether a combination of these two enhancers is required to regulate Slp1 and Slp2
206 expression in medulla neuroblasts, we used CRISPR-Cas9 to delete the second enhancer in the
207 strain that had the first enhancer deleted. Since the fly strain containing deletions of two
208 enhancers was homozygous lethal, we placed the double enhancer deletion line (slp^{DED}) over a
209 deficiency line (slp^{S37A}) that lacks the *slp1* transcription unit and all intervening sequences up to
210 16bp downstream of the slp2 transcriptional start site [60], and examined Slp1/2 expression in
211 larval brains. In such brains, both Slp1 and Slp2 expression are lost specifically in medulla
212 neuroblasts and their progenies, but their expression in lamina neurons and glia are not
213 affected (Fig. 2D-D’’’’). As controls, heterozygous slp^{S37A} or slp^{DED} brains show wild-type Slp1
214 and Slp 2 expression patterns (Fig. 2E-F’’’’). This result confirms that these two enhancers acting

215 together are necessary and specific enhancers for Slp1 and Slp2 expressions in medulla
216 neuroblasts and progeny.

217

218 **Bio-informatics analysis of enhancers identified binding sites for transcription factors Ey, Slp1,**
219 **Scro/Vnd and Su(H).**

220 We analyzed the sequences of the u8772 220bp and the d5778 850bp enhancers using a web-
221 based tool that uses the MEME suite [61] application FIMO [62] for predicting potential transcription
222 factor binding sites (Dr. Bart Deplancke and Michael Frochaux, personal communication). This
223 tool can be accessed at https://biss.epfl.ch. This initial analysis predicted the occurrence of
224 putative binding sites for the previous TTF Ey, the CSL transcription factor Su(H), Slp1 itself, and
225 an Nk2-class homeodomain transcription factor Ventral nervous system defective (Vnd) (Fig. 3,
226 Table 2, Supplementary Table 2) in our enhancers. The previous TTF Ey was shown to be
227 required but not sufficient for activating Slp genes' expression in medulla neuroblasts[18], but it
228 was unclear whether this regulation is direct. Vnd is not expressed in medulla neuroblasts
229 according to our single-cell RNA-sequencing data [16], but a related homologous NK-2 homeobox
230 transcription factor Scarecrow [63] (Scro) is expressed around the same time as Slp1 [16]. Also, the
231 loss of Scro leads to significantly reduced Slp expression level [16]. The CSL transcription factor
232 Su(H) is the *Drosophila* homolog of RBP-J[64,65] and the critical DNA-binding component of the
233 active Notch transcriptional complex. The Notch signaling pathway plays an overarching role as
234 a master regulator of development and differentiation in neuroblasts, but it has not been

235 shown to regulate the expression of temporal patterning genes in neural progenitors.

236 Therefore, we next tested whether Slp1/2 expression is regulated by Notch signaling.

237

238 **<u>The Notch pathway regulates Slp1 and Slp2 expression in medulla neuroblasts</u>**

239 We observed the expression of Slp1 and Slp2 in RNAi knockdown clones of key Notch pathway

240 components induced by *ay-Gal4* (*actin>FRT-y^{+}-STOP-FRT-Gal4*, in which *actin* promoter drives

241 Gal4 expression only after a STOP cassette is excised by the action of heat shock activated

242 Flippase[66]). Since *slp1* and *slp2* are two homologous genes located in close proximity in the

243 genome [67] and are expressed in similar patterns with Slp1 expression slightly preceding Slp2

244 (Fig. 1B-B'''), in all subsequent figures we have shown data for Slp2 assuming that Slp1

245 expression follows the same pattern . On inducing RNAi knockdowns of the critical Notch

246 pathway components Notch and Su(H) – members of the tripartite core of the active Notch

247 transcriptional complex [68], it is seen that Slp2 expression is delayed within the RNAi knockdown

248 clones marked by GFP expression (Fig. 4A-A''', B-B''' respectively) compared to wild type

249 neuroblasts of the same age (i.e., in the same vertical 'stripe'). Since the lateral to medial

250 spatial axis is a proxy of the neuroblast age, we counted the number of neuroblast when Slp2 is

251 first turned on. In control regions, Slp2 is turned on at the 4th- 5th neuroblast from the lateral

252 edge, while in N-RNAi clones (n=12), Slp2 is turned on at the 10th-15th neuroblast. Similarly,

253 Slp2 expression initiates between the 7th-10th neuroblasts inside Su(H)-RNAi clones (n=11). A

254 similar effect is seen when a dominant-negative variant of the third core component of the

255 Notch transcriptional complex Mastermind (Mam) is expressed under the control of *ay*-Gal4

256 (Fig. 4C-C'''). Within *mamDN* expressing clones (n=6), Slp2 is initiated between the 7th-10th
257 neuroblast as with *Su(H) RNAi* clones. These data suggest that timing of Slp1/2 expression in
258 medulla neuroblasts is regulated by the Notch pathway.

259 To identify Notch's cognate ligand that activates Notch signaling in medulla neuroblasts, we
260 examined expression of known Notch ligands- Delta [69], Serrate[70,71] and Weary[72] in medulla
261 neuroblasts (data not shown). Of these only *UAS-GFP* driven by *delta-Gal4* was seen to be
262 expressed in medulla neuroblasts and in their progeny GMCs. We then examined whether loss
263 of Dl recapitulates the effects we observe on Slp1/2 expression with loss of function of core
264 Notch transcription complex components, as would be expected if Dl is required for activating
265 Notch signaling in these cells. In neuroblasts within Dl-RNAi expression clones, Slp2 expression
266 is initiated at the 6th-10th neuroblasts from the medulla lateral edge (Fig. 4D-D''') (n=5),
267 consistent with our observations of Slp2 expression in mutants of other Notch pathway
268 components discussed above.

269 **Genetic interactions between Notch, Ey and Scro in the regulation of Slp expression.**

270 Since Ey is required for Slp expression, the delay of Slp expression with loss of N signaling might
271 be due to a delay in earlier temporal transitions resulting in late Ey onset, or a specific delay in
272 the Ey to Slp transition, or both. To test this, we examined the expression of Ey with loss of N
273 pathway components. Ey is normally turned on in the 2nd-3rd neuroblast. In *N-RNAi* clones, Ey is
274 turned on in the 5th-8th neuroblast (n=6) (Fig. 5A1-8), suggesting that Notch signaling is required
275 for the timely transition into the Ey stage. However, this does not preclude an additional direct
276 role for Notch signaling in the Ey to Slp transition. To examine this, we counted the number of

277 Ey+ neuroblast in which the transition to Slp stage occurs. We observed that in wild type
278 neuroblasts, Slp2 starts to be expressed at a weak level in the 2nd-3rd Ey+ neuroblast, and the
279 level becomes stronger one or two neuroblasts later and then remains strong for several
280 neuroblasts, thus the transition to the Slp stage occurs in the 3rd -4th Ey+ neuroblast, and after
281 the transition, Ey level starts to decrease because of repression by Slp. In *N-RNAi* clones, the
282 transition to the Slp stage occurs in the 6th-9th Ey+ neuroblast (n=6) (Fig. 5A1-8). In *Su(H)*^{47}
283 mutant clones, the transition occurs after the 6th-8th Ey+ neuroblasts (n=5)(Fig. 5B-C''). To make
284 sure the delayed Slp transition is not mediated through Ey with loss of Su(H), we supplied Ey
285 using a *dpn*-Gal4 and UAS-Ey in *Su(H)*^{47} mutant clones. In such clones, Ey is over-expressed, but
286 the transition to Slp stage is still delayed to the 6th-7th Ey+ neuroblast (n=6) (Fig. 5D-E''). These
287 results suggest that Notch signaling also facilitates the Ey to Slp transition in addition to an
288 earlier indirect role through Ey.

289 We next examined if the expression of earlier TTFs or later TTFs is also affected by loss of N
290 signaling. One of the first TTFs, SoxN, is not significantly affected in *Su(H)-RNAi* clones (Figure
291 5—figure supplement 1A-A'''). Opa, the TTF upstream of Ey, is normally expressed in two
292 stripes. In *Su(H)-RNAi* clones, the first Opa stripe appears expanded, while the second stripe is
293 delayed (Figure 5—figure supplement 1B-B'''). Furthermore, the expression of later factors D
294 and BarH1 are severely delayed or mostly lost when we knocked down Su(H) (Fig. 5G-H'). Thus
295 N signaling may affect multiple temporal transitions.

296 Since Notch signaling is active throughout the neuroblast life, and may facilitate multiple
297 temporal transitions, we reasoned that Notch signaling may require the previous TTF for
298 specificity. Therefore, we tested if supplying active Notch signaling can rescue Slp expression

299 when Ey is knocked down. Supplying NICD using a *dpn>FRT-stop-FRT3-FRT-NICD* transgene
300 (which drives the expression of NICD from the *dpn* enhancer in presence of heat shock
301 activated Flippase; see Methods) was not sufficient to rescue Slp expression in *ey-RNAi* clones
302 (Fig. 5I-I''). This result is consistent with our hypothesis that Notch signing, as a general
303 signaling pathway active in all neuroblasts, requires the previous TTF Ey for its specificity to
304 facilitate Slp expression and promote the transition. Furthermore, overexpression of Scro was
305 also not sufficient to rescue Slp expression in *ey-RNAi* clones (Fig. 5J-J''). Taken together, these
306 results suggest that the previous TTF Ey is required to initiate Slp expression, while Notch
307 signaling and Scro require Ey to further activate Slp expression and facilitate the timely
308 transition to the Slp stage.

309

310 **Notch pathway and Ey regulate the activity of *slp* enhancers.**

311 Since Su(H) and Ey are required for regulate Slp expression, we next tested whether these
312 regulations are mediated through the identified enhancers. We tested whether knockdown of
313 each factor would affect GFP reporter expression driven by these enhancers. We reasoned that
314 if any of the factors we had identified binding sites for bound to the enhancers and activated
315 Slp1/2 transcription, GFP reporter expression driven by these enhancers would be lost in the
316 loss of function clones of these transcription factors. We induced RNAi knockdown clones for Ey
317 and Su(H) using ay-Gal4 in transgenic flies expressing wild type GFP reporters driven by these
318 two enhancers, and then compared the expression of Slp2 and GFP in wild-type neuroblasts
319 and in neuroblasts where each of these TFs had been individually knocked down.

320 For both enhancers, GFP reporter expression and Slp2 expression were lost in *ey-RNAi* clones
321 (Fig 6A-B'''), confirming an earlier observation that Ey is required for initiating Slp1/2
322 expression. It also strengthened the evidence that these two were indeed bona-fide enhancers
323 activating Slp1/2 expression. Similarly, GFP reporter expression was lost or delayed in s*u(H)-*
324 *RNAi* clones for both enhancers (Fig 6C-D'''), consistent with the changes in Slp2 expression.
325 Since Slp binding sites were also identified in the *slp* enhancers, we next tested the effect of
326 loss of Slp1/2 function on the expression of our GFP reporters. To this end we induced *slp1/2*
327 loss of function (LOF) mutant clones in flies carrying the *GFP reporter and UbiRFP FRT40A*. In
328 Fig. 6E-F' *slp* LOF clones are visible as dark regions devoid of RFP whereas wild type neuroblasts
329 are marked by RFP expression from the Ubiquitin promoter. Reporter expression driven by both
330 enhancers within *slp* LOF neuroblasts is normal as in wild-type neuroblasts. Though this
331 suggests that Slp1/2 are not required to initiate their own expression, it does not preclude a
332 possible role of Slp1/2 in sustaining their own expression in older Slp1/2 stage neuroblasts or
333 progeny, but the perdurance of the GFP reporter prevents us from testing this possible role. In
334 summary, our genetic experiments confirmed that identified enhancers of *slp1/2* respond to
335 activation by Ey and Su(H).

336

337 **Mutations of potential binding sites for Ey, Su(H) and Scro in *slp1/2* enhancers impair**
338 **expression of the reporters**

339 To further test whether the regulators we identified regulate Slp1/2 expression directly through
340 binding to the enhancers, we set out to mutate all possible binding sites for each of the

341 regulators- Ey, Su(H), Scro and Slp1, on each enhancer. We identified all potential matches to
342 consensus binding motifs for these factors using the DNA Pattern Find Tool within the Sequence
343 Manipulation Suite[73] (Figure 3, Table2) and using the FIMO based web-application to predict
344 transcription factor binding sites mentioned earlier (accessible at https://biss.epfl.ch) (please
345 see Methods for details). We adopted this combined approach instead of solely mutating FIMO
346 predicted binding sites for a TF since mutation of FIMO predicted binding sites alone did not
347 always result in GFP reporter expression patterns that were consistent with our observations
348 from genetic experiments. For instance, in the u8772 220bp enhancer, deletion of the Su(H)
349 binding site that was predicted using FIMO (220-Su(H)-site1 in Table 2) did not result in a loss of
350 reporter GFP expression (Fig. 7- figure supplement 1). This contradicted our result from genetic
351 experiments with the wild type u8772 220bp GFP reporter, where GFP expression from the
352 reporter is lost or delayed in *su(H)-RNAi* knockdown clones (Figure 6C-C'''). We suspected this
353 lack of correspondence between phenotypes from genetic experiments and those observed
354 from our transgenic GFP reporters could be explained by our failure to identify all potential
355 transcription factor binding sites using FIMO alone.

356 The "DNA Pattern Find" pattern recognition tool accepts transcription factor (TF) binding
357 consensus sequences and DNA sequences to search within for TF binding sites as inputs, and
358 returns the locations of sites matching the consensus within the provided sequence. Consensus
359 DNA sequences recognized by transcription factors were obtained for Ey, Su(H) and Slp1 from
360 Fly Factor Survey, JASPAR databases and from published literature (for Ey) [74] (Figure3). We
361 noticed that predicted binding sites identified by FIMO such as the 220-Ey-Site2 and 850-Ey-
362 Site1 often had minor mismatches to the consensus binding sequence (for example, the 220-Ey-

363 Site2 had two mismatches to the consensus). Therefore, we also considered sites with a
364 maximum of two mismatches on non-critical bases to our consensus sequences as potential
365 binding sites for a particular transcription factor. For Scro, no consensus sequences could be
366 found, hence we searched d5778 850 bp enhancer using available binding consensus sequences
367 for a closely related NK-2 transcription factor Vnd and 19 other related NK-2 transcription
368 factors (Figure 3—Figure supplement1) and selected seven most commonly occurring
369 sequence motifs for these factors as putative Scro binding sites. Given the small size of the
370 u8772 220bp enhancer we identified just the binding site predicted for Vnd within this
371 enhancer as the probable Scro binding site to avoid mutating a significant fraction of its
372 sequence length. We then designed strategies to either delete or mutate the identified binding
373 sites for each TF based on their proximity; when two sites for any two or more TFs overlapped,
374 we used mutations that would not disrupt binding of the other factor. We also tried to keep the
375 lengths of the mutated enhancer variants as close as possible to the wild-type enhancers. We
376 then checked our mutant sequences through the FIMO and DNA Pattern Find to select
377 mutation sequence designs that minimized disruptions of other predicted binding sites. Table 2
378 lists the original TF binding sites identified and the sequences to which they were mutated.
379 Custom-designed gene blocks (Supplementary Table 3) containing the mutated enhancer
380 sequences were cloned upstream of the GFP reporter in pJR12 vector as before, and transgenic
381 flies expressing these reporter constructs were then made using the same landing site in the
382 genome as the wild-type reporters. We next compared the expression patterns and intensities
383 of GFP reporters with mutated TF binding sites against GFP reporter expression driven by the
384 'wild type' version of that same enhancer (Fig. 7A-A''', Fig. 8A-A'''). To compare GFP reporter

385 intensities between wild-type and mutated variants of an enhancer, identical microscope
386 illumination, and imaging settings were used for all variants of the same enhancer.

387 For the u8772 220bp enhancer, individual deletion of one Ey binding site (220-Ey-Site1) or
388 mutation of another Ey binding site (220-Ey-Site2) nearly eliminated GFP expression (Fig. 7B-
389 C’’’,H). There are four predicted Su(H) binding sites, and among them 220-SuH-Site1 and 4 are
390 perfect matches to the consensus, but only site1 was predicted by FIMO. Site 2 and 3 each has
391 two mis-matches to the consensus on non-critical bases. Mutation of all four predicted Su(H)
392 sites in the u8772 220bp enhancer led to a complete loss of GFP expression from the reporter
393 (Fig. 7D-D’’’,H). We also generated another reporter mutating only the two Su(H) sites that
394 were perfect matches to the consensus, and this caused a dramatic reduction of the reporter
395 expression (Fig. 7E-E’’’,H). Mutation of the Scro/Vnd site in the u8772 220bp enhancer greatly
396 reduced the level of GFP expression (Fig. 7F-F’’’,H), Mutation of Slp1 binding sites significantly
397 reduced the level of GFP expression, but preserved the pattern of GFP expression as the wild
398 type GFP reporter (Fig. 7G-G’’’,H).

399 For the d5778 850 bp reporter, combined deletion and mutation of three predicted Ey binding
400 sites abolished the reporter expression, while deletion of seven possible Scro binding sites
401 reduced the reporter expression greatly (Fig. 8 B-C’’’,E). Deletion of the putative Slp1 binding
402 site did not significantly change the GFP reporter expression (Fig. 8 D-D’’’).

403 Six potential Su(H) binding sites were identified in the d5778 850bp enhancer (sites 850-SuH-
404 Site 1 through 6 in Table 2). The DNA Pattern Finder tool predicted three Su(H) binding sites
405 that were perfect matches to consensus Su(H) binding sites (Figure 3). These were 850-SuH-

406 Site2, 3 and 6. Among them, Site 3 was also predicted by the FIMO-based analysis. 850-SuH-
407 Site1 has one mismatch, while sites 4 and 5 have two mismatches to the Su(H) binding
408 consensus on non-critical bases. We created two different Su(H) site variants. The 850-SuH-
409 1m2m3m6m construct mutated sites 1,2,3 and 6, and the 850-SuH-1-6m construct had all
410 potential Su(H) binding sites mutated. For both variants, GFP expression is greatly intensified in
411 glial cells, making it difficult to assess the neuroblast expression (Figure 9 —figure supplement
412 1). Therefore, we used *repoGal4* to knock down GFP expression in glial cells using *UAS-GFP-*
413 *RNAi* , and found that the neuroblast GFP expression was actually increased compared to the
414 wild-type reporter for both variants (Figure 9 B-C''', D). These data suggest that Notch signaling
415 does not activate this enhancer directly. This is likely the reason why the d5778 850bp
416 enhancer drives a delayed expression pattern than the u8772 220bp enhancer and the
417 endogenous Slp.

418 Taken together, our data suggest that Notch signaling may activate *slp1/2* expression by acting
419 on the u8772 220bp enhancer alone. Although loss of all Su(H) binding sites in the 220bp
420 enhancer caused a complete loss of reporter expression, endogenous Slp expression is only
421 delayed when Notch or Su(H) is knocked down. This can be explained by our finding that the
422 d5778 850 bp enhancer directs a delayed expression of Slp and this expression is not
423 dependent on Notch signaling.

424

425 **DamID-sequencing confirms binding of Ey and Su(H) to identified enhancers of Slp1/2.**

426 DamID-sequencing can be used to profile genome-wide binding patterns for transcription
427 factors and chromatin proteins [75,76]. We used a *SoxN*-Gal4 expressed in all medulla neuroblasts
428 [16] to drive the expression of DamSu(H) or DamEy fusion proteins under *UAS* control and
429 inferred the genome-wide binding patterns of Ey and Su(H) through DamID-sequencing. For
430 each transcription factor two biological replicates were sequenced. Reproducibility of peaks of
431 transcription factor binding was determined using the Irreproducibility Discovery Rate (I.D.R.)
432 program to comply with recommended standards of reproducibility specified for genomic data
433 consortia such as ENCODE [77] and all further analyses were done based on I.D.R. reproducible
434 data. Reproducible peaks of Ey and Su(H) binding were observed in both replicates in the
435 genomic region corresponding to the identified enhancers of Slp1/2 transcription, although
436 reproducible Su(H) peaks were observed only in a smaller region toward the 3' end of the
437 d5778 enhancer, in contrast to the u8772 220bp enhancer where Su(H) peaks are distributed
438 prominently throughout the enhancer body (Fig. 10). We also observed peaks of Ey binding in
439 the genomic region of *scro* gene (Fig. 10-figure supplement1A), consistent with the observation
440 that Scro expression is initiated in medulla neuroblasts at about the same time as Slp1/2.

441 Additionally, our experiments also revealed that a list of genes were bound reproducibly both
442 by Ey and by Su(H) (Supplementary Table 4). Using DAVID, we conducted a functional
443 annotation clustering analysis of this gene list. Genes related to the Notch pathway and
444 participating in the cell division cycle were strikingly enriched within this list of co-bound genes
445 (Supplementary Table 5), thus raising the possibility that in medulla neuroblasts, TTFs such as
446 Ey can modulate the responsiveness of Notch target genes in the medulla to mitogenic Notch
447 signaling as has been seen in Type II neuroblasts[78] (note that Ey can function as both

448 transcriptional activator and repressor). Another set of genes were bound reproducibly only by
449 Ey (Supplementary Table 4). For example, only Ey I.D.R peaks were observed in the genomic
450 region of the *hmx* gene (Fig. 10-figure supplement1B), encoding a transcription factor
451 expressed in a type of Notch-off neurons born from the Ey stage [17,79]. DAVID analysis of genes
452 bound uniquely by Ey showed an enriched representation of genes involved in axon guidance
453 and maintenance, and interestingly, of genes that participate within or interact with the Hippo
454 pathway and Ras pathway (Supplementary Table5). It remains to be studied whether Ey
455 regulates the expression of these genes. Finally, a third set of genes were bound reproducibly
456 only by Su(H) (Supplementary Table 4). For example, an I.D.R peak only for Su(H) was found in
457 the *dll* genomic region (Fig. 10-figure supplement1C). Since Notch-on neurons born from the Tll
458 stage neuroblasts express Dll [17], it will be interesting to test whether Notch signaling activates
459 Dll expression directly. DAVID analysis of the gene list bound uniquely by Su(H) shows a
460 representation of genes participating in the EGFR/MAPK pathway such as p38 MAPK and in
461 BMP signaling (Supplementary Table 5). These preliminary data indicate that the Notch
462 pathway may interact with other signaling pathways such as MAPK and BMP in medulla
463 neuroblasts and present a promising opportunity for future studies.

464 Taken together our DamID data support evidence from our genetics studies and suggests that
465 Ey and Su(H)/N pathway activate Slp1/2 transcription by direct binding to Slp1/2 enhancers.

466 **<u>Notch signaling is dependent on cell-cycle progression.</u>**

467 Although it has been well-established that GMCs generated by the asymmetric division of
468 neuroblasts signal to their sister neuroblasts to provide the Notch signaling[32,33], it hasn't been
469 demonstrated whether Notch signaling is lost in cell-cycle arrested medulla neuroblasts since

470 they fail to generate GMCs. We used a regional Gal4, *vsx-Gal4* that is expressed in the center
471 domain of the medulla crescent starting in the neuroepithelium[80], to drive *UAS-DCR2* and a
472 RNAi against Proliferating Cell Nuclear Antigen (PCNA),which is essential for DNA replication
473 and S phase progression[81]. Blocking cell cycle progression caused premature transformation of
474 neuroepithelial cells to neuroblasts, as has been previously reported [82]. These neuroblasts
475 express the normal neuroblast marker Deadpan (Dpn) (Fig. 11A-A'''), but produce few
476 progenies, and some neuroblasts are present in the deep layers which would normally be
477 occupied by neuronal progenies (Fig. 11D). In the region where PCNA is knocked down, a large
478 fraction of neuroblasts don't express E(spl)mγGFP, a Notch signaling reporter [69], while all
479 neuroblasts in the control regions express E(spl)mγGFP (Fig. 11A-A'''). Thus, Notch signaling is
480 largely lost in cell-cycle arrested neuroblasts.
481
482 **<u>The role of cell cycle progression in the medulla TTF cascade.</u>**
483 Next, we tested whether blocking cell-cycle progression also affected the medulla TTF cascade
484 progression. In *vsx-Gal4>PCNA-RNAi* brains, neuroblasts in the affected region have reduced
485 expression of Ey, and loss of Slp1/2, but they keep expressing SoxN (Fig. 11B-D''). This suggests
486 that an earlier temporal transition step is blocked which is required for Ey expression, and this
487 prevents us from examining whether the Ey to Slp transition also requires cell cycle progression.
488 To circumvent this problem, we used the *ay*-Gal4 to drive *UAS-DCR2* and *PCNA-RNAi*. By
489 adjusting heat shock timing to induce clones, we were able to obtain a condition where Ey
490 expression is minimally affected, and at this condition we observed that Slp2 expression is still
491 severely delayed (Fig. 11E-F''). In addition to the timing of clone induction, the *ay-Gal4* is also

492 likely to be weaker than *Vsx-Gal4* at inducing RNAi, and the cell cycle is likely only slowed down
493 rather than arrested when using *ay-Gal4*, because there are still some progenies produced in
494 such clones. Furthermore, Slp1/2 expression is also significantly delayed when we knock down
495 String /Cdc25 required for the G2 to M phase transition[83], or overexpress Dacapo (Dap, a Cyclin-
496 dependent kinase inhibitor in the CIP/KIP family)[84] using *ay-Gal4*, while Ey is slightly delayed
497 (Figure 11—figure supplement 1A-D'''). Thus, cell cycle progression is also required for the
498 precise timing of Ey to Slp1/2 transition.
499
500 **Notch signaling can rescue Slp expression delay caused by cell cycle defects.**
501 Finally, we tested if supplying Notch signaling to cell-cycle arrested or delayed neuroblasts can
502 rescue the timing of the Ey to Slp transition. We supplied active Notch in neuroblasts using the
503 *dpn>FRT-stop-FRT3-FRT-NICD* transgene, while simultaneously inducing knockdown of PCNA
504 using *ay-Gal4* under the same heat shock condition that leaves Ey expression largely
505 unaffected. Supplying NICD was sufficient to rescue Slp2 expression in *PCNA-RNAi* clones (Fig.
506 11G-H''). This suggests that for the Ey to Slp transition, the presence of active Notch signaling
507 can substitute for the requirement of the cell-cycle progression. In wild type condition,
508 supplying active NICD did not significantly affect the timing of the Ey to Slp transition, which is
509 still around 3rd-4th Ey+ neuroblast (Figure 11I-J'''), possibly because that wild type cycling
510 neuroblasts already have active Notch signaling.
511
512 ## Discussion
513 **Evidence of direct transcriptional activation in the medulla TTF cascade.**

514 *Drosophila* neuroblasts are temporally patterned by sequentially expressed TTFs. Although the
515 expression pattern and mutant phenotypes suggest that TTFs form a transcriptional cascade,
516 direct transcriptional regulation between TTFs has not been demonstrated in most cases. This
517 work has characterized two enhancers of the *slp* genes that enable the expression of Slp1 and
518 Slp2 in medulla neuroblasts. The u8772 220bp enhancer is activated at an earlier stage relative
519 to the d5778 850bp enhancer. In these two enhancers, we identified sites for the previous TTF -
520 Ey and Scro-a TTF expressed at around the same time as Slp1. Deleting either enhancer alone
521 did not eliminate the expression of endogenous Slp1 and Slp2, suggesting that they act partially
522 redundantly with one another. Deletion of both enhancers completely eliminates Slp1 and Slp2
523 expression in medulla neuroblasts but does not affect their expression in lamina neurons or
524 glia, confirming the specificity and necessity of these two enhancers. Using GFP reporter assays,
525 we have shown that mutation of Ey binding sites in these enhancers abolishes reporter
526 expression similar to genetic experiments where we observe a loss of GFP reporter within *ey*
527 RNAi clones. Our results are also consistent with previous studies that showed a complete loss
528 of endogenous Slp1/2 expression in *UAS-ey-RNAi* expressing neuroblasts [18]. We also confirmed
529 the *in vivo* binding of Ey to the identified enhancers of Slp by Dam-ID sequencing. The
530 expression of the TTF Scro is initiated simultaneously as Slp1/2, and it has been shown that loss
531 of Scro significantly reduces Slp expression level. Mutation of most probable Scro binding sites
532 on the u8772 220bp or d5778 850bp enhancers led to a dramatic reduction of GFP reporter
533 expression. Thus, the combined effect of mutating Scro binding sites on both enhancers
534 recapitulates the observed impact of Scro knock-down on endogenous Slp1/2 expression, which
535 is reduced expression of Slp1/2 in neuroblasts expressing *UAS scro-RNAi* and a consequent loss

536 of neural fates specified by Slp1/2 in their progeny[16]. It is interesting to note that our
537 observation of multiple enhancers regulating Slp1/2 expression (Fig. 12) is consistent with
538 regulation of Slp1/2 in other developmental contexts. Previous studies have noted the presence
539 of multiple enhancers of Slp1/2 expression in the vicinity of the *slp1* and *slp2* coding loci . Many
540 of these regulatory DNA segments function as stripe enhancers enabling Slp1/2 to function as
541 pair-rule genes during embryonic segmentation[55]. Though these enhancers share some
542 overlapping functions and domains of activation, a full complement of stripe enhancers is
543 required for maintaining parasegment boundaries and wingless expression [85, 55].
544

545 **Notch signaling regulates temporal transitions in medulla neuroblasts.**

546 It was previously demonstrated that although Ey is necessary for activating Slp1/2 expression it
547 is not sufficient [18]. There is always a time delay after the start of Ey expression to the start of Slp
548 expression to ensure the sufficient duration of the Ey window. How is the timing controlled?
549 From our analyses of the *slp1/2* enhancer sequences we found several binding sites for the CSL
550 transcription factor Su(H), most prominently known as a central component of the ternary
551 Notch transcription complex and the primary DNA binding component. To confirm the
552 involvement of the Notch pathway in regulating Slp1/2, we observed the effects of knocking
553 down key Notch pathway components on endogenous Slp1/2 expression. In all cases we
554 observed a delay in the expression of Ey and a further delay in the transition to the Slp1/2 stage
555 in neuroblasts expressing the RNAi knockdowns. Mutating Su(H) binding sites in the u8772
556 220bpenhancer led to a loss or reduction of GFP reporter expression in neuroblasts. However,
557 mutating Su(H) binding sites in the d5778 850bp enhancer did not decrease the reporter

558 expression. These results suggest that Notch signaling directly regulates Slp expression through
559 the u8772 220bp enhancer, but not the d5778 850bp enhancer, and this is consistent with the
560 delayed expression driven by the d5778 850bp enhancer. However, Ey still plays a more critical
561 role in activating Slp1/2 expression than the Notch pathway, since Slp1/2 are still expressed
562 albeit later in the absence of Su(H) and other Notch components, and Notch signaling requires
563 Ey to speed up the Ey to Slp transition. As with Ey, we confirmed Su(H) binding to the u872
564 220bp enhancer using DamID-seq. Thus, our work provided strong evidence that N signaling, a
565 general signaling pathway involved in neuroblast development, regulates the timing of
566 activation of a TTF gene directly (Fig. 12). In addition, our results also raised the interesting
567 hypothesis that Notch signaling might be involved in facilitating all temporal transitions,
568 because the turning on of Opa and Ey is also delayed, and we observed a further and further
569 delay in turning on of later TTFs. Whether Notch signaling regulates other TTF expression
570 directly or indirectly still awaits further investigation.
571
572 **Cooperative regulation of target genes including *slp* by the TTF Ey and Notch signaling**
573 What might explain the delay in Slp1/2 expression in the absence of Notch signaling? Recent
574 developments in single-molecule Fluorescence In Situ Hybridization (smFISH) technology and
575 live imaging techniques using the MS2-MCP system have enabled studying the transcription
576 process in molecular detail. Imaging transcription driven by Notch responsive enhancers in
577 native contexts has shown this process to be inherently 'bursty', i.e., episodes of transcription
578 (enhancer 'On' state) are punctuated with gaps in activity (enhancer in 'Off' state) [86,87]. The
579 dosage of NICD modulates the duration of the 'On' phase in one context studied by live imaging

580 [86,87]. Additionally, binding of tissue-specific regional factors to these Notch responsive
581 enhancers may prime these enhancers and help synchronize transcription and sustain a steady
582 transcriptional output upon Notch binding to enhancers; this helps integrate important
583 positional cues and the perception of context [86]. Applying these insights to our system, we
584 suggest that Ey may act by priming the Notch responsive enhancer of *slp* providing crucial
585 contextual information, and this is required for Notch to further activate Slp1/2 transcription,
586 land speed up the transition (Fig. 12).

587 **<u>The role of cell cycle progression and Notch signaling in the medulla TTF cascade</u>**

588 Notch targeting genes and Dpn are transcriptional repressors that act partially redundantly to
589 maintain neuroblast identity. In type II NBs, Dpn depends on Notch signaling, and loss of Dpn
590 causes premature differentiation[37,88]. However, in type I NBs, Dpn is not lost when Notch
591 signaling is lost, and Notch signaling seems dispensable for the self-renewing abilities of NBs[39-
592 41]. In the medulla neuroblasts, we also observed that in *Su(H)* mutant clones, the clone size and
593 neuroblast proliferation are not significantly affected. On the other hand, we observed that N
594 signaling is dependent on cell-cycle progression, and the Notch target gene is lost when cell
595 cycle progression is blocked.
596 In the medulla, blocking cell cycle progression in neuroepithelial cells prematurely transform
597 them into neuroblasts, and these neuroblasts seem to be arrested or severely delayed in the
598 TTF cascade. When we arrested or slowed down the cell cycle later in neuroblasts to preserve
599 Ey expression, we observed Slp expression is still delayed. Therefore, cell cycle progression also
600 has a role in the Ey to Slp transition. Further we showed that supplying Notch signaling is
601 sufficient to rescue the delay in the Ey to Slp transition caused by cell cycle defect. Thus at the

602 Ey to Slp transition, the cell cycle effect is mediated through the direct regulation of Slp
603 transcription by Notch signaling. Taken together, our results suggest that in Ey stage
604 neuroblasts, Ey is required to initiate Slp expression but not sufficient to activate it to a strong
605 level right away, and after each asymmetric division, activation of Notch signaling in the
606 neuroblast enhances Slp expression, until Slp expression reaches a certain level to repress Ey
607 expression and make the transition (Fig. 12). This can be part of a mechanism to coordinate the
608 TTF temporal transition with the cell cycle progression to generate the appropriate number of
609 neural progenies at a given temporal stage.

610

611 ## Methods

612 **Fly stocks and genetics**

613 Flies were reared on yeast food at 25°C unless otherwise stated.

614 Enhancer identification- Flies carrying the *GMR35H02-Gal4* insertion (BDSC 49923) were
615 crossed with transgenic flies expressing *UAS-GFPnls* (BDSC 4776). GFP driven by the
616 *GMR35H02-Gal4* was then compared to endogenous Slp1 and Slp2 expression. The procedure
617 for making transgenic constructs and strains is described separately.

618 Clonal experiments using *ay-Gal4*- The following RNAi lines or *UAS* lines were used for RNAi
619 knockdown experiments or over-expression experiments: *UAS-ey-RNAi* (BDSC 32486), *UAS-scro-*
620 *RNAi* (BDSC 33890), *UAS-N-RNAi* (BDSC 7078), *UAS-Su(H)-RNAi* (VDRC 103597), *UAS-Dl-RNAi*

621 (VDRC 32788), *UAS-PCNA-RNAi* (VDRC 51253), *UAS-stg-RNAi* (VDRC 17760), *UAS-Dap* (BDSC
622 83338), *UAS-Scro* (FlyORF: F000666).

623 *ay-Gal4* (*actin*>FRT-y^+-STOP-FRT-Gal4, in which *actin* promoter drives Gal4 expression after a
624 STOP cassette is excised by the action of heat shock activated Flippase) was used to drive RNAi
625 lines or *UAS* lines. Flies of genotype *ywhsFlp; ay-Gal4>UAS-GFP; UAS-Dcr2/Tm6B* were crossed
626 to the RNAi lines. Larvae were heat shocked at 37°C for 10 minutes 48 hours after egg laying
627 and then raised at 29°C, until brains of third instar larvae were dissected and stained.

628 For observing the effect of *ey-RNAi* on the GFP reporter expression (Fig 3) flies of genotype
629 *ywhsFlp; ay-Gal4>UAS-lacZ; ey-RNAi* (made by combining *ay-Gal4>UAS-lacZ* on chromosome II
630 (BDSC 4410) with *UAS-ey-RNAi* on chromosome III) were crossed to flies with genotype
631 *ywhsFlp; Sp/CyO; u8772 220bp>GFP* (enhancer1) or *ywhsFlp; Sp/CyO; d5778 850bp>GFP*
632 (enhancer2).

633 For studying effects of *Su(H)-RNAi* on GFP reporter expression, flies of genotype *ywhsFlp; ay-*
634 *Gal4>lacZ; Tm2/Tm6B* were crossed to flies of genotype *UAS-Dcr2; Su(H)-RNAi; u8772 220>GFP*
635 (enhancer 1) or *UAS-Dcr2; Su(H)-RNAi; d5778 870> GFP* (enhancer 2).

636 Heat shock protocols for RNAi experiments driven by *ay-Gal4* in the presence of GFP reporters
637 were the same as described above for *ay-Gal4* driven RNAi by themselves (i.e., without GFP
638 reporters).

639 <u>*Su(H)* MARCM experiment with *UAS-Ey.*</u> Flies of genotype *ywhsFlp UAS-GFP; FRT40A tubGal80;*
640 *dpn-Gal4* were crossed to flies of genotype *yw; FRT40A Su(H)^{47}/CyO; UAS-Ey/+.* The progeny
641 larvae were heat-shocked at 37°C for 45 minutes 48 hours after egg laying and then raised at

642 25°C, until brains of third instar larvae were dissected and stained. Anti-Ey staining is used to
643 distinguish brains carrying UAS-Ey from those that do not.

644 Expression of NICD in *ey-RNAi* knockdown clones- Flies of genotype *ywhsFlp; Sp/CyO; UAS-*
645 *eyRNAi* were crossed to flies of genotype *ywhsFlp; ay-Gal4 UAS-lacZ/CyO; dpn>hsNICD/Tm6B.*
646 Progeny larvae were heat-shocked at 37°C for 12 minutes 72 hours after egg-laying. Third instar
647 larval brains were dissected 48 hours after heat shock treatment.

648 Expression of Scro in *ey-RNAi* knockdown clones- Flies of genotype *ywhsFlp; ay-Gal4>UAS-GFP;*
649 *UAS-eyRNAi /Tm6B* were crossed to flies of genotype *UAS-Scro/Tm3.* Progeny larvae were
650 heat-shocked at 37°C for 9 minutes 48 hours after egg-laying. Third instar larval brains were
651 dissected 72 hours after heat shock treatment.

652 Cell cycle arrest experiments- For some experiments examining the effect of cell cycle arrest on
653 Slp1/2 expression and on the expression of the Notch reporter E(spl)mγGFP, *Vsx-Gal4* was used
654 to drive the expression of *UAS-PCNA-RNAi* and *UAS-Dcr2* in neuroblasts. Flies of genotype *Vsx-*
655 *G4; E(spl)mγGFP;UAS-Dcr2/Tm6B* were crossed to those with genotype *ywhsFlp; UAS-PCNA-*
656 *RNAi*. Larvae were shifted to 29°C 48 hours after egg-laying. Brains of third instar larvae were
657 observed. For other experiments, flies of genotype *ywhsFlp; UAS-PCNA-RNAi* were crossed to
658 flies of genotype *ywhsFlp; ay-Gal4>UAS-GFP; UAS-Dcr2/Tm6B*. Larvae with genotype *ywhsFLP;*
659 *ay-Gal4 UAS-GFP /UAS-PCNA-RNAi; UAS-DCR2/+* were heat shocked for 8 minutes at 37°C 50
660 hours after egg-laying (70 hours before they develop into climbing third instar larvae) and were
661 then dissected. For rescuing Notch expression in cell cycle arrested neuroblasts flies of
662 genotype *ywhsFlp; ay-Gal4>UAS-GFP; UAS-Dcr2/Tm6B* were crossed to those with genotype

663 *ywhsFlp; UAS-PCNA-RNAi; dpn>hsNICD*. Larvae of genotype *ywhsFLP; ay-Gal4 UAS-GFP /UAS-*
664 *PCNA-RNAi; UAS-DCR2/dpn>hsNICD* were then heat shocked for 8 minutes at 37°C 50 hours
665 after egg laying (70 hours before the third instar stage) as before and then dissected.

666 Negative labeling of *slp* loss of function clones- *Ubi-RFP FRT40A/CyO* flies (BDSC 34500) were
667 crossed with flies of genotype *ywhsFlp;Sp/CyO; u8772 220bp>GFP* (enhancer1) and *ywhsFlp*
668 *;Sp/CyO; d5778 870bp>GFP* (enhancer2) to create strains with genotypes *ywhsFlp; Ubi-RFP*
669 *FRT40A; u8772 220bp>GFP* and *ywhsFlp; Ubi-RFP FRT40A; d5778 870bp>GFP* respectively. Flies
670 of genotype *ywhsFlp; slp^{S37A}/Sm6-Tm6B* flies (a kind gift from Dr. Andrew Tomlinson) were then
671 crossed to *ywhsFlp; Ubi-RFP FRT40A; u8772 220bp>GFP* and *ywhsFlp; Ubi-RFP FRT40A; d5778*
672 *870bp>GFP* and larvae were heat shocked for 45 minutes 48 hours after egg laying. Third instar
673 larvae were then dissected. Clones carrying two copies of this deficiency are seen as dark
674 regions amidst Ubi>RFP marked wild type neuroblasts.

675 **Bioinformatic identification of transcription factor binding sites (TFBS)**

676 Initially, to identify a list of possible candidate TFs with binding sites within our enhancers, we
677 analyzed our enhancer sequences using the MEME suite tools[61], TOMTOM[89], and especially
678 using an analytic tool developed at EPFL (https://biss.epfl.ch) that uses FIMO[62] to identify
679 motifs on a sequence (Michael Frochaux, Dr.Bart Deplancke personal communication).
680 However, mutating sites identified by this initial round of analysis did not always result in GFP
681 reporter expression patterns that were consistent with our observations from the genetic
682 experiments as explained earlier. To remedy this, we employed a slightly different strategy to
683 identify all potential binding sites of Ey, Su(H), Slp1, and Scro. We searched for consensus

684 motifs of transcription factor binding sites for Ey, Su(H), Slp1 in JASPAR[90,91] and Fly Factor
685 Survey[92]. We then searched for potential matches to these consensus sequences in our
686 enhancers using the DNA Pattern Find program in Sequence Manipulation Tool[73]. Since
687 consensus motifs for binding sites of Scro were not reported in either JASPAR or Fly Factor
688 Survey, we picked 20 related transcription factors of the NK-domain TF family with known
689 binding motifs as templates for finding possible Scro binding sequences (NK2 TFs used are listed
690 in Figure3-figure supplement1). We looked for potential matches to these motifs within our
691 enhancers using the Pattern Recognition Tool of the Sequence Manipulation Suite. Sequences
692 that were most shared between the 20 NK domain containing TFs were scored as the most
693 likely motifs for Scro binding in the d5778 870bp enhancer. Given the smaller size of the u8772
694 220bp enhancer, only motifs corresponding to Vnd binding sites were mutated since Scro has
695 been suggested to share the greatest homology to Vnd of all NK domain containing TFs[63].

696 The consensus sequences we used for identifying binding sites for each of our candidate
697 regulators Ey, Su(H), and Scro in the DNA Pattern Recognition program are detailed in Figure 3.
698 Using this approach, we found additional potential binding sites for Ey and Su(H) than what
699 were predicted using FIMO. We noticed that predicted binding sites identified by FIMO such as
700 the 220-Ey-Site2, 850-Ey-Site1 and 850-Scro-Site 1 and 6, often had minor mismatches to the
701 consensus binding sequence used as input (for example, the 220-Ey-Site2 had two mismatches
702 to the consensus). Therefore, we also considered sites with a maximum of two mismatches to
703 our consensus sequences for the DNA Pattern Find program as potential binding sites for a
704 particular transcription factor. We detected such potential binding sites that deviated by at

705 most two base pairs from the consensus search sequence using less stringent pattern search
706 conditions in the DNA Pattern Find program.

707 To test this binding site search method's validity, we cloned custom gene blocks of enhancer
708 segments containing mutated binding sites for each transcription factor into the pJR12 vector.
709 We subsequently made transgenic flies expressing these 'mutant' reporters as described
710 elsewhere in Methods. All transgenes were inserted at the same chromosomal location as the
711 wild-type GFP reporters. Reporter GFP expressions driven by these mutation-carrying
712 enhancers were consistent with evidence from genetic experiments where wild-type GFP
713 reporter expressions were observed in Ey, Su(H), or Scro knockdown or loss of function clones,
714 thus demonstrating the reliability of this approach.

715

716 **Plasmids constructs and the making of transgenic fly stocks**

717 Primer sequences for all cloning are provided in a supplementary table (Supplementary Table
718 1).

719 For making all constructs DNA was amplified from the template using Expand High-Fidelity
720 Polymerase (Roche) unless stated otherwise and all constructs were verified by sequencing. All
721 fly embryo injections for making transgenic flies were carried out either by Bestgene Inc, Chino
722 Hills, CA or by Rainbow Transgenic Flies.

723 Generating constructs for reporter assays and enhancer bashing and making transgenic
724 reporter expressing stocks- Sequences corresponding to the fragments of regulatory DNA

725 encoded in GMR35H02 and the d5778 REDfly enhancer were cloned from the BAC clone CH321-
726 94O18[93] (BACPAC resources). Sequences were PCR amplified from this BAC and cloned into the
727 pJR12 vector (a kind gift from Dr. Jens Rister) between *AscI* and *NotI* sites. Transgenes were
728 inserted at the landing site VK00027 on the third chromosome (BL9744) by ϕC31 integrase
729 mediated transgenesis[94] and positive transformants were screened using the w+ marker
730 originally present in the pJR12 plasmid. Mutated enhancers were custom synthesized as gene
731 blocks (gBlocks, IDT DNA) (Supplementary Table 3) and cloned as stated above. Split gBlocks
732 were custom made for making the d5778 ey site mutant and the d5778 su(h) site mutants.
733 These split gBlocks were then PCR spliced and cloned between NotI and AscI sites of the pJR12
734 vector. A custom-made gBlock was used for making the d5778 scro mutant reporter. All
735 reporters were integrated at the same genomic site to ensure comparability across constructs
736 and experiments.

737 Generation of CRISPR enhancer deletion constructs and transgenic stocks- CRISPR gRNAs were
738 designed by entering sequences of genomic DNA of the target +/- 20 kbp into the CRISPR
739 Optimal Target Finder web utility [95] (https://www.targtfinder.flycrispr.neuro.brown.edu). Four
740 gRNAs-two upstream and two downstream of the target region to be deleted were then
741 selected. All four gRNAs were then cloned into the vector pCFD5[96] (Addgene plasmid #73914 a
742 kind gift from Dr. Simon Bullock) using NEB-Builder HiFi DNA Assembly master mix. Constructs
743 were then injected into fly strain containing *M{nos-cas9}ZH-2A* (BL54591) along with a 120 bp
744 repair oligonucleotide that contained 60bp of wild type genome sequence flanking both ends of
745 the expected double-stranded break. After injection, the *nos-cas9* source was eliminated in the
746 subsequent generations by crossing individual G0 progeny flies to a double balancer of

747 genotype *ywhsFlp; Sp/CyO; Tm2/Tm6B* and selecting male G1 progeny. Individual G1 males
748 were then crossed to the same double balancer line to create stocks. The G1 males were then
749 genotyped by PCR to identify whether their genome had been edited, using RedExtract-n-Amp
750 tissue PCR kit (Sigma-Aldrich). The G2 progeny of genome-edited males were then raised until
751 homozygous stocks were established. To delete both enhancers, gRNAs for the d5778 enhancer
752 was injected into a fly line carrying nos-Cas9 and deletion of the u8772 enhancer and
753 genotyped as previously. Genomic DNA from CRISPR-Cas9 edited flies was extracted using
754 Qiagen DNeasy Blood and Tissue kit according to the manufacturer's instructions. Fragments of
755 genomic DNA flanking the expected deletion sites were amplified by PCR using Platinum
756 SuperFi II PCR master mix (Invitrogen). They were then sequenced by Sanger sequencing to
757 confirm the outcome of the genome modification procedure. The deleted sequences are shown
758 in Supplementary file 1.

759

760 <u>Generation of the heat shock inducible NICD construct</u>: We modified the pJR12 vector used in
761 enhancer bashing experiments to replace the GFP coding sequence with coding sequences of
762 our interest. First, we generated a DNA fragment that matched the sequences of the pJR12
763 vector flanking the eGFP sequence but that did not contain the eGFP sequence itself by PCR
764 splicing. We then cut-out the eGFP segment from the pJR12 vector and replaced it with our GFP
765 deleted fragment using *NsiI* and *XhoI*. Next, an *FRT-stop-FRT3-FRT* segment was cloned from
766 the CoinFlp plasmid[97] (Addgene plasmid # 52889, a kind gift from Dr. Iswar Hariharan) and PCR
767 spliced with a fragment of Notch Intracellular Domain (NICD). Sequences corresponding to the
768 Notch Intracellular Domain were PCR amplified from Notch cDNA LD34134 (DGRC). The *FRT-*

769 *stop-FRT3-FRT-NICD* fragment was then cloned into the modified pJR12 vector between the
770 *PmeI* and *AgeI* restriction sites. The *deadpan* enhancer sequence amplified from the BAC clone
771 CH321-86A18 (BACPAC resources) was then cloned into the modified pJR12 vector to drive the
772 heat shock inducible NICD expressing construct in presence of a heat shock activated Flippase
773 or *hsFlp* (this construct is abbreviated as *dpn> hsNICD*). The construct was inserted at the
774 VK00027 landing site (BL 9744) by ϕC31 integrase mediated transgenesis. Positive
775 transformants were identified by the w+ eye color marker expression and stocks were created
776 by crossing to a double balancer of genotype *ywhsFlp; Sp/CyO; Tm2/Tm6B*.

777 Generation of DamID-fusion constructs (*UAS Dam-Ey* and *UAS-Dam-Su(H)*) and transgene
778 expressing stocks- Su(H) coding sequence was amplified from a cDNA clone GH10914 (DGRC) by
779 PCR. The amplified Su(H) coding sequence was cloned into the pUAST-Dam-attB vector[76] (a kind
780 gift from Dr. Andrea Brand) between the *NotI* and *XhoI* sites. A gBlock of Ey coding sequence
781 was ordered from IDT and cloned into the pUAST-LT3- UAS Dam- vector. Constructs were then
782 incorporated at the VK00027 landing site (BL 9744) by ϕC31 mediated integration.
783 Transformants were identified by expression of the w+ marker gene. Final stocks were
784 established by crossing to a double balancer line of genotype *ywhsFlp; Sp/CyO; Tm2/Tm6B*.

785 **Immunofluorescence staining**

786 Antibody staining was carried out as described in [18] with a few modifications. The protocol is
787 described briefly as follows: brains from climbing third instar larvae were dissected in 1XPBS
788 and fixed in 4% Formaldehyde solution in 1X PBS for 30 minutes on ice. Brains were then
789 incubated in primary antibody solution overnight at 4°C, washed three times for 30 minutes

790 each at 4°C, then incubated in fluor conjugated- secondary antibody solution overnight at 4°C
791 and then washed again thrice at room temperature each time for 30 minutes. Samples were
792 mounted in Slowfade Gold antifade reagent (Invitrogen). Images are acquired using a Zeiss
793 LSM500 Confocal Microscope.

794 Antibodies used in the study are as follows: rabbit anti-Slp1, guinea-pig anti-Slp2, rabbit anti-Ey
795 (all used at 1:500) were kind gifts from Dr. Claude Desplan, guinea-pig anti-Dpn (1:500) (a kind
796 gift from Dr. Chris Doe). Commercially available antibodies include - sheep anti-GFP (1:500,
797 AbD Serotec, 4745-1051), Chicken anti-beta-gal (1:500, Abcam ab9361), Rat anti-Deadpan
798 [11D1BC7] (1:200, Abcam, ab195173) mouse anti-PCNA (1:50, Abcam ab29). These antibodies
799 are provided by the Developmental Studies Hybridoma Bank (DSHB): mouse anti-eyeless (1:10),
800 mouse anti-Pros (MR1A 1:20). Secondary antibodies are from Jackson or Invitrogen.

801 **Fluorescence In situ hybridization (FISH)**

802 FISH was carried out using custom Stellaris probe sets (LGC Biosearch) as described in [98] except
803 that incubation with sodium borohydride was skipped. Probes were generated using the *slp1*
804 mRNA (Flybase annotation symbol CG16738-RA) and *slp2* mRNA (Flybase annotation symbol
805 CG2939-RA) as templates. Tiling probes for the *slp1* mRNA were conjugated to the fluorophore
806 Quasar 670 Dye, while probes for *slp2* mRNA were conjugated to the fluorophore Quasar 570
807 Dye. Concurrent FISH and immunofluorescence staining were carried out as described in the
808 same publication.

809 **DamID-Seq**

810 Flies of genotype *ywhsFlp; Sp/CyO; UAS-Dam/ Tm6B, ywhsFlp; Sp/CyO; UAS-Ey-Dam/ Tm6B* or
811 *ywhsFlp; Sp/CyO; UAS-Su(H)-Dam /Tm6B* were crossed with *UAS-Dcr2; tubGal80ts; SoxN-Gal4*.
812 Mating crosses were incubated at 25 °C. Eggs laid within an 8-hour window were then shifted to
813 18°C for three days until they hatched. The expressions of the Dam-fusion proteins were then
814 induced in larval brains by shifting the larvae to 29°C for 72 hours. Climbing third instar larvae
815 were then dissected. Only the optic lobes were used for further sample preparation. For each
816 sample around 100 brains were dissected.

817 Dam-ID libraries were made as described in [99]. Briefly, fly brains were dissected in 1X PBS and
818 genomic DNA was isolated using the QIAamp DNA Micro kit (Qiagen). Genomic DNA was then
819 digested with DpnI and purified using spin column purification (Qiagen PCR-purification kit). To
820 the DpnI digested DNA DamID-PCR adaptors were ligated. Subsequently the adaptor-ligated
821 DNA fragments were digested with DpnII. The DpnII digested genomic DNA fragments were
822 then amplified by PCR to enrich for bound GATC fragments. To make sequencing libraries the
823 PCR enriched genomic DNA sample was sonicated using a Bioruptor bath sonicator
824 (Diagenode), purified using AMPure XP beads, end-repaired and 3'-adenylated. Illumina
825 sequencing indexes were then ligated to these fragments. Index-labeled DNA fragments were
826 then further enriched by PCR amplification, checked for quality and fragment size distribution
827 on an Agilent Bioanalyzer and by qPCR (Quality control of all libraries was carried out at the
828 Functional Genomics Unit of Roy J. Carver Biotechnology Center, UIUC). Libraries that were
829 deemed acceptable were then sequenced on a single SP100 lane of an Illumina NovaSeq
830 sequencer. Read lengths were 100bp. Two Biological replicates of *Ey-Dam*, *Su(H)-Dam* and
831 *Dam*-only samples were sequenced, and each biological replicate is defined as one library

832 generated from ~100 dissected brains. The number of reads obtained were as follows: Dam
833 replicate1: 53745480 reads, Dam replicate 2: 85637355 reads, Ey-Dam replicate 1: 81121107
834 reads, Ey-Dam replicate 2: 82085708 reads, SuH-Dam replicate 1: 77448608 reads, replicate 2:
835 80015207 reads. All samples exhibited good QC scores.

836 **DamID-Seq data analysis**

837 DamID-seq data was analyzed using the damidseq-pipeline [100]. Duplicate samples of Ey-Dam
838 and Su(H)-Dam samples and Dam-only controls were aligned to the Drosophila reference
839 genome UCSC dm6. Alignment rate for individual samples were as follows:(Ey-Dam replicate 1-
840 97.04%, Ey-Dam replicate 2 -97.82%, Su(H)-Dam replicate 1- 97.91% and Su(H)-Dam replicate 2
841 – 97.82%. The main utility- the damid-seqpipeline was used to align reads to the genome using
842 bowtie2, bin and count reads, normalize counts and generate log-2 ratio bedgraph files for each
843 DamID-sample and its corresponding Dam-only control. The provided gatc.track file was used
844 for running the script. Next, the findpeaks utility was used with an F.D.R. <0.01 to identify
845 peaks. We then used the provided peaks2genes utility to assign peaks to genes. To assess the
846 reproducibility of our data we also ran the findpeaks script using F.D.R <0.1 to discover peaks
847 with weaker statistical confidence and used this as input for the I.D.R. Python package
848 (https://github.com/nboley/idr). 984 of 1810 (54.4.%) Ey-Dam and 972 of 1996 (48.7%) of
849 Su(H)-Dam peaks passed an I.D.R. threshold of 0.05. All replicate tracks for Ey and for Su(H) as
850 well as reproducible peaks identified using I.D.R. were visualized in IGV [101]. To generate the lists
851 of genes bound reproducibly by Ey or Su(H), files containing lists of peaks that had passed the
852 I.D.R. cutoff were processed using the peaks2genes utility provided along with the damidseq-

853 pipeline. Peaks were mapped to particular genes if they were within a 1000bp neighborhood of
854 the gene loci.

855 **Image quantification and statistical analysis.**

856 No statistical method was used to predetermine sample size. Sample size /replicate numbers
857 were decided based on the routine in the field and previous experience. All data were obtained
858 from at least two independent experiments. The numbers of animals or clones analyzed can be
859 found in figure legends or this section (see below). All data are highly reproducible. No outliers
860 are excluded. For specific quantification methods and statistical analysis see below.

861 Imaging and image analysis for comparison of wild-type and mutant GFP reporter intensities-
862 All images were acquired using a Zeiss LSM 500 confocal microscope. Samples were imaged at
863 sub-saturating illumination conditions, with stack intervals of 1 micron. Same laser settings and
864 imaging conditions were used across all variants of the same enhancers. Image analysis was
865 carried out using Fiji [102]. Signal intensities in the GFP and the Dpn channels were measured over
866 a small rectangular selection for all variants. For the same enhancer a 'scaling factor' was
867 calculated for each mutant by dividing the Dpn channel intensity for the mutant reporter by the
868 channel intensity of the corresponding wild-type reporter. The GFP channel intensities for each
869 variant were then multiplied by this scaling factor. Finally, a ratio of the scaled GFP channel
870 intensity to the Dpn channel intensity was calculated for each GFP reporter variant. Ratios of
871 scaled GFP/Dpn intensities were then plotted using GraphPad Prism. For each enhancer,
872 Ordinary One-way ANOVA and Dunnett's multiple comparisons test were carried out between
873 reporter variants of the same enhancer. For the d5778 870bp enhancer, five sets of data from

874 twenty different optic lobes were acquired for each enhancer (one set- wild type and all
875 mutant variations all imaged using the same conditions). For the u8772 220bp enhancer three
876 sets of data were used for quantification. For the *UAS-GFP-RNA*i; d5778 850- Su(H) binding sites
877 mutants crossed with *Repo-Gal4*, three sets of data were used for quantification.

878 Image analysis for CRISPR enhancer deletion experiments- All images were acquired using a
879 Zeiss LSM 500 confocal microscope under sub-saturating illumination conditions. For each
880 sample width of Slp1, Slp2 and Dpn expression domains were measured in Fiji at five different
881 locations and averaged. The brain size of the sample was estimated by measuring the length of
882 the brain at its widest point perpendicular to the neuroblast division axis. The width of each
883 protein expression domain was divided by the brain size to normalize expression domain size
884 estimates to the brain size. For each protein Slp1, Slp2 and Dpn- these ratios were then plotted
885 in GraphPad Prism and ordinary one way ANOVA and Dunnett's multiple comparisons tests
886 were carried out between wild-type and CRISPR enhancer deleted brains. Data from seven
887 brains of each genotype was analyzed and quantified.

888 All images were processed in Adobe Photoshop and assembled using Adobe Illustrator.

889 Data Availability

890 The raw and processed DamID-seq data have been deposited to GEO, and the accession
891 number is GSE188643 (reviewer's token qncnwyyidtsndcp).

892 Acknowledgments

893 We thank the Functional Genomics Unit and the DNA-Sequencing Services Unit of the Roy J.
894 Carver Biotechnology Center at the University of Illinois at Urbana-Champaign for assistance
895 with the quality control and sequencing of Dam-ID sequencing libraries. We thank the fly
896 community, especially Claude Desplan, Andrea Brand, Chris Doe, Bruce Edgar, Kenneth Irvine,
897 Miki Fujioka and James B. Jaynes for generous gifts of antibodies and fly stocks. We are grateful
898 to Bart Deplancke's team for help with the YIH pipeline to predict transcription factor binding
899 sites within enhancers. We thank the Bloomington Drosophila Stock Center, the Vienna
900 Drosophila RNAi Center, the Developmental Studies Hybridoma Bank, and TriP at Harvard
901 Medical School (NIH/NIGMS R01-GM084947) for fly stocks and reagents. We thank members of
902 the Li lab Dr. Yu Zhang and Hailun Zhu for helpful discussions. This work was supported by the
903 National Eye Institute (Grant 1 R01 EY026965-01A1) and start-up funds from the University of
904 Illinois at Urbana-Champaign.

905 **Competing interests.**

906 The authors declare no competing or financial interests.

907 **Materials & Correspondence.** Publicly available fly lines (those from BDSC or VDRC) should be
908 requested directly from the corresponding stock centers: https://bdsc.indiana.edu/ or
909 https://stockcenter.vdrc.at/control/main. Fly lines generated in this study can be requested
910 without restriction. Correspondence and requests for materials should be addressed to Xin Li
911 (lixin@illinois.edu).

912

Figure legends:

Figure 1. Expression of *slp1* and *slp2* genes in medulla neuroblasts is controlled at transcription. (A) Schematic of *Drosophila* brain at the third instar larval stage highlighting the location of the optic lobe medulla. Medulla NBs (shown as circles), located on the surface of the optic lobe, are transformed from neuroepithelial cells (NE) as a neurogenesis wave spreads in a medial to lateral direction. As a result, medulla NBs of different ages are aligned on the lateral (L) to medial (M) spatial axis. Schematic to the right shows part of the temporal patterning program of medulla NBs with a focus on the Ey to Slp1/2 transition. NBs undergo asymmetric divisions to self-renew and to produce intermediate progenitors called Ganglion Mother Cells that each divide once to produce two neurons. In the Ey stage, NBs undergo a few divisions while gradually activating Slp expression resulting in a significant overlap between Ey and Slp expression in NBs. After Slp level reaches a certain threshold Ey expression is down-regulated and eventually deactivated completely. This process repeats as subsequent temporal patterning factors are activated and earlier factors down-regulated over several neuroblast division cycles. After several temporal stages that are not shown here indicated by the dashed arrow, neuroblasts express TTF Gcm and exit the cell cycle. The larval brain graphic was created using BioRender. (B-B’’’) Expression patterns of endogenous Slp1 and Slp2 proteins in medulla neuroblasts identified by their expression of Deadpan (Dpn) a neuroblast marker. (C-C’’’) Expression patterns of Slp1 and Slp2 mRNAs in Dpn expressing medulla neuroblasts closely parallels the corresponding protein expression patterns. (D-D’’’’) Detection of *slp2* mRNA and Slp2 protein in the same brain shows spatial co-localization of *slp2* transcripts and Slp2 protein in the same neuroblasts. Two distinct neuroblasts indicated by arrowheads shown for emphasis. These cells express the neuroblast marker Dpn (D, D’’’’) and Slp2 in the nucleus and the *slp2* mRNA is localized to the cytoplasm. Scale bar for panels (B-B’’’) and (C-C’’’): 20 microns. Scale bar for (D-D’’’’) 6 microns.

Figure 2. Transcription of *slp1* and *slp2* in medulla neuroblasts is regulated by two enhancers of lengths 220bp and 850bp respectively. (A) A schematic of the enhancer screening. *slp1* and *slp2* genes and transcriptional enhancers identified as regulating their expression are shown as black and grey boxes, respectively. Positions of slp1 coding locus (2L:3,825,675..3,827,099 [+]), slp2 coding locus (2L:3,836,840..3,839,185 [+]), GMR35H02 (2L:3,817,265..3,821,014) and the REDfly enhancers u8772 (2L:3,816,967..3,818,532) and d5778 (2L:3,842,530..3,844,660) are shown relative to one another. A 220 bp enhancer located within the genomic segment covered by GMR35H02 and an 850 base pair enhancer element within the REDFly enhancer d5778 were identified as potential cis-regulatory elements of *slp1* and *slp2* genes. The distance between the start of GMR35H02 and the end of d5778 is around 27.394 kbp. Other fragments that were screened /cloned are shown as black bars with names on top. (B-B’’’) A 220bp enhancer element located within the REDfly enhancer u8772 activates GFP expression in medulla neuroblasts in the same pattern as endogenous Slp1 and Slp2 in reporter assays. (C-C’’’) Reporter GFP expression driven by an 850-bp enhancer segment located within the REDfly enhancer d5778 also closely coincides with the expressions of endogenous Slp1 and Slp2, although it is initiated at a slightly later temporal stage than the 220bp enhancer. (D-D’’’’) A CRISPR-Cas9 edited chromosome 2 with both enhancers deleted (indicated as Slp^{DED}) when placed over the Slp^{S37A} chromosome results in loss of Slp1 and Slp2 expression in medulla

neuroblasts in affected flies (n=11). The effect is confined to neuroblasts, as Slp2 expression is retained in both lamina (la) and in surface glial cells (arrows), and Slp1 is also seen in laminar cells. This also confirms that coding sequences of *slp1* and *slp2* genes are unaffected by the CRISPR-Cas9 editing procedure. Control experiments where Slp^{DED} was placed against a wild type chromosome 2 (indicated by '+') (E-E'''') (n=9) and where the Slp^{S37A} chromosome was placed against a wild type chromosome 2 (F-F'''')(n=11) show normal expression of Slp1 and Slp2 in medulla neuroblasts. Scale bars 20 microns.

Figure 2—figure supplement 1. The identification of the 220bp enhancer by promoter bashing. (A-A''') UAS-GFP driven by GMR35H02-Gal4 is initiated at the same time as endogenous Slp1 and Slp2 in neuroblasts marked by Dpn. (B-D'') Expression of GFP reporters driven by SlpL1.5 (B-B'') and its sub-segments Slpf1-220bp(C-C''), Slpf2-592bp (D-D''), and Slpf3-123bp (E-E''). Of the three sub-segments of SlpL1.5, only the Slpf1 fragment (220bp in size) shows enhancer activity. Scale bars 20 microns.

Figure 2—figure supplement 2. The two enhancers act partially redundantly. CRISPR-Cas9 deletions of the u8772 enhancer (A-A''') and the d5778 enhancer (B-B''') individually do not abolish Slp1/2 expression suggesting possible redundance. Scale bars: 20 microns. (C) Middle panel: comparison of widths of expression domains normalized to brain size for Slp1 in wild type and enhancer deleted brains. P value of ordinary one way ANOVA is < 0.0001 and is statistically significant because p <0.05. Adjusted p values from Dunnett's multiple comparison test between wild type and the u8772 220bp enhancer deletion is 0.0041, between wild type and d5778 850bp enhancer deletion is 0.0187. Both are statistically significant since p<0.05. Data from seven brains of each genotype are quantified (n=7). Right panel: expression domain width normalized to brain size for Slp2 compared between wild type and enhancer deleted brains shows no statistically significant differences relative to wild type (Adjusted p values from Dunnett's multiple comparison test relative to wild type are as follows: for u8772 220bp enhancer deletion p=0.0730, for d5778 850bp enhancer deletion p= 0.0965. Neither are statistically significant since p>0.05). The difference between u8772 deletion and d5778 deletion is significant (p value from ordinary one way ANOVA =0.0019, statistically significant because p<0.05). Data from seven brains of each genotype are quantified (n=7). Left panel: expression domain width normalized to brain size for Dpn also shows no significant differences between wild type and enhancer deletion mutants (p value from ordinary one-way ANOVA is 0.5277 and is >0.05, hence not statistically significant. Adjusted p values from Dunnett's multiple comparisons test between enhancer deletion mutants and the wild type are as follows: for the u8772 220bp enhancer deletion p=0.6310, for the d5778 850bp enhancer deletion p=0.9414. Neither are statistically significant being >0.05.) Data from seven brains of each genotype are quantified (n=7). This shows that deletion of the enhancers doesn't affect Dpn expression.

Figure 2—figure supplement 3. Screen of REDfly enhancers identifies d5778 as an enhancer of slp1/2 transcription in medulla neuroblasts. (A-R'') Results of the screen showing lacZ reporter expressions driven by REDfly enhancers. Of the reporters tested, u8772 (A-A'') and u8781 (B-B'') recapitulated the expression patterns driven by the previously identified 220bp slp enhancer, thereby supporting our findings. Both u8772 and u8781 contain within them the 220

bp enhancer element. Additionally, patterns of lacZ expression driven by u8166 (D-D'') and u5547 (F-F'') are also interesting in that they somewhat overlap with the expression of endogenous Slp2. However, the u5547 enhancer was contained within the GMR35H02 sequence, and enhancer bashing experiments encoding this part of GMR35H02 did not show reporter expression. The u8166 line drove reporter expression primarily in neurons than in neuroblasts. For these reasons, the u5547 and u8166 enhancers were not considered for further analysis. However, the screen of REDfly enhancers identified d5778 as a potential enhancer of slp1 and slp2 transcription since it drove reporter expression in neuroblasts in a pattern overlapping endogenous Slp2 (Q-Q''). Scale bars 20 microns.

Figure 2—figure supplement 4. The d5778 850bp enhancer drives reporter expression predominantly in neuroblasts. (A-A''') The d5778 850 bp enhancer is activated slightly after the initiation of Slp2 expression. The wild type d5778 850bp reporter drives GFP expression (A') predominantly in neuroblasts identifiable by their expression of the neuroblast marker Dpn (A''''). Slp2 is expressed in some surface glial cells expressing the marker Repo (A, A'', A'''). (B-B'''') Neuroblast specific suppression of 850bp reporter GFP expression by GFP-RNAi results in no visible GFP signals from neuroblasts. (C-C'''') Glial specific suppression of 850 bp reporter GFP by GFP-RNAi preserves GFP expression in neuroblasts and establishes that the d5778 enhancer is indeed prominently active in medulla neuroblasts. Scale bars: 20 microns.

Figure 3. Predicted binding sites for Ey, Su(H), Scro, and Slp1 in the two enhancers. (A-D) Position weight matrix of for Ey (A), Su(H) (B), Scro /Vnd (C) and Slp1 (D) from Fly Factor Survey, JASPAR and literature are considered together to make a consensus sequence. Arrows of different colors are underlying these consensus binding sites. Critical invariant bases are in bold. Grey boxes indicate the corresponding positions of the Position weight matrix from two sources. (E,F) Predicted binding sites for Ey, Su(H), Scro, and Slp1 in the 220bp enhancer (E) and 850bp enhancer (F). Arrows are color coded as in (A-D). Right-pointing arrow indicates the binding site is on direct strand, while left-pointing arrow indicated the binding site is on reverse strand. Star* indicates that the binding site is also predicted by the FIMO pipeline.

Figure 3—figure supplement 1. NK-2 family transcription factors with known binding consensus motifs were used to identify potential Scro binding sites in the d5778 850bp enhancer. The transcription factor is listed in the column to the left. Its position weight matrix, either from JASPAR or Fly Factor Survey, is shown in the column in the middle. The consensus binding motif of the transcription factor inferred from the position weight matrix and used as input for the Sequence Manipulation Suite DNA Pattern Find program is listed in the column on the right.

Figure 4. The Notch pathway regulates expression of *slp* genes in medulla neuroblasts. White arrow to the right indicates the neuroblast age from young to old. All clones are generated with *ay-Gal4 UAS-GFP* and clone boundaries are shown in dotted lines. The dash-dotted lines indicate where Slp2 should be turned on, and the curvature is due to the curvature of the Dpn initiation. (A) RNAi knockdown of Notch in GFP marked clones leads to a delay in expression of Slp2 compared to contemporaneous wild type neuroblasts outside the GFP marked clones. While in wild-type brains Slp2 expression is seen in the 4th-5th neuroblast from the lateral edge of the medulla, inside *N-RNAi* clones Slp2 expression is first noted in the 10th -15th neuroblast

(n=12 clones). (B) In *Su(H) RNAi* clones marked by GFP, Slp2 expression begins at the 7th-10th neuroblast (n=11 clones). (C) In clones expressing the dominant negative mutant variant of Mastermind, Slp2 expression is also delayed and start at the 7th-10th neuroblasts (n= 6 clones) (D) Knockdown of Dl, a Notch ligand, caused a similar delay in Slp2 expression, with Slp2 expression being initiated at the 6th to 10th NB (n=5 clones). Clonal data from at least 3 brains were observed for each mutant to infer delay in Slp2 expression initiation. Scale bar 20 microns.

Figure 5. Genetic interactions between Notch, Ey and Scro in the regulation of Slp expression. In all panels, dotted lines outline clone margins. Dash-dotted lines mark the expected transition front for Dpn or TTFs (white for Dpn, pink for Ey, cyan for Slp2, and yellow for D). The curvature of the dash-dotted lines is determined by the curvature of Dpn or the previous TTF. (A1-A8) In N-RNAi clones marked by GFP in green, Ey is turned on in the 5th-8th NB (6.50±1.05, n=6), and the transition to Slp stage occurs in the 6th -9th Ey+ NB (7.67±1.21, n=6). In control regions (not marked by GFP), Ey is turned on in the 2nd -3rd NB (2.50±0.55, n=6), and the transition to Slp stage occurs on the 3rd -4th Ey+ NB (3.83±0.41, n=6). The delay of Ey expression and the further delay of Slp transition are significant by t-test ($p=4.8x10^{-5}$, and p=0.0003, respectively). (B-B'''') In *Su(H)*^{47} mutant clones marked by GFP, Ey expression is delayed and the transition to Slp stage is further delayed: Slp2 is still barely detectable or very weak at the 6th -8th Ey+ NBs (6.80±0.84, n=5). In control regions, the transition to Slp2 stage occurs in the 4th Ey+ NBs (n=5). The further delay of Ey to Slp transition is significant by t-test (p=0.002). (C-C'') Magnified view of the rectangle area containing three clones shown in B. (D-D'''') In *Su(H)*^{47} mutant clones over-expressing Ey, the transition to Slp2 stage is still delayed to the 6th-7th Ey+ NBs (6.40± 0.55, n=5). In control regions, the transition occurs in the 3rd-4th Ey+ NBs (3.80±0.45, n=5), The further delay of Ey to Slp transition is significant by t-test ($p=4.50x10^{-5}$). (E-E") Magnified view of the rectangle area containing one clone shown in D. (F-H') The expression of Ey and Slp2 (F-F''), Dichaete and Dpn (G-G''), and BarH-1 (H,H') in *Su(H)*-RNAi clones marked by GFP. (I-I'') Supplying active NICD using *hsFlp; dpn>FRT-STOP-FRT-NICD* (heat shocked for 40min 3 days before dissection) is not sufficient to activate Slp2 expression in Ey-RNAi clones marked by bGal. (J-J'''') Supplying Scro is not sufficient to activate Slp2 expression in Ey-RNAi clones marked by GFP. Scale bars 20 microns.

Figure 5—figure supplement 1. Notch signaling is also involved in early temporal transitions. (A-A'''') SoxN expression is not significantly affected in Su(H)RNAi clones marked by GFP. (B-B'''') The TTF Opa is expressed at two different 'stripes'. The earlier expression stripe is expanded in width within Su(H) RNAi clones, while Opa expression in the second stripe in older neuroblasts is delayed. (C-C'''') Expression of Ey is delayed in Su(H) RNAi clones. Representative images of at least four brains are shown. Scale bars 20 microns.

Figure 6. Eyeless and the Notch pathway act through the 220 bp and 850 bp enhancers to regulate expression of *slp* genes. (Panels A-A''' through D-D'''') RNAi clones in which Ey or Su(H) is knocked down are marked by *Beta-galactosidase* (*bGal*) in blue, while regions unmarked by *bGal* are populated by wild type neuroblasts. (A-A'''') The expression of a GFP reporter driven by the 220 bp enhancer and endogenous Slp2 in *ey RNAi* clones and wild type neuroblasts. Expressions of both the GFP reporter and endogenous Slp2 are similarly abolished in *ey* knockdown clones (representative data shown, n=5 brains). (B-B'''') The expression of a GFP

reporter driven by the d5778 850 bp enhancer and endogenous Slp2 in *ey RNAi* knockdown clones and in wild type neuroblasts. Knockdown of Ey leads to loss of both the GFP reporter expression and the endogenous Slp2 protein (representative data shown, n=15 brains). (C-C''') The expression of the GFP reporter driven by 220bp enhancer and endogenous Slp2 in *Su(H) RNAi* clones and in wild type neuroblasts (representative data shown, n=11 brains). (D-D''') The expression of the GFP reporter driven by 850bp enhancer and of endogenous Slp2 in *Su(H) RNAi* clones and in wild type neuroblasts (representative data shown, n=14 brains). In case of both enhancers the expression of the GFP reporter is lost or delayed. (E, E') The expression of the 220 bp GFP reporter in *slp1* and *slp2* loss of function mitotic clones ('dark' regions) and in wild type neuroblasts (marked by RFP) (representative data shown, n=24 brains). (F,F') Expression of the 850 bp enhancer GFP reporter in *slp* LOF clones and wild type neuroblasts similar to (E,E') (representative data shown, n=16 brains). Slp1 binding sites were identified in both enhancer elements which indicate that Slp1 may auto-regulate its expression. However, GFP reporter expression driven by these two enhancers is not significantly affected within *slp* LOF neuroblasts, suggesting that Slp1/2 are not required to initiate their own expression in neuroblasts. Representative images are provided. Scale bar 20 microns.

Figure 7. Mutations of predicted binding sites for transcription factors Ey, Su(H) and Scro in the u8772 220 bp enhancer establish their requirement for activating *slp1/slp2* mRNA transcription in medulla neuroblasts. Expression of GFP reporter driven by the wild-type 220 bp enhancer (A-A''') was compared against GFP reporters driven by mutated versions of the 220 bp enhancer in which predicted binding sites for specific transcription factors had been mutated: (B-B''') with a predicted site for Ey binding (220-Ey-site1 in Table 2) deleted, (C-C''') with a different predicted site for Ey binding (site 220-Ey-Site2 in Table 2) mutated, (D-D''') with four predicted Su(H) binding sites mutated (sites 220-SuH-Site1 to 4), (E-E''') with two Su(H) binding sites mutated (sites 220-SuH-Site1 and 220-SuH-Site4 in Table 2), (F-F''') with a predicted site for Scro binding mutated (220-Scro-Site1 in Table 2), (G-G''') with two predicted Slp1 binding sites mutated (sites 220-Slp1-Site1 and 220-Slp1-Site2). Loss of binding sites for Ey, Su(H) and Scro in the 220 bp enhancer led to a loss or reduction of GFP reporter expression. Scale bar: 20 microns. (H) Intensity comparisons of mutated and wild type GFP reporters of the u8772 220bp enhancer. The decrease in intensity of GFP expression for Ey , Scro, Su(H) and Slp1 binding site mutated reporters relative to wild type are all statistically significant. Ordinary one way ANOVA was performed to determine statistical significance between the wild type and the mutated enhancer variants. The differences in GFP expressions were statistically significant for all enhancer variants relative to the wild type enhancer. Adjusted p values from Dunnett's multiple comparisons test between wild type and mutants are as follows: for both Ey site mutants, the 220-Scro-1m mutant, and the 220-Slp-1m2m, p values were <0.0001. For the 220-SuH-1-4m, p value was also <0.0001, but for the 220-SuH-1m4m the p value was 0.0001. 3 different sets of observations were used for analyses (n=3). The graph shows the distribution of individual observations about the median and within 95% confidence intervals.

Figure 7—figure supplement 1. Deletion of one Su(H) site identified by FIMO in the u8772 220bp enhancer GFP reporter does not abolish GFP expression. Deletion of the 220-Su(H)-site1 in the u8772 220bp enhancer (B-B'') did not change the intensity of GFP reporter expression compared to wild type u8772 220bp GFP reporter (A-A'').

Figure 8. Mutations of putative binding sites for Ey and Scro in the d5778 850bp enhancer show their requirement for activating Slp1/Slp2 gene expressions in medulla neuroblasts. A parallel comparison was made for GFP reporter expression driven by the wild type 850 bp enhancer (A-A''') to the GFP reporter expression driven by versions of the 850 bp enhancer with binding sites for specific transcription factors Scro, Ey, and Slp1 mutated (B-B''', C-C''', and D-D''' respectively). For the Ey site mutant 850-Ey-1m2d3d shown in (B-B''') three potential binding sites for Ey were mutated (850-Ey-Site1 in Table 2 was mutated as indicated, 850-Ey-Site2 and 850-Ey-Site3 were deleted). For the Scro sites mutant 850-Scro-1-7d, seven of the potential Scro binding sites (850-Scro-Site1 through 850-Scro-Site7 in Table 2) were deleted. Loss of binding sites for Ey obliterated GFP reporter expression in neuroblasts, while loss of potential Scro binding sites resulted in a noticeable reduction of GFP expression from the d5778 850bp reporter. (E) Quantitation of d5778 850bp reporter intensities of the wild type and the factor binding site mutated variants shows that the reduction of GFP intensity compared to wild type for Ey binding site and Scro binding site mutated reporters is statistically significant. Scale bars: 20 microns. Ordinary one way ANOVA was performed to compare differences in GFP expression between the wild type d5778 850bp enhancer and the transcription factor binding site mutants. Adjusted p values from Dunnett's multiple comparisons test between the wild type d5778 850bp enhancer and both the Ey and Scro sites mutants were less than 0.0001. Five different sets of observations were used for analyses (n=5). The graph shows the distribution of individual observations about the median and within 95% confidence intervals.

Figure 9. Mutation of potential Su(H) binding sites in the d5778 850bp enhancer does not decrease GFP reporter expression in neuroblasts. To measure GFP intensities in medulla neuroblasts unimpeded by GFP fluorescence from glial cells, *UAS-GFP-RNAi; d5778 850 bp >GFP* wild type reporter or *UAS-GFP-RNAi; d5778 850 Su(H) binding site mutant GFP* reporters were mated with a *UAS-Dcr2; Repo-Gal4* expressing line, and phenotypes in the resulting progeny were observed. Mutation of four Su(H) binding sites in the 850-SuH-1m2m3m6m mutant (B-B''') and all six possible Su(H) binding sites in the 850-SuH-1-6m mutant (C-C''') showed no loss of GFP expression relative to the wild type d5778 850bp GFP reporter (A-A'''). Instead, GFP expression was upregulated in Su(H) site mutants of the d5778 850bp reporter. This indicates that Su(H) does not activate *slp1/slp2* expression through the d5778 850bp enhancer directly. Scale bars: 20 microns. (D) Three sets of observations were used for statistical analyses (n=3). Ordinary one-way ANOVA was used to compare relative GFP intensities between Su(H) site mutants and the wild type d5778 850bp enhancer. Adjusted p values by Dunnett's multiple comparisons test between the wild type d5778 850bp reporter and the Su(H) site mutant reporters are as follows: for the 850-SuH-1m2m3m6m reporter p= 0.0019, and the 850-SuH-1-

6m reporter is p=0.0005. Difference of means of each sample relative to wild type are statistically significant as p<0.005, below the significance threshold of p<0.05. The graph shows the distribution of individual observations about the median and within 95% confidence intervals.

Figure 9 —figure supplement 1. Mutation of Su(H) binding sites in the d5778 850bp enhancer causes intensified GFP expression in glia. (A-A''') The expression of 850-SuH-1-6m mutant reporter is very strong in glial cells marked by Repo, preventing us to assess the expression in neuroblasts (marked by Dpn). The 850-SuH-1m2m3m6m mutant reporter has a similar pattern (not shown). Arrows point to examples of cell bodies of glia marked by Repo. Scale bars 20 microns.

Figure 10. DamID-seq demonstrates reproducible binding of Ey and Su(H) to the *slp1/2* enhancers *in vivo*. Prominent reproducible peaks of Ey and Su(H) binding are seen in neighborhood of the *slp1* and *slp2* gene loci including at the genomic locations of identified 220bp and 850 bp enhancers in both replicates of Ey-Dam and Su(H)-Dam experiments. Peaks at the u8772 220bp and the d5778 850bp enhancers have passed IDR< 0.05 cut-off supporting their reproducibility.

Figure 10 —figure supplement 1. **Examples of DamID-seq profiles on selected genes**. The IDR tracks are showing peaks that have passed the IDR< 0.05 cut-off. (A) IDR Peaks for Ey but not Su(H) are observed in the vicinity of the *scro* gene locus. (B) IDR Peaks for Ey but not Su(H) are observed within the intron of *Hmx* gene locus. (C) IDR Peaks for Su(H) but not Ey are observed in the *dll* gene locus.

Figure 11. Cell cycle progression is required for the precise timing of Slp expression and this is mediated in part through Notch signaling. (A-A''') The expression of PCNA, Dpn (red) and E(spl)mγGFP (cyan) in *vsx-Gal4* driving *UAS-DCR2* and *UAS-PCNA-RNAi* (VDRC51253) optic lobes (n=5). The affected region is indicated by loss of PCNA staining. (B-B''') The expression of Dpn and SoxN in *vsx-Gal4* driving *UAS-DCR2* and *UAS-PCNA-RNAi* optic lobes (n=5). (C-D''') The expression of Dpn, Ey and Slp2 in *vsx-Gal4* driving *UAS-DCR2* and *UAS-PCNA-RNAi* optic lobes (n=9) showing the surface neuroblast layer view (C-C'''') and the deep progeny layer view (D-D''') of the same brain. (C-C'''') In affected region marked by loss of PCNA staining, Ey expression is reduced and Slp2 expression is lost in Dpn+ neuroblasts. Some glia express Slp2 but not Dpn are indicated by white arrows. (D-D''') Dpn expressing neuroblasts are observed in deep layers in the affected region, but they don't express Ey or Slp2. (E-E''') Larvae of genotype *ywhsFLP; ay-Gal4 UAS-GFP /UAS-PCNA-RNAi; UAS-DCR2/+* were heat shocked at 37C for 8min 70 hours before dissection at 3rd instar larval stage. Ey expression (blue) is minimally affected in clones marked by GFP (green), while Slp2 (red) expression is delayed (n=17 clones). (F-F'') Magnified view of the boxed region in E'''. (G-G''') Larvae of genotype *ywhsFLP; ay-Gal4 UA-SGFP /UAS-PCNA-RNAi; UAS-DCR2/dpn>FRT-STOP-FRT-NICD* were heat shocked at 37C for 8min 70 hours before dissection at 3rd instar larval stage. Ey expression (blue) is minimally affected in clones marked by GFP (green), while Slp2 (red) expression initiation is rescued (n=10 clones). (H-H'') Magnified view of the boxed region in G'''. (I-J''') The expression of Ey, Slp2 and Dpn in *ywhsFLP; dpn>FRT-STOP-FRT-NICD* (I-I''') and *yw* control (J-J''') optic lobes (n=5 each) (heat shocked 37C for 8min 70 hours before dissection). Scale bars 20 microns.

Figure 11--figure supplement 1. Cell cycle progression is required for the temporal cascade progression. (A-A''') Larvae of genotype *ywhsFLP; ay-Gal4 UAS-GFP /+; UAS-DCR2/UAS-stgRNAi* (VDRC 17760) were heat shocked at 37C for 8min 70 hours before dissection at 3rd instar larval stage. Exd expression (co-factor of Hth, and always expressed in the same pattern) is normal in clones marked by GFP (gray), Ey expression is slightly delayed, while Slp2 expression is severely delayed (11 clones). (B-B''') Magnified view of the boxed region in A''''. (C-C'''') Larvae of genotype *ywhsFLP; ay-Gal4 UAS-GFP /+; UAS-DCR2/UAS-Dap* (BDSC 83338) were heat shocked at 37C for 8min 70 hours before dissection at 3rd instar larval stage. Exd expression is normal in clones marked by GFP (gray), Ey expression is slightly delayed, while Slp2 expression is severely delayed (8 clones). (D-D'') Magnified view of the boxed region in C''''.

Figure 12. A coordinated action of temporal patterning factors Eyeless (Ey) and Scarecrow (Scro) and the Notch signaling pathway regulates the expressions of Slp1 and Slp2 in medulla neuroblasts. (A) A schematic summarizing the main findings of this study. In medulla neuroblasts, transcription of the *slp1* and *slp2* genes is regulated by other temporal patterning factors Ey and Scro and by the Notch pathway. Ey and Scro both activate *slp1/2* transcription by binding to the identified enhancers u8772 220bp and d5778 850bp. Su(H) activates slp1/2 transcription by binding to the u8772 220bp enhancer. (B) The cell cycle in neuroblasts is required for continued activation of Notch signaling in medulla neuroblasts. We show that the cell cycle influences expression of *slp1* and *slp2* genes via its effects on the Notch signaling pathway; Slp1/2 expression is lost in cell cycle arrested neuroblasts due to a failure of Notch signaling. Restoration of Notch signaling rescues Slp1/2 expression in cell cycle arrested neuroblasts. Cellular processes like the neuroblast cell cycle cooperate with temporal patterning and Notch signaling to attain precise developmental outcomes. Graphic A created using BioRender.

Table 1. Fragments screened or cloned for identifying enhancers of *slp1/2* transcription in medulla neuroblasts. Table summarizing names and chromosomal locations of enhancer fragments screened or cloned. Those with names beginning with GMR are Janelia FlyLight Gal4 lines. Enhancer fragments with names beginning in u, i, or d are enhancers from the study (Fujioka and Jaynes 2012).

Screened fragments	**Start base**	**End base**	**Expression in medulla neuroblasts**
GMR35H02	3817265	3821014	Yes
GMR79H09	3830094	3833128	No
GMR35G02	3821714	3825360	No
GMR79H08	3832497	3833703	No
u8772	3816967	3818532	Yes
u8781	3816967	3817608	Yes
u8172	3817605	3818532	No
u8166	3817605	3819171	Mainly in neurons
u5534	3820168	3822240	unspecific broad expression
u5547	3820168	3821009	weak expression
u3925	3821751	3823158	No
u3725	3822001	3823158	No
u2316	3823356	3824032	No
u1609	3824033	3824739	No
i1523	3827196	3827972	No
i2330	3827970	3828686	No
i4053	3829629	3830998	No
i4060	3829629	3831819	No
i5882	3831440	3833928	No
d2445	3839285	3841364	No
d5778	3842530	3844660	Yes
d6383	3843114	3845187	No
Cloned fragments	**Start base**	**End base**	**Expression in medulla neuroblasts**
35H02-L1.5	3817261	3818808	Yes
35H02-M1.0	3818785	3819757	No
35H02-R2.2	3818872	3821014	No
slpf1-220bp (u8772 220bp)	3817298	3817517	Yes
slpf2-592bp	3817782	3818373	No
slpf3-123bp	3818686	3818808	No
d5778 850bp	3842770	3843619	Yes

Table 2. List of predicted binding sites and mutagenesis strategy. Sequences of 21bp fragments including the underlined binding sites are shown. The critical invariant bases are in bold. For sites on the reverse strand (-), the reserve strand sequence is shown. For deletions, all 21bps are deleted. Mutated bases are shown as lower-case letters. * indicates that the binding site is predicted by the FIMO pipeline.

Site Name	Strand	Original Sequence	Mutate to	Constructs (Size in bp)
220-Ey-Site1	+	TAATTC**C**GTT**T**A**A**A**TG**ATTTC	Deleted	220-Ey-1d (199 bp)
220-Ey-Site2*	-	TTTTCA**C**GGC**T**C**A**G**TG**GCCTT	TTTTCACGGCTatGTGGCCTT	220-Ey-2m (220 bp)
220-SuH-Site1*	+	GGTGAGCGATAG**TT**TT**CA**CAT	GGTGAGCGActaggagacgAT	220-SuH-1d has the first site deleted.
220-SuH-Site2	+	TTTGAGC**TT**TG**CA**CGTAATCA	TTTGAGCTTaGactGTAATCA	220-SuH-1-4m (220 bp) has all four sites mutated.
220-SuH-Site3	-	AAATTCA**TT**TC**CA**CTTGATTA	AAATcCAcTTCCACTTGATTA	
220-SuH-Site4	-	CTGATAT**TT**TT**CA**CGGCTCAG	CTGActcgcTTtACGGCTCAG	220-SuH-1m4m (220 bp) has site 1 and site 4 mutated.
220-Scro-Site1	+	CACGTAA**T**C**AAG**TGGAAATGA	CACGTAATCgtGTGGAAATGA	220-Scro-1m (220bp)
220-Slp1-Site1	+	TTCACA**TGTT**TTGTTCGAGCA	TTCACATGTaccaagCGAGCA	220-Slp1-1m2m has both sites mutated (220 bp)
220-Slp1-Site2	-	CTCTTG**TGTT**GGTCAAATTCA	CTCTTGgagTcGatcAATTCA	
850-Ey-Site1*	+	TTGTGC**C**CTG**T**GTG**TG**TGAAA	aTGTGgCtTGTGTGTGTGAAA	850-Ey-1m2d3d has site 1 mutated, and sites 2 and 3 deleted (808 bp).
850-Ey-Site2	+	TGATTC**C**AAT**T**G**A**C**TG**ATTTC	Deleted	
850-Ey-Site3	-	ATGTGAGC**C**ACT**T**GTG**TG**GCA	Deleted	
850-SuH-Site1	-	TTTTTGT**TT**CA**CA**CACACAGG	TaTcTGTcgCACACACACAGG	850-SuH-1m2m3m6m has sites 1, 2, 3 and 6 mutated (850 bp).
850-SuH-Site2	-	CGTCTGT**TT**CC**CA**ACACCGTA	CGTCTGTaTCCgtACACCGTA	
850-SuH-Site3*	-	TCCAAAG**TT**CC**CA**CAGTGCGC	TCCAAAGaTCCgACAGTGCGC	850-SuH-1-6m has sites 1 to 6 mutated (850 bp) .
850-SuH-Site4	+	GCATTT**TT**AA**CA**ACTTTAAGC	GCATTTcTAAgtACTTTAAGC	
850-SuH-Site5	+	GTCGACC**TT**GT**CA**AGTACCTT	GTCGACCaTGTCAAGTACCTT	
850-SuH-Site6	-	AGCAGCGTT**TT**CT**CA**ACTTTG	AGCAGCGTTaTCTgAACTTTG	
850-Scro-Site1*	+	TTGATG**T**T**AAG**TGTCTGCCAC	Deleted	850-Scro-1-7d has all 7 sites deleted (724 bp)
850-Scro-Site2	-	CATAGTGTCC**T**A**AA**TGCTGTT	Deleted	
850-Scro-Site3	+	CAAGCCAAAACT**A**A**T**GGGTAT	Deleted	
850-Scro-Site4,5	-	TCG**T**T**AA**AGG GG**T**T**AA**ATAGG	Deleted	
850-Scro-Site6*	+	TTG**T**C**AA**GTACCTTGTTAGCT	Deleted	
850-Scro-Site7	+	CGT**T**T**AA**TTGACAATTGAACC	Deleted	
850-Slp1-Site1*	+	TGACTT**TGTT**TTTGCTACTCA	Deleted	850-Slp1-1d (829 bp)

References

913 1 Lin, S. & Lee, T. Generating neuronal diversity in the Drosophila central nervous system. *Dev Dyn*
914 **241**, 57-68, doi:10.1002/dvdy.22739 (2012).
915 2 Allan, D. W. & Thor, S. Transcriptional selectors, masters, and combinatorial codes: regulatory
916 principles of neural subtype specification. *Wiley Interdiscip Rev Dev Biol* **4**, 505-528,
917 doi:10.1002/wdev.191 (2015).
918 3 Holguera, I. & Desplan, C. Neuronal specification in space and time. *Science* **362**, 176-180,
919 doi:10.1126/science.aas9435 (2018).
920 4 Sagner, A. & Briscoe, J. Establishing neuronal diversity in the spinal cord: a time and a place.
921 *Development* **146**, doi:10.1242/dev.182154 (2019).
922 5 Pearson, B. J. & Doe, C. Q. Specification of temporal identity in the developing nervous system.
923 *Annu Rev Cell Dev Biol* **20**, 619-647, doi:10.1146/annurev.cellbio.19.111301.115142 (2004).
924 6 Oberst, P., Agirman, G. & Jabaudon, D. Principles of progenitor temporal patterning in the
925 developing invertebrate and vertebrate nervous system. *Curr Opin Neurobiol* **56**, 185-193,
926 doi:10.1016/j.conb.2019.03.004 (2019).
927 7 Maurange, C. Temporal patterning in neural progenitors: from Drosophila development to
928 childhood cancers. *Dis Model Mech* **13**, doi:10.1242/dmm.044883 (2020).
929 8 Doe, C. Q. Temporal Patterning in the Drosophila CNS. *Annu Rev Cell Dev Biol* **33**, 219-240,
930 doi:10.1146/annurev-cellbio-111315-125210 (2017).
931 9 Miyares, R. L. & Lee, T. Temporal control of Drosophila central nervous system development.
932 *Curr Opin Neurobiol* **56**, 24-32, doi:10.1016/j.conb.2018.10.016 (2019).
933 10 Brody, T. & Odenwald, W. F. Programmed transformations in neuroblast gene expression during
934 Drosophila CNS lineage development. *Dev Biol* **226**, 34-44, doi:10.1006/dbio.2000.9829 (2000).
935 11 Isshiki, T., Pearson, B., Holbrook, S., and Doe, C.Q. . Drosophila neuroblasts sequentially express
936 transcriptional factors which specify the temporal identity of their neuronal progeny. *Cell* **106**,
937 51-5211 (2001).
938 12 Grosskortenhaus, R., Robinson, K. J. & Doe, C. Q. Pdm and Castor specify late-born motor
939 neuron identity in the NB7-1 lineage. *Genes Dev* **20**, 2618-2627, doi:10.1101/gad.1445306
940 (2006).
941 13 Baumgardt, M., Karlsson, D., Terriente, J., Diaz-Benjumea, F. J. & Thor, S. Neuronal subtype
942 specification within a lineage by opposing temporal feed-forward loops. *Cell* **139**, 969-982,
943 doi:10.1016/j.cell.2009.10.032 (2009).
944 14 Babaoglan, A. B., Housden, B. E., Furriols, M. & Bray, S. J. Deadpan contributes to the robustness
945 of the notch response. *PLoS One* **8**, e75632, doi:10.1371/journal.pone.0075632 (2013).
946 15 Suzuki, T., Kaido, M., Takayama, R. & Sato, M. A temporal mechanism that produces neuronal
947 diversity in the Drosophila visual center. *Dev Biol* **380**, 12-24, doi:10.1016/j.ydbio.2013.05.002
948 (2013).
949 16 Zhu, H., Zhao, S. D., Ray, A., Zhang, Y. & Li, X. A comprehensive temporal patterning gene
950 network in Drosophila medulla neuroblasts revealed by single-cell RNA sequencing. *Nat*
951 *Commun* **13**, 1247, doi:10.1038/s41467-022-28915-3 (2022).
952 17 Konstantinides, N. *et al.* A complete temporal transcription factor series in the fly visual system.
953 *Nature* **604**, 316-322, doi:10.1038/s41586-022-04564-w (2022).
954 18 Li, X. *et al.* Temporal patterning of Drosophila medulla neuroblasts controls neural fates. *Nature*
955 **498**, 456-462, doi:10.1038/nature12319 (2013).

19 Tang, J. L. Y. *et al.* NanoDam identifies Homeobrain (ARX) and Scarecrow (NKX2.1) as conserved temporal factors in the Drosophila central brain and visual system. *Dev Cell* **57**, 1193-1207 e1197, doi:10.1016/j.devcel.2022.04.008 (2022).
20 Maurange, C., Cheng, L. & Gould, A. P. Temporal transcription factors and their targets schedule the end of neural proliferation in Drosophila. *Cell* **133**, 891-902, doi:10.1016/j.cell.2008.03.034 (2008).
21 Averbukh, I., Lai, S. L., Doe, C. Q. & Barkai, N. A repressor-decay timer for robust temporal patterning in embryonic Drosophila neuroblast lineages. *Elife* **7**, doi:10.7554/eLife.38631 (2018).
22 Hirono, K., Margolis, J. S., Posakony, J. W. & Doe, C. Q. Identification of hunchback cis-regulatory DNA conferring temporal expression in neuroblasts and neurons. *Gene Expr Patterns* **12**, 11-17, doi:10.1016/j.gep.2011.10.001 (2012).
23 Grosskortenhaus, R., Pearson, B. J., Marusich, A. & Doe, C. Q. Regulation of temporal identity transitions in Drosophila neuroblasts. *Dev Cell* **8**, 193-202, doi:10.1016/j.devcel.2004.11.019 (2005).
24 Mettler, U., Vogler, G. & Urban, J. Timing of identity: spatiotemporal regulation of hunchback in neuroblast lineages of Drosophila by Seven-up and Prospero. *Development* **133**, 429-437, doi:10.1242/dev.02229 (2006).
25 van den Ameele, J. & Brand, A. H. Neural stem cell temporal patterning and brain tumour growth rely on oxidative phosphorylation. *Elife* **8**, doi:10.7554/eLife.47887 (2019).
26 Okamoto, M. *et al.* Cell-cycle-independent transitions in temporal identity of mammalian neural progenitor cells. *Nat Commun* **7**, 11349, doi:10.1038/ncomms11349 (2016).
27 Moore, R. & Alexandre, P. Delta-Notch Signaling: The Long and The Short of a Neuron's Influence on Progenitor Fates. *J Dev Biol* **8**, doi:10.3390/jdb8020008 (2020).
28 Fortini, M. E. Notch signaling: the core pathway and its posttranslational regulation. *Dev Cell* **16**, 633-647, doi:10.1016/j.devcel.2009.03.010 (2009).
29 Kopan, R. & Ilagan, M. X. The canonical Notch signaling pathway: unfolding the activation mechanism. *Cell* **137**, 216-233, doi:10.1016/j.cell.2009.03.045 (2009).
30 Bray, S. a. F., M. . Notch pathway: Making sense of Suppressor of Hairless. *Current Biology* **11**, 217-221 (2001).
31 Walsh, K. T. & Doe, C. Q. Drosophila embryonic type II neuroblasts: origin, temporal patterning, and contribution to the adult central complex. *Development* **144**, 4552-4562, doi:10.1242/dev.157826 (2017).
32 Knoblich, J. A., Yan, L.Y., and Jan, Y.N. . Asymmetric segregation of Numb and Prospero during cell division. *Nature* **377**, 624-627 (1995).
33 Rhyu, M. S., Jan, L.Y.,and JAn, Y.N. . Asymmetric division of the Numb protein during division of the sensory organ precursor cell confers distinct fates to daughter cells. *Cell* **76**, 477-491 (1994).
34 Roegiers, F. & Jan, Y. N. Asymmetric cell division. *Curr Opin Cell Biol* **16**, 195-205, doi:10.1016/j.ceb.2004.02.010 (2004).
35 Fuerstenberg, S., Broadus, J. and Doe, C.Q. Asymmetry and cell fate in the Drosophila embryonic CNS. *International Jounal of Developmental Biology* **42**, 379-383 (1998).
36 Wang, H. *et al.* Aurora-A acts as a tumor suppressor and regulates self-renewal of Drosophila neuroblasts. *Genes Dev* **20**, 3453-3463, doi:10.1101/gad.1487506 (2006).
37 Bowman, S. K. *et al.* The tumor suppressors Brat and Numb regulate transit-amplifying neuroblast lineages in Drosophila. *Dev Cell* **14**, 535-546, doi:10.1016/j.devcel.2008.03.004 (2008).
38 Weng, M., Golden, K. L. & Lee, C. Y. dFezf/Earmuff maintains the restricted developmental potential of intermediate neural progenitors in Drosophila. *Dev Cell* **18**, 126-135, doi:10.1016/j.devcel.2009.12.007 (2010).

1004 39 Zacharioudaki, E., Magadi, S. S. & Delidakis, C. bHLH-O proteins are crucial for Drosophila
1005 neuroblast self-renewal and mediate Notch-induced overproliferation. *Development* **139**, 1258-
1006 1269, doi:10.1242/dev.071779 (2012).
1007 40 Almeida, M. S. & Bray, S. J. Regulation of post-embryonic neuroblasts by Drosophila Grainyhead.
1008 *Mech Dev* **122**, 1282-1293, doi:10.1016/j.mod.2005.08.004 (2005).
1009 41 Magadi, S. S. *et al.*, doi:10.1101/2020.03.25.007187 (2020).
1010 42 Ulvklo, C. *et al.* Control of neuronal cell fate and number by integration of distinct daughter cell
1011 proliferation modes with temporal progression. *Development* **139**, 678-689,
1012 doi:10.1242/dev.074500 (2012).
1013 43 Bivik, C. *et al.* Control of Neural Daughter Cell Proliferation by Multi-level Notch/Su(H)/E(spl)-
1014 HLH Signaling. *PLoS Genet* **12**, e1005984, doi:10.1371/journal.pgen.1005984 (2016).
1015 44 Kageyama, R., Ohtsuka, T., Shimojo, H. & Imayoshi, I. Dynamic regulation of Notch signaling in
1016 neural progenitor cells. *Curr Opin Cell Biol* **21**, 733-740, doi:10.1016/j.ceb.2009.08.009 (2009).
1017 45 Pfeiffer, B. D., Jenett, A., Hammonds, A.S., Ngo, T.B., Misra, S., Murphy, C., Scully, A., Carlson,
1018 J.W., Wan , K.H., Laverty, T.R., Mungall, C., Svirkas, R., KAdonaga, J.T., Doe, C.Q., Eisen, M.B.,
1019 Celniker, S.E., and Rubin, G.M. . Tools for neuroanatomy and neurogenetics in Drosophila. *PNAS*
1020 **105**, 9715-9720 (2008).
1021 46 Jenett, A. *et al.* A GAL4-driver line resource for Drosophila neurobiology. *Cell Rep* **2**, 991-1001,
1022 doi:10.1016/j.celrep.2012.09.011 (2012).
1023 47 Pfeiffer, B. D. *et al.* Refinement of tools for targeted gene expression in Drosophila. *Genetics*
1024 **186**, 735-755, doi:10.1534/genetics.110.119917 (2010).
1025 48 Brody, T. *et al.* cis-Decoder discovers constellations of conserved DNA sequences shared among
1026 tissue-specific enhancers. *Genome Biol* **8**, R75, doi:10.1186/gb-2007-8-5-r75 (2007).
1027 49 Awgulewitsch, A., and Jacobs, D. . Deformed autoregulatory element from Drosophila functions
1028 in a conserved manner in transgenic mice *Nature* **358**, 341-344 (1992).
1029 50 Malicki, J., Cianetti, L.C., Peschle, C., and, McGinnis, W. A human HOX4B regulatory element
1030 provides head-specific expression in Drosophila embryos. *Nature* **358**, 345-347 (1992).
1031 51 Wray, G. A. *et al.* The evolution of transcriptional regulation in eukaryotes. *Mol Biol Evol* **20**,
1032 1377-1419, doi:10.1093/molbev/msg140 (2003).
1033 52 Odenwald, W. F., Rasband, W., Kuzin, A., and, Brody, T. . EVOPRINTER, a multigenomic
1034 comparative tool for rapid identification of functionally important DNA. *PNAS* **102**, 14700-14705
1035 (2005).
1036 53 Rister, J., Razzaq, A., Boodram, P.,Desai, N., Tsanis, C., Chen, H., Jukam, D., and Desplan, C.
1037 Single-base pair differences in a shared mtif determine differential Rhodopsin expression.
1038 *Science* **350**, 1258-1261 (2015).
1039 54 Frankel, N. *et al.* Phenotypic robustness conferred by apparently redundant transcriptional
1040 enhancers. *Nature* **466**, 490-493, doi:10.1038/nature09158 (2010).
1041 55 Fujioka, M. & Jaynes, J. B. Regulation of a duplicated locus: Drosophila sloppy paired is replete
1042 with functionally overlapping enhancers. *Dev Biol* **362**, 309-319,
1043 doi:10.1016/j.ydbio.2011.12.001 (2012).
1044 56 Ghiasvand, N. M. *et al.* Deletion of a remote enhancer near ATOH7 disrupts retinal
1045 neurogenesis, causing NCRNA disease. *Nat Neurosci* **14**, 578-586, doi:10.1038/nn.2798 (2011).
1046 57 Lagha, M., Bothma, J. P. & Levine, M. Mechanisms of transcriptional precision in animal
1047 development. *Trends Genet* **28**, 409-416, doi:10.1016/j.tig.2012.03.006 (2012).
1048 58 Gallo, S. M., Li, L., Hu, Z. & Halfon, M. S. REDfly: a Regulatory Element Database for Drosophila.
1049 *Bioinformatics* **22**, 381-383, doi:10.1093/bioinformatics/bti794 (2006).

1050 59 Rivera, J., Keranen, S. V. E., Gallo, S. M. & Halfon, M. S. REDfly: the transcriptional regulatory
1051 element database for Drosophila. *Nucleic Acids Res* **47**, D828-D834, doi:10.1093/nar/gky957
1052 (2019).
1053 60 Sato, A. & Tomlinson, A. Dorsal-ventral midline signaling in the developing Drosophila eye.
1054 *Development* **134**, 659-667, doi:10.1242/dev.02786 (2007).
1055 61 Bailey, T. L., Johnson, J., Grant, C. E. & Noble, W. S. The MEME Suite. *Nucleic Acids Res* **43**, W39-
1056 49, doi:10.1093/nar/gkv416 (2015).
1057 62 Grant, C. E., Bailey, T. L. & Noble, W. S. FIMO: scanning for occurrences of a given motif.
1058 *Bioinformatics* **27**, 1017-1018, doi:10.1093/bioinformatics/btr064 (2011).
1059 63 Zaffran, S., Das, G., and Frasch, M. . The NK-2 homeobox gene scarecrow (scro) is expressed in
1060 pharynx, ventral nerve cord and brain of Drosophila embryos. *Mechanisms of Development* **94**,
1061 237-241 (2000).
1062 64 Bailey, A. M., and Posakony, J. W. . Suppressor of Hairless directly activates transcription of
1063 *Enhancer of Split* complex genes in response to Notch receptor activity. *Genes and Development*
1064 **9**, 2609-2622 (1995).
1065 65 Furukawa, T., Kobayakawa, Y.,Tamura, K., Kawaichi, M., Tanimura, T., and Honjo, T. . Suppressor
1066 of Hairless, the *Drosophila* homolog of RBP-Jκ, transactivates the neurogenic gene E(spl)m8.
1067 *Japan Journal of Genetics.* **70**, 505-524 (1995).
1068 66 Ito, K., Awano, W., Suzuki, K, Hiromi, Y., and Yamamoto, D.,. The Drosophila mushroom body is a
1069 quadruple structure of clonal units each of which contains a virtually identical set of neurones
1070 and glial cells. *Development* **124**, 761-771 (1997).
1071 67 Nusslein-Volhard, C., Weischaus, E., and Kluding, E. Mutations affecting the pattern of the larval
1072 cuticle in *Drosophila melanogaster*. I. Zygotic loci on the second chromosome. . *Roux's Archives*
1073 *of Developmental Biology* **193**, 267-282 (1984).
1074 68 Bray, S. J. Notch signalling: a simple pathway becomes complex. *Nat Rev Mol Cell Biol* **7**, 678-
1075 689, doi:10.1038/nrm2009 (2006).
1076 69 Campos-Ortega, J. A. Cellular interactions during early neurogenesis of *Drosophila*
1077 *melanogaster*. . *Trends in Neurosciences* **11**, 400-405 (1988).
1078 70 Fleming, R. J., Scottgale, T.N., Diederich, R.J., and Artavanis-Tsakonas, S. The gene Serrate
1079 encodes a putative EGF-like transmembrane protein essential for proper ectodermal
1080 development in *Drosophila melanogaster*. . *Genes and Development* **4**, 2188-2201 (1990).
1081 71 Rebay, I., Fleming, R.J., Fehon, R.G. , Cherbas, L., Cherbas, P., and Artavanis-Tsakonas, S. .
1082 Specific EGF repeats of Notch mediate interactions with Delta and Serrate: implications for
1083 Notch as a multifunctional receptor. *Cell* **67**, 687-699 (1991).
1084 72 Kim, I. M., Wolf, M. J. & Rockman, H. A. Gene deletion screen for cardiomyopathy in adult
1085 Drosophila identifies a new notch ligand. *Circ Res* **106**, 1233-1243,
1086 doi:10.1161/CIRCRESAHA.109.213785 (2010).
1087 73 Stothard, P. The Sequence Manipulation Suite: Javascript programs for analyzing and formatting
1088 protein and DNA sequences *BioTechniques* **28**, 1102-1104 (2000).
1089 74 Tanaka-Matakatsu, M., Miller, J. & Du, W. The homeodomain of Eyeless regulates cell growth
1090 and antagonizes the paired domain-dependent retinal differentiation function. *Protein Cell* **6**,
1091 68-78, doi:10.1007/s13238-014-0101-9 (2015).
1092 75 van Steensel, B., and Henikoff, S. Identification of in vivo DNA targets of chromatin proteins
1093 using tethered Dam methyltransferase. *Nature Biotechnology* **18**, 424-428 (2000).
1094 76 Southall, T. D. *et al.* Cell-type-specific profiling of gene expression and chromatin binding
1095 without cell isolation: assaying RNA Pol II occupancy in neural stem cells. *Dev Cell* **26**, 101-112,
1096 doi:10.1016/j.devcel.2013.05.020 (2013).

1097 77 Landt, S. G. *et al.* ChIP-seq guidelines and practices of the ENCODE and modENCODE consortia.
1098 *Genome Res* **22**, 1813-1831, doi:10.1101/gr.136184.111 (2012).
1099 78 Farnsworth, D. R., Bayraktar, O. A. & Doe, C. Q. Aging Neural Progenitors Lose Competence to
1100 Respond to Mitogenic Notch Signaling. *Curr Biol* **25**, 3058-3068, doi:10.1016/j.cub.2015.10.027
1101 (2015).
1102 79 Kurmangaliyev, Y. Z., Yoo, J., Valdes-Aleman, J., Sanfilippo, P. & Zipursky, S. L. Transcriptional
1103 Programs of Circuit Assembly in the Drosophila Visual System. *Neuron* **108**, 1045-1057 e1046,
1104 doi:10.1016/j.neuron.2020.10.006 (2020).
1105 80 Erclik, T. *et al.* Integration of temporal and spatial patterning generates neural diversity. *Nature*
1106 **541**, 365-370, doi:10.1038/nature20794 (2017).
1107 81 Moldovan, G. L., Pfander, B. & Jentsch, S. PCNA controls establishment of sister chromatid
1108 cohesion during S phase. *Mol Cell* **23**, 723-732, doi:10.1016/j.molcel.2006.07.007 (2006).
1109 82 Zhou, L. & Luo, H. Replication protein a links cell cycle progression and the onset of
1110 neurogenesis in Drosophila optic lobe development. *J Neurosci* **33**, 2873-2888,
1111 doi:10.1523/JNEUROSCI.3357-12.2013 (2013).
1112 83 Edgar, B. A., and O'Farrell, P. Genetic control of cell division patterns in *Drosophila* embryo *Cell*
1113 **57**, 177-187 (1989).
1114 84 Lane, M. E. *et al.* Dacapo, a Cyclin-Dependent Kinase Inhibitor, Stops Cell Proliferation during
1115 Drosophila Development. *Cell* **87**, 1225-1235, doi:10.1016/s0092-8674(00)81818-8 (1996).
1116 85 Cadigan, K. M., Grossniklaus,U., and Genring, W.J. . Localized expression of sloppy paired protein
1117 maintains the polarity of Drosophila parasegments. . *Genes and Development* **8**, 899-913 (1994).
1118 86 Falo-Sanjuan, J., Lammers, N. C., Garcia, H. G. & Bray, S. J. Enhancer Priming Enables Fast and
1119 Sustained Transcriptional Responses to Notch Signaling. *Dev Cell* **50**, 411-425 e418,
1120 doi:10.1016/j.devcel.2019.07.002 (2019).
1121 87 Lee, C., Shin, H. & Kimble, J. Dynamics of Notch-Dependent Transcriptional Bursting in Its Native
1122 Context. *Dev Cell* **50**, 426-435 e424, doi:10.1016/j.devcel.2019.07.001 (2019).
1123 88 San Juan, B. P., Andrade-Zapata, I. & Baonza, A. The bHLH factors Dpn and members of the E(spl)
1124 complex mediate the function of Notch signalling regulating cell proliferation during wing disc
1125 development. *Biol Open* **1**, 667-676, doi:10.1242/bio.20121172 (2012).
1126 89 Gupta, S., Stamatoyannopoulos, J. A., Bailey, T. L. & Noble, W. S. Quantifying similarity between
1127 motifs. *Genome Biol* **8**, R24, doi:10.1186/gb-2007-8-2-r24 (2007).
1128 90 Sandelin, A., Alkema, W., Engstrom, P., Wasserman, W. W. & Lenhard, B. JASPAR: an open-
1129 access database for eukaryotic transcription factor binding profiles. *Nucleic Acids Res* **32**, D91-
1130 94, doi:10.1093/nar/gkh012 (2004).
1131 91 Fornes, O. *et al.* JASPAR 2020: update of the open-access database of transcription factor
1132 binding profiles. *Nucleic Acids Res* **48**, D87-D92, doi:10.1093/nar/gkz1001 (2020).
1133 92 Zhu, L. J. *et al.* FlyFactorSurvey: a database of Drosophila transcription factor binding
1134 specificities determined using the bacterial one-hybrid system. *Nucleic Acids Res* **39**, D111-117,
1135 doi:10.1093/nar/gkq858 (2011).
1136 93 Venken, K. J. *et al.* Versatile P[acman] BAC libraries for transgenesis studies in Drosophila
1137 melanogaster. *Nat Methods* **6**, 431-434, doi:10.1038/nmeth.1331 (2009).
1138 94 Groth, A. C., Fish, M., Nusse, R., and Calos, M.P. . Construction of transgenic Drosophila by using
1139 the site specific integrase from Phage PhiC31 *Genetics* **166**, 1775-1782 (2004).
1140 95 Gratz, S. J. *et al.* Highly specific and efficient CRISPR/Cas9-catalyzed homology-directed repair in
1141 Drosophila. *Genetics* **196**, 961-971, doi:10.1534/genetics.113.160713 (2014).
1142 96 Port, F. & Bullock, S. L. Augmenting CRISPR applications in Drosophila with tRNA-flanked sgRNAs.
1143 *Nat Methods* **13**, 852-854, doi:10.1038/nmeth.3972 (2016).

1144 97 Bosch, J. A., Tran, N. H. & Hariharan, I. K. CoinFLP: a system for efficient mosaic screening and
1145 for visualizing clonal boundaries in Drosophila. *Development* **142**, 597-606,
1146 doi:10.1242/dev.114603 (2015).
1147 98 Long, X., Colonell, J., Wong, A. M., Singer, R. H. & Lionnet, T. Quantitative mRNA imaging
1148 throughout the entire Drosophila brain. *Nat Methods* **14**, 703-706, doi:10.1038/nmeth.4309
1149 (2017).
1150 99 Marshall, O. J., Southall, T. D., Cheetham, S. W. & Brand, A. H. Cell-type-specific profiling of
1151 protein-DNA interactions without cell isolation using targeted DamID with next-generation
1152 sequencing. *Nat Protoc* **11**, 1586-1598, doi:10.1038/nprot.2016.084 (2016).
1153 100 Marshall, O. J. & Brand, A. H. damidseq_pipeline: an automated pipeline for processing DamID
1154 sequencing datasets. *Bioinformatics* **31**, 3371-3373, doi:10.1093/bioinformatics/btv386 (2015).
1155 101 Robinson, J. T. *et al.* Integrative genomics viewer. *Nat Biotechnol* **29**, 24-26,
1156 doi:10.1038/nbt.1754 (2011).
1157 102 Schindelin, J. *et al.* Fiji: an open-source platform for biological-image analysis. *Nat Methods* **9**,
1158 676-682, doi:10.1038/nmeth.2019 (2012).

List of Supplementary files:

1) Supplementary file 1. Sequences deleted in the *slp* double enhancer deletion line.

2) Supplementary Table 1. List of primers used for experiments described.

3) Supplementary Table 2. Predicted transcription factor binding sites by the web-based FIMO analysis.

4) Supplementary Table 3. List of gene blocks used for reporter assays and for cloning Ey coding sequence into the pUAST-Dam-attB plasmid.

5) Supplementary Table 4. Gene lists that have IDR peaks for both Su(H) and Ey, Ey only, and Su(H) only from the DamID-seq data.

6) Supplementary Table 5. DAVID analysis of gene lists that have IDR peaks for both Su(H) and Ey, Ey only, and Su(H) only from the DamID-seq data.

Figure 1

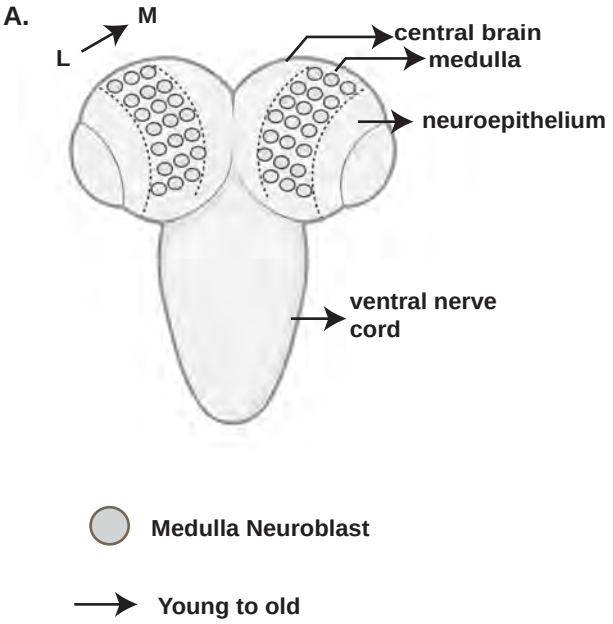
A.
M
L
central brain
medulla
neuroepithelium
ventral nerve cord
Medulla Neuroblast
Young to old

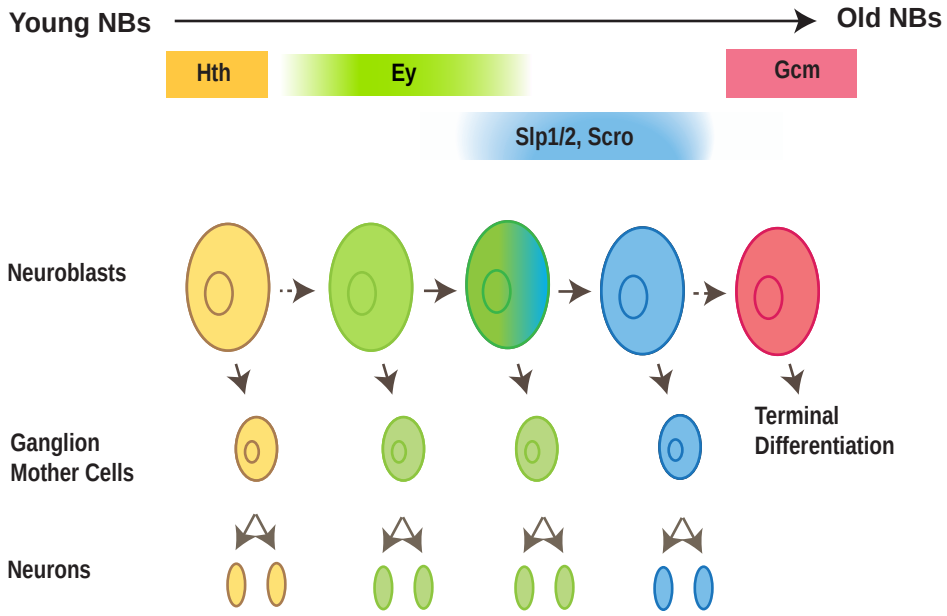
Young NBs
Old NBs
Hth
Ey
Gcm
Slp1/2, Scro
Neuroblasts
Ganglion Mother Cells
Neurons
Terminal Differentiation

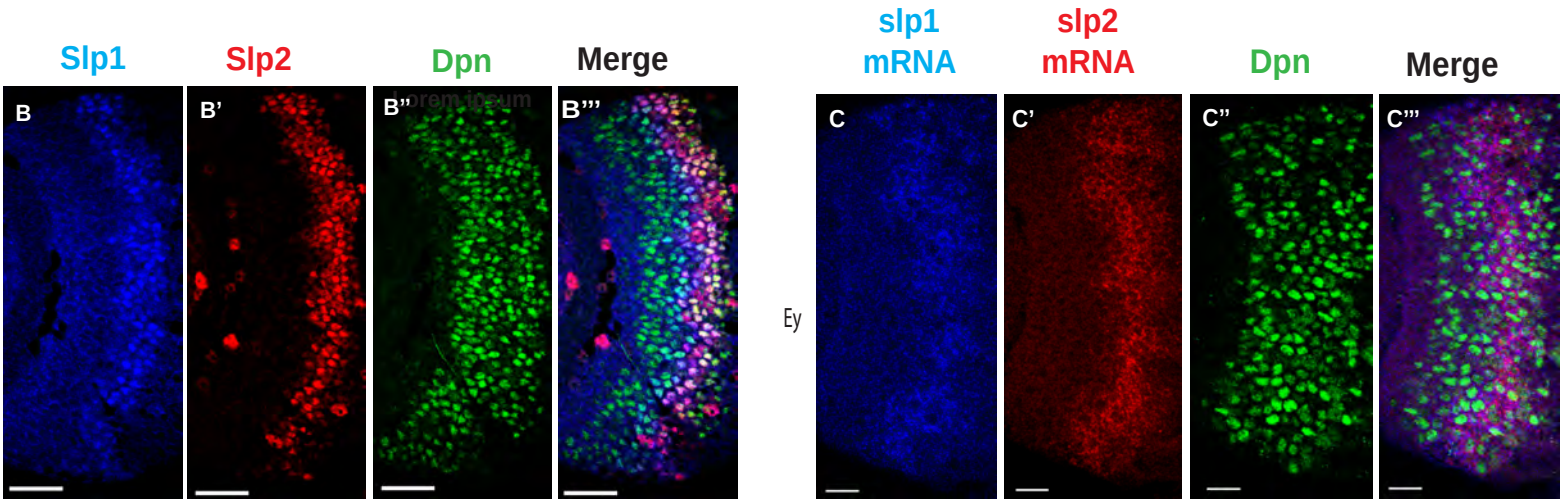
Slp1
Slp2
Dpn
Merge
B
B'
B''
B'''
slp1 mRNA
slp2 mRNA
Dpn
Merge
Ey
C
C'
C''
C'''

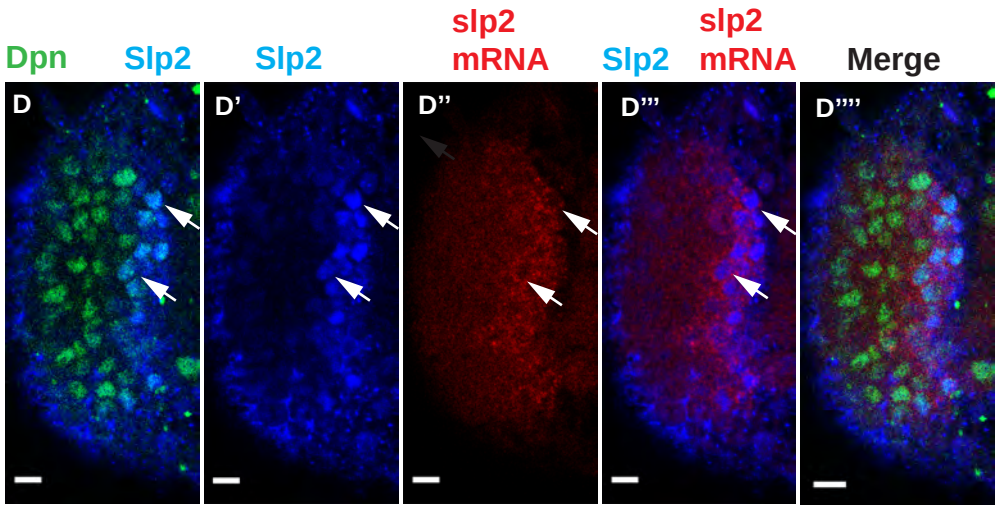
Dpn
Slp2
Slp2
slp2 mRNA
Slp2
slp2 mRNA
Merge
D
D'
D''
D'''
D''''

Figure 2

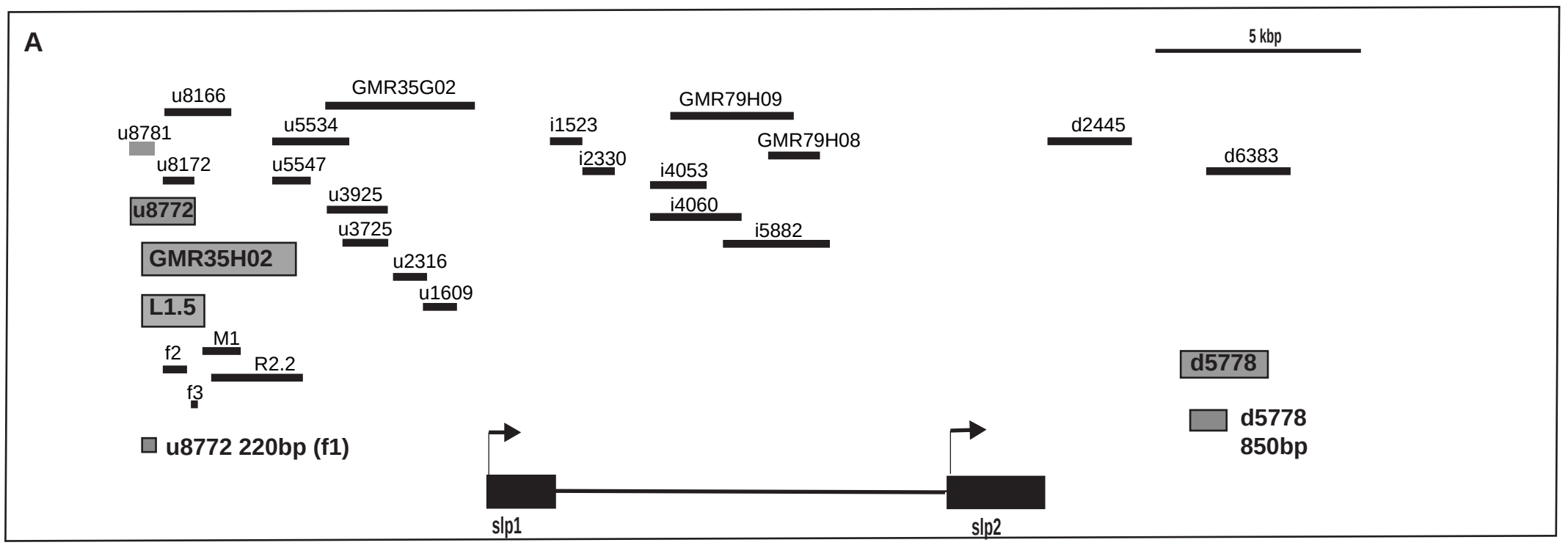
A
5 kbp
u8166
GMR35G02
GMR79H09
u8781
u5534
i1523
GMR79H08
d2445
u8172
u5547
i2330
i4053
d6383
u3925
u8772
i4060
u3725
i5882
GMR35H02
u2316
u1609
L1.5
M1
f2
R2.2
f3
d5778
u8772 220bp (f1)
d5778
850bp
slp1
slp2

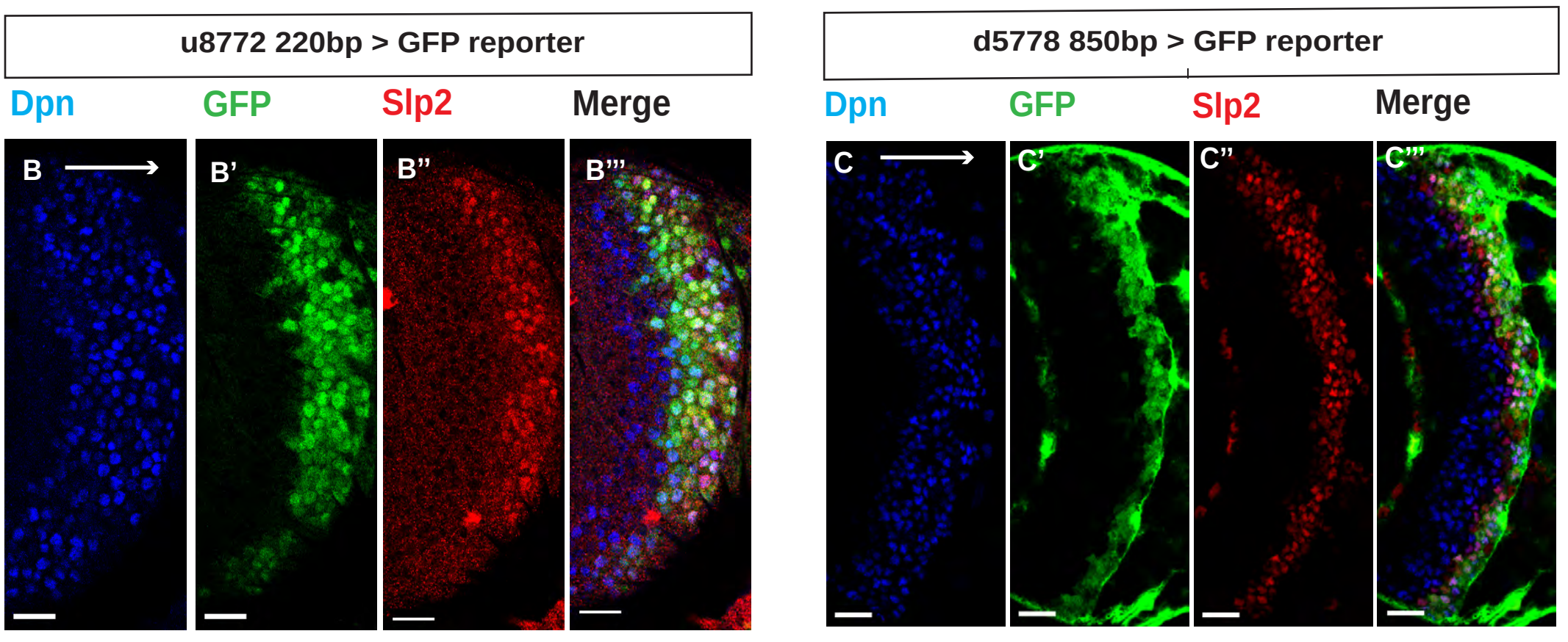
u8772 220bp > GFP reporter
d5778 850bp > GFP reporter
Dpn
GFP
Slp2
Merge
B
B'
B''
B'''
C
C'
C''
C'''

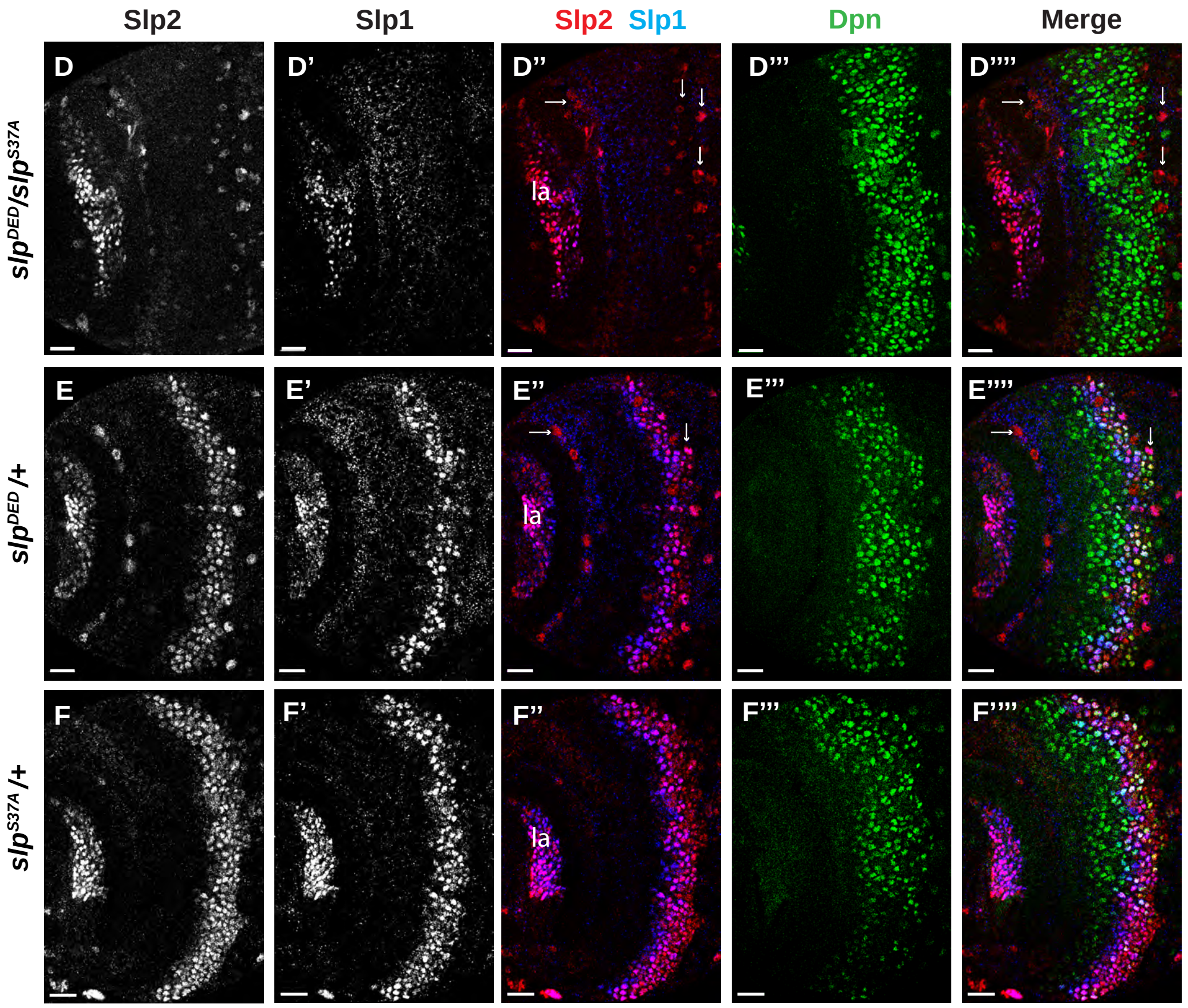
Slp2
Slp1
Slp2 Slp1
Dpn
Merge
slpDED/slpS37A
slpDED /+
slpS37A /+
D
D'
D''
D'''
D''''
E
E'
E''
E'''
E''''
F
F'
F''
F'''
F''''
la

Figure 2—figure supplement 1

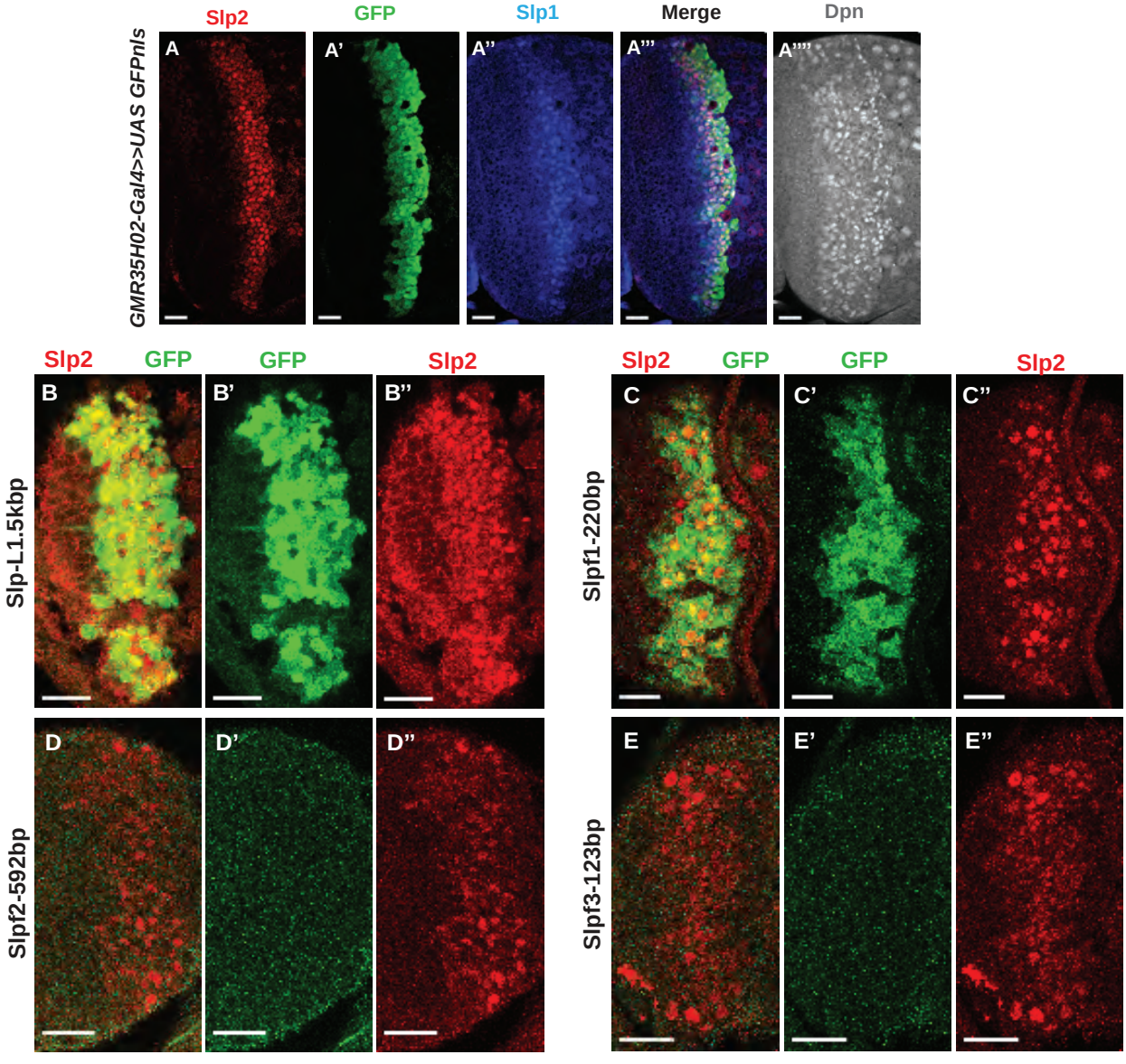

Figure 2—figure supplement 2

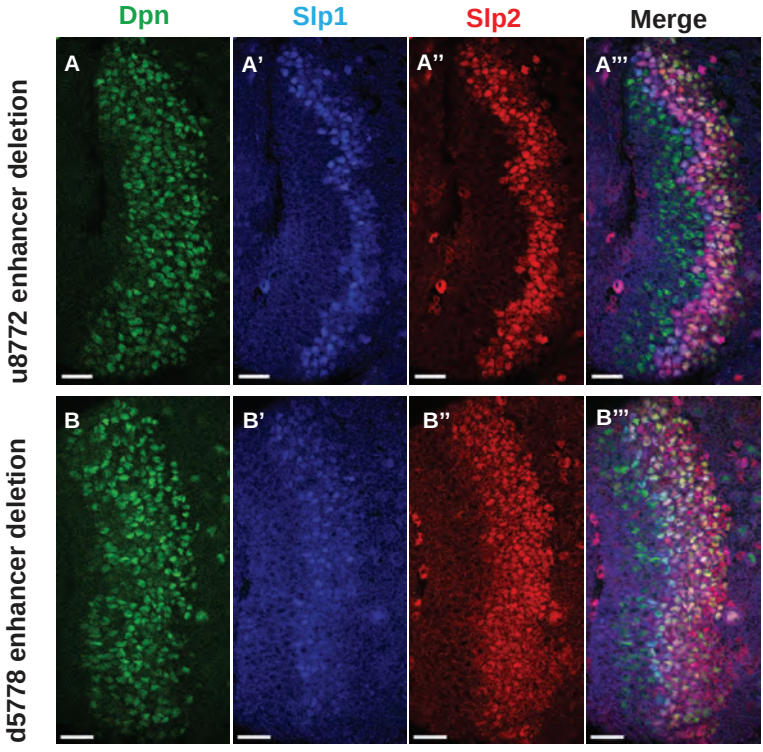

C

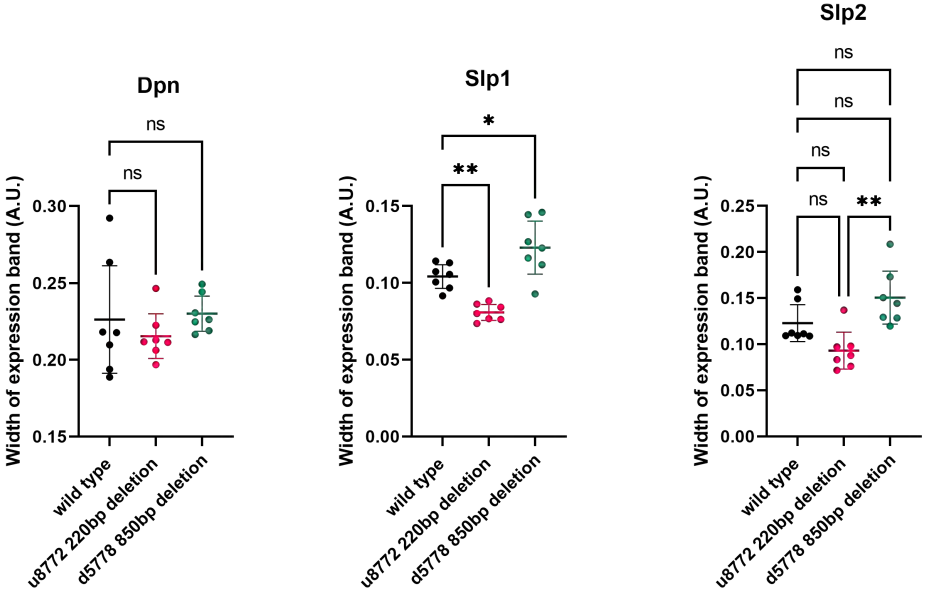

Figure2-figure supplement3

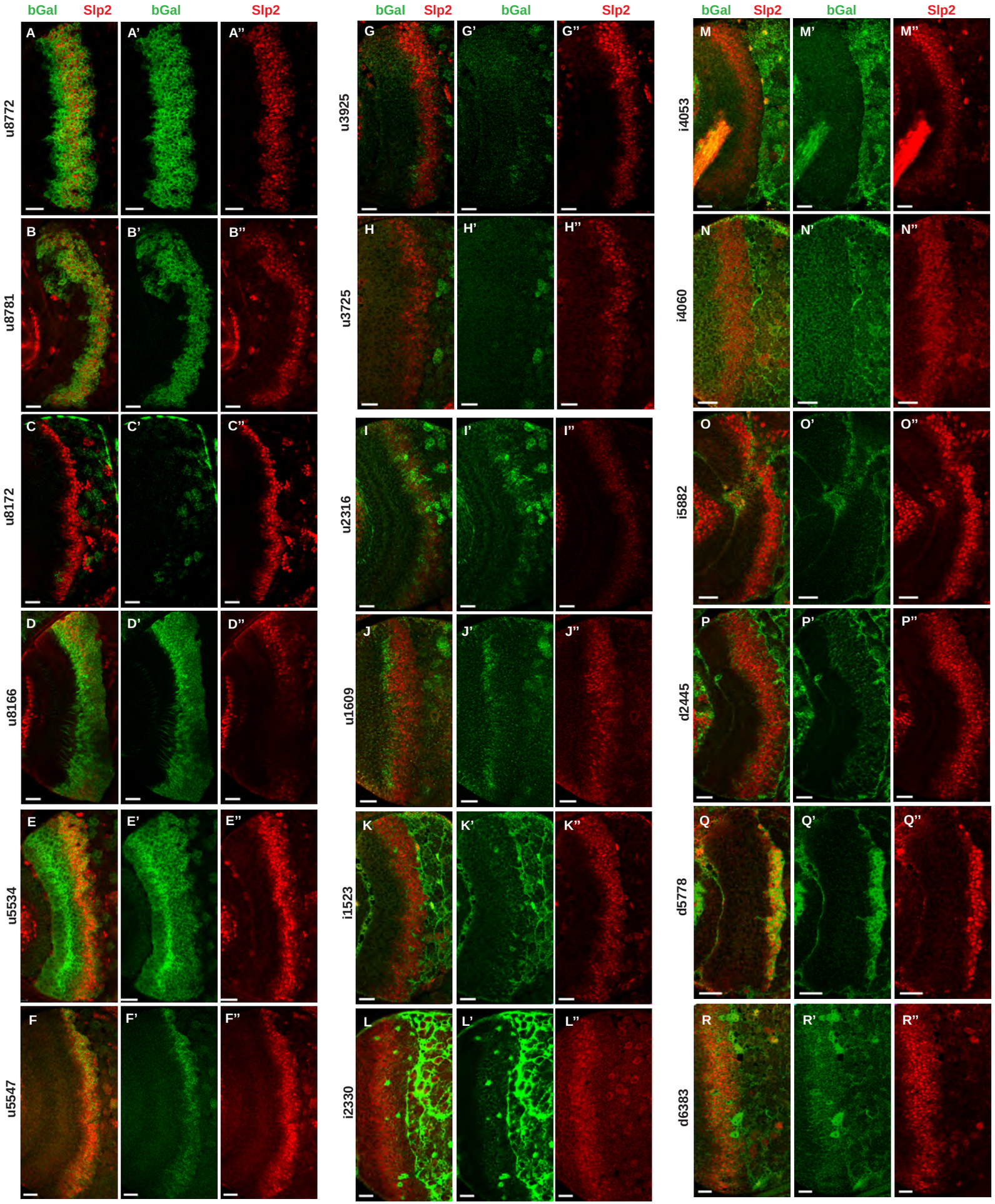

Figure2-figure supplement4

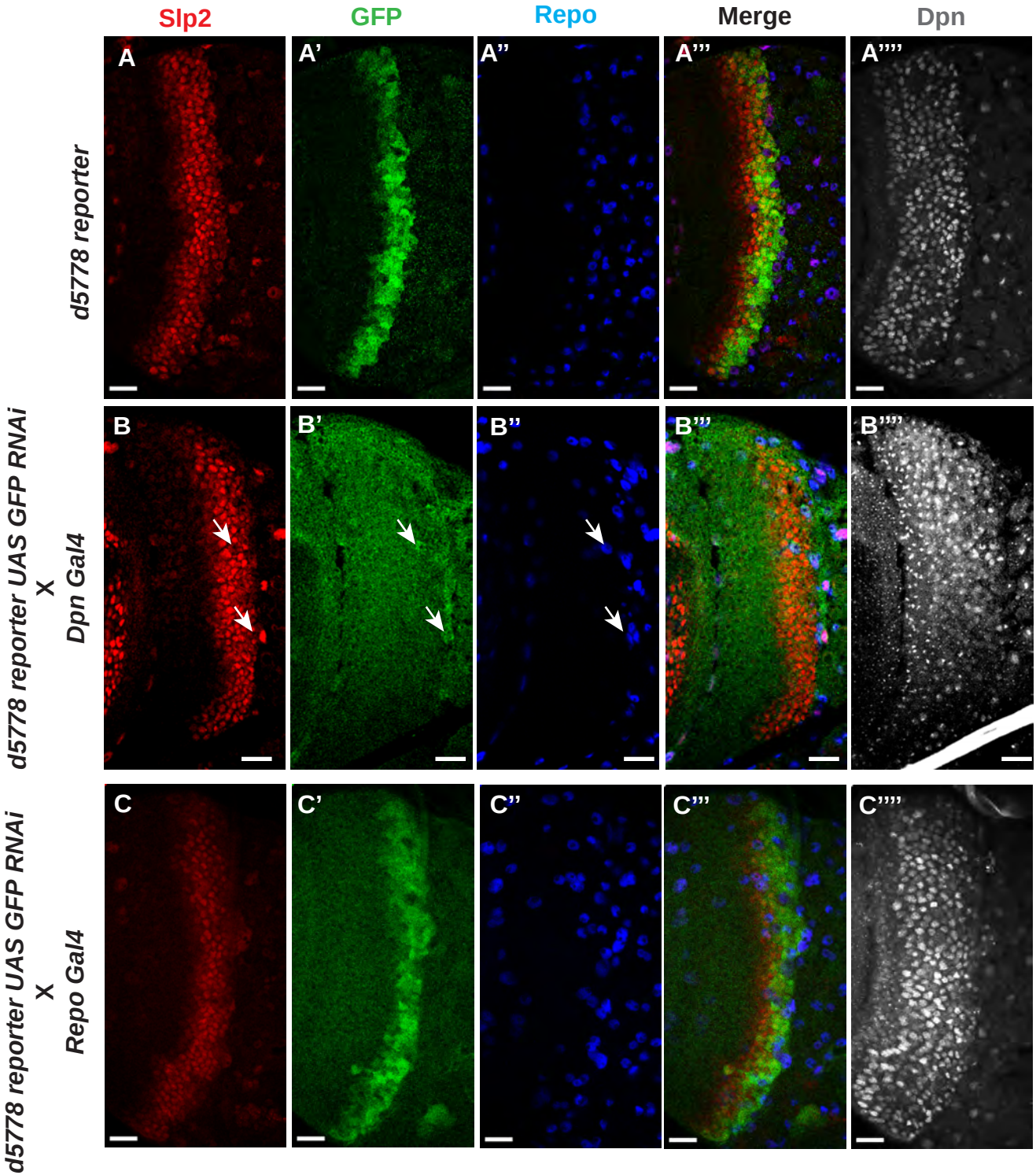

Figure 3

A

Ey

Fly Factor Survey

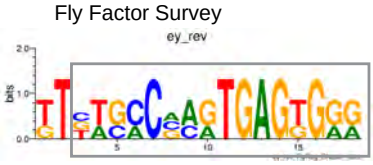

Literature

WWNM**C**RMN**T**S**A**N**TG**RRY

[AT][AT][ATCG][AC]**C**[AG][AC][ATCG]**T**[GC]**A**[ATCG]**TG**[AG][AG][CT]

Consensus used:

[ATCG][AT][ATCG][AC]**C**[ACG][AC][ATCG]**T**[GC]**A**[ATCG]**[TG]G**[AG][AG]

B

Su(H)

Fly Factor Survey

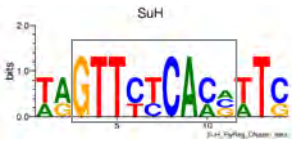

JASPAR

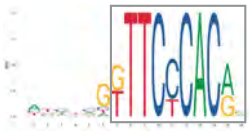

Consensus used

[GT]**TT**[CT][TC]**CA**[CA][AGC]

C

Scro/Vnd

Fly Factor Survey

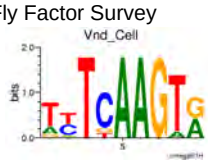

Fly Factor Survey

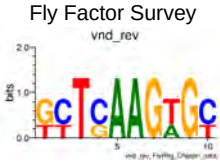

Consensus used

[TAG][TC]**T**[CGT]**AAG**[TA][GA]

D

Slp1

Fly Factor Survey

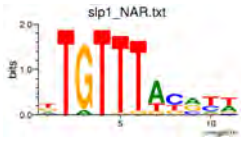

JASPAR

Consensus used

TGTTT[ATG][CTG][AGC][TCA]

E

GAATCGAGTGGTGAGCGATAGTTTTCACATGTTTTGTTCGAGCATTAATTCCGTTTAAATGATTTCCGCAACAGATT

TGAGCTTTGCACGTAATCAAGTGGAAATGAATTTGACCAACACAAGAGGTTTATACACACATCACATTTTCTGCCTT

TATGTTTTTGCGGTGTCCCATTAGTTTGATTGTTTCGAAGGCCACTGAGCCGTGAAAAATATCAGA

F

CATTAACTCGAGTCTGGTTTCCGATTCCGATTTCGCTTCCTCCTGCCAACTTATTTCTATATCTTCTCCCTTTGTGC

CCTGTGTGTGTGAAACAAAAACGTTTGTTTCAATACGTTGGCTTCGTGCATTTTACGGTGTTGGGAAACAGACGAAA

TGGACTCATTGATTCCAATTGACTGATTTCAATTGATGTTAAGTGTCTGCCACAGTCGCAGCCGCAAATTCAGTGGC

ACAACTCCGTCGCAGCCAAATGCCATTTGCTTTTCACATCCAGGTCGAACGGCGTTGCCTTGTTGACTTTGTTTTTG

CTACTCATTGCCGCGATTTGGGTTAGGCATGGGGTATGTGCGCACTGTGGGAACTTTGGATTACTCAGATGAAACAG

CATTTAGGACACTATGCAGCTGGAAAGATAAACTAGTTGATAGCTACTCATTTACTCATTTACTACTTACTACTAAT

TTAATGCATTTTTAACAACTTTAAGCTACACAAGCCAAAACTAATGGGTATTTTATAGTCCTATTTAACCCCTTTAA

CGAATGCATCCTTTTACCTTTTTTGGTCACGGCAGCTGAACTCTGCCCTTTCGTTGGGGGTGACTCCTCCCTCCCGT

ACTCCCTCCCTCCCTCCCCTCCCTCTCCGCGCCACAGTCGACCTTGTCAAGTACCTTGTTAGCTGTTGGGCAAATGT

GCCACACAAGTGGCTCACATCAGCGGGATCGAAAATAAAAAGCGAAACGCATCGAGAACTTCCCAAGAAAACGGCGA

GTCAAAGTTGAGAAAACGCTGCTTCCGTTTAATTGACAATTGAACCCGAACCCGGACCGAACTCCTGGAGAATATGT

ACG

Transcription Factor	Position Weight Matrix	Pattern searched (SMS)
Bap	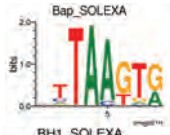	[TCA]TA[AC][GT][TGA][GA]
BH1	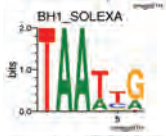	TAA[TA][TCG][GA]
BH2	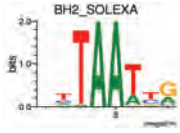	[TCA]TAA[TAG][TCG][GA]
Bsh	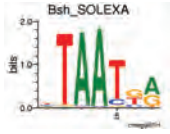	TAA[TCG][GTC][AG]
C15	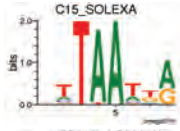	[TAGC]TAA[TAC][TGA][AG]
CG11085	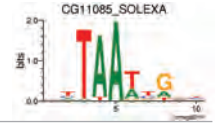	[TGA]T[AT]A[TAG][TC-G][GAT]
Ems	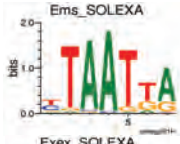	[TCG][TGA][AGC]A[TG][T-GA][AG]
Exex	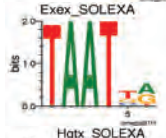	TAAT[TGC][AGT]
Hgtx	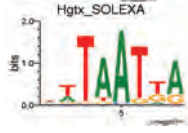	[TAG]T[ATG]A[TG][T-GA][AG]
Hmx	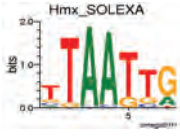	[TGCA][TG]A[AC][TG][TG-C][GAT]
inv	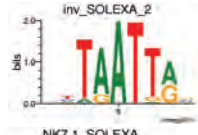	[TA][AG]AT[TGA][AG]
NK7.1	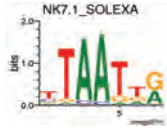	[TCGA][TGA][AC][AC][T-GA][TGA][GA]

Transcription Factor	Position Weight Matrix	Pattern searched (SMS)
CG15696	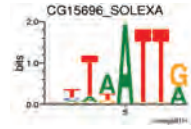	[TGAC][TAG][ATG]ATT[GA]
CG18599	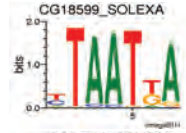	[TCAG]T[AC][AC][TG][T-GA][AG]
CG34031	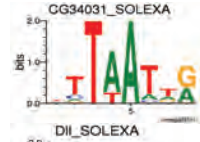	[TCAG]T[AT]A[TAC][TAG][-GA]
Dll	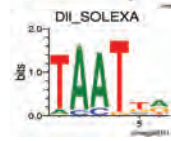	[TA][AC][AC][TG][TG-C][AGT]
Dr	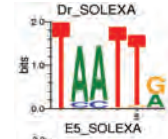	T[AC][AC]T[TG][GA]
E5	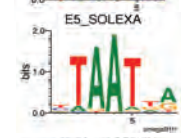	[TCG][TA][AGT]A[TAG][T-GA][AGT]
Unpg	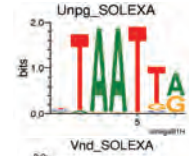	[TA]AAT[TGC][AG]
Vnd	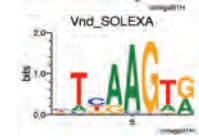	[TAC][CT-G][AG][AG]G[TAG][GA]

Figure 4

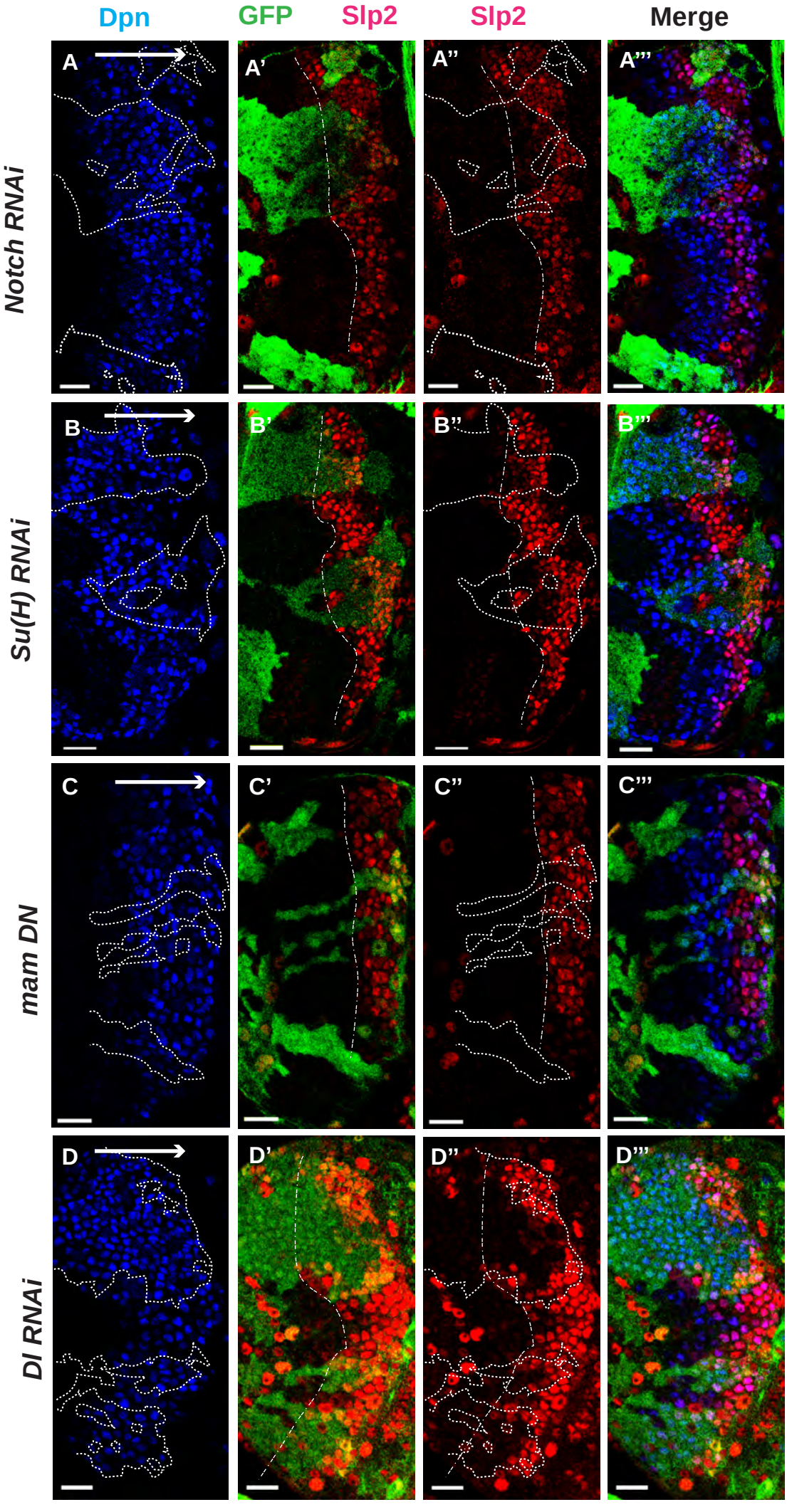
Dpn
GFP
Slp2
Slp2
Merge
Notch RNAi
Su(H) RNAi
mam DN
Dl RNAi
A
A'
A''
A'''
B
B'
B''
B'''
C
C'
C''
C'''
D
D'
D''
D'''

Figure 5

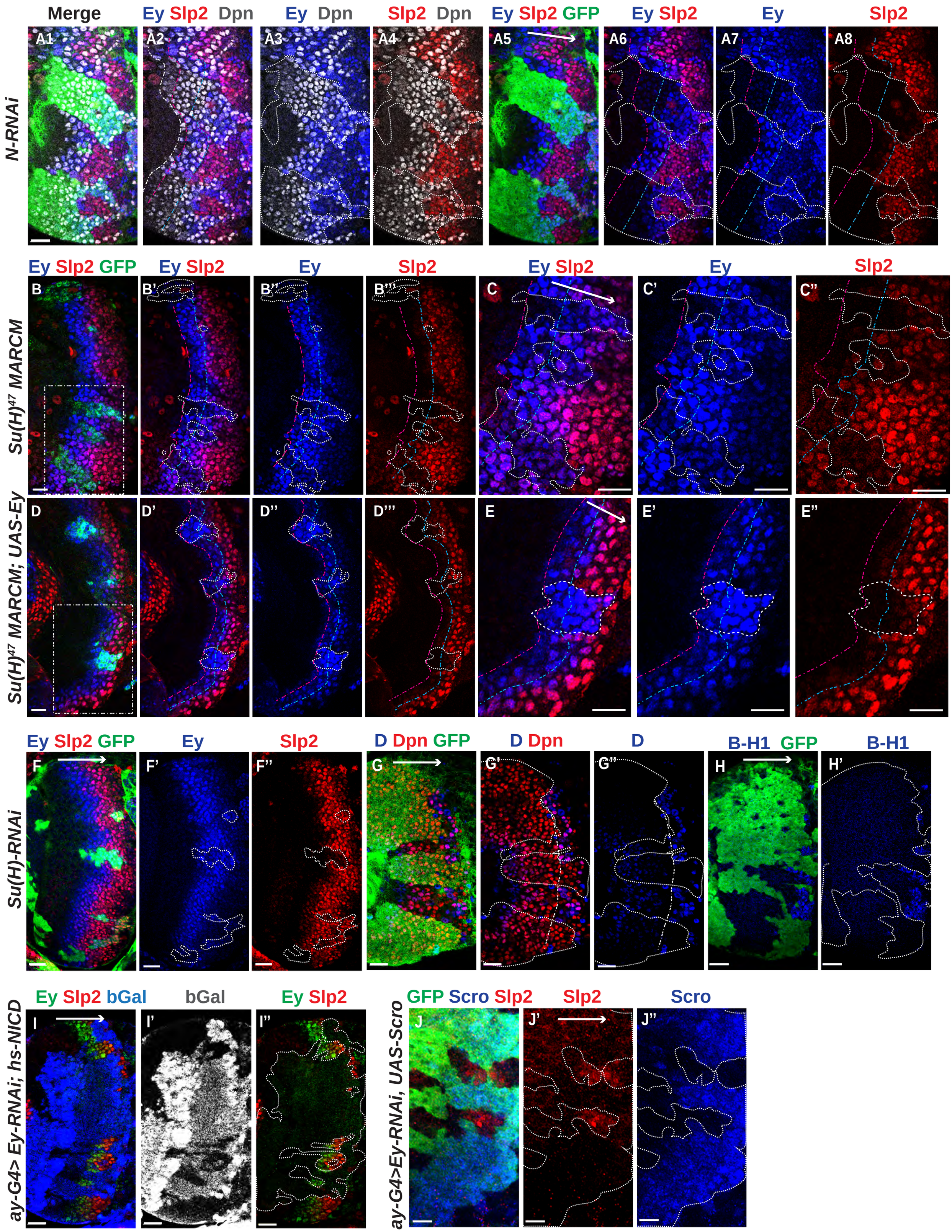
Merge
Ey Slp2 Dpn
Ey Dpn
Slp2 Dpn
Ey Slp2 GFP
Ey Slp2
Ey
Slp2
N-RNAi
A1
A2
A3
A4
A5
A6
A7
A8
Ey Slp2 GFP
Ey Slp2
Ey
Slp2
Ey Slp2
Ey
Slp2
Su(H)47 MARCM
B
B'
B''
B'''
C
C'
C''
Su(H)47 MARCM; UAS-Ey
D
D'
D''
D'''
E
E'
E''
Ey Slp2 GFP
Ey
Slp2
D Dpn GFP
D Dpn
D
B-H1 GFP
B-H1
Su(H)-RNAi
F
F'
F''
G
G'
G''
H
H'
Ey Slp2 bGal
bGal
Ey Slp2
ay-G4> Ey-RNAi; hs-NICD
I
I'
I''
GFP Scro Slp2
Slp2
Scro
ay-G4>Ey-RNAi, UAS-Scro
J
J'
J''

Figure5-figure supplement1

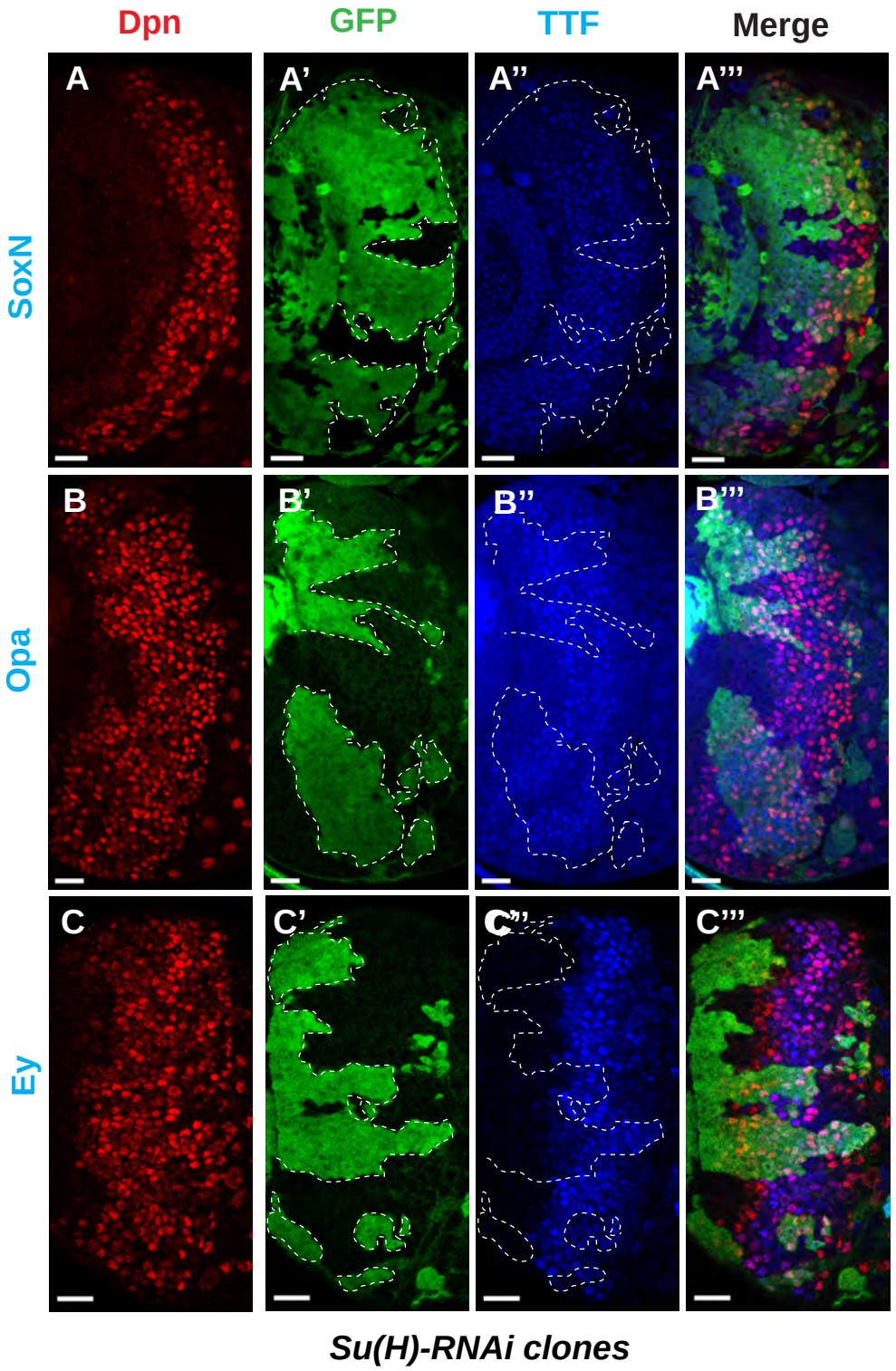

Figure 6

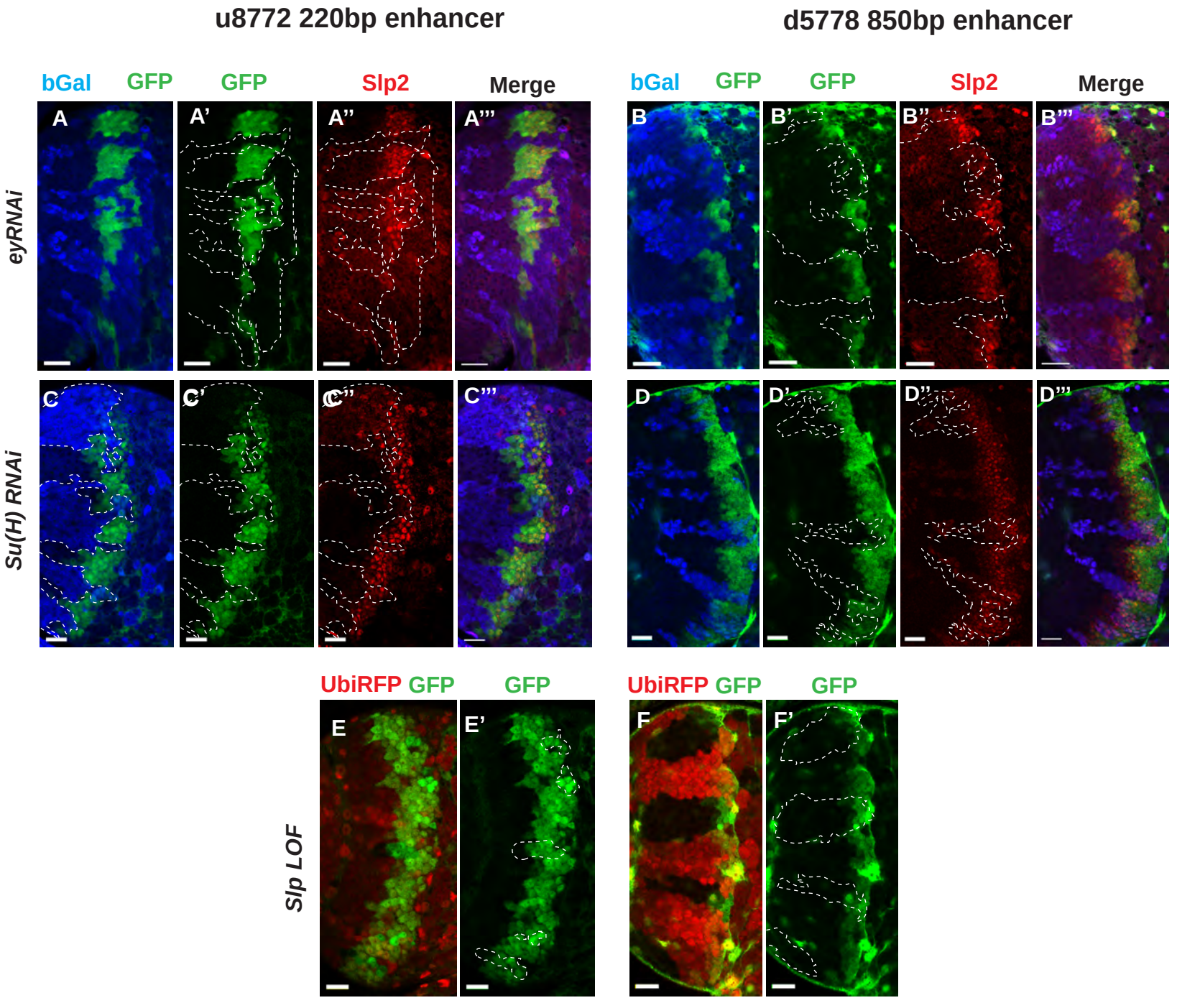
u8772 220bp enhancer
d5778 850bp enhancer
bGal
GFP
GFP
Slp2
Merge
eyRNAi
Su(H) RNAi
Slp LOF
UbiRFP
A
A'
A''
A'''
B
B'
B''
B'''
C
C'
C''
C'''
D
D'
D''
D'''
E
E'
F
F'

Figure 7

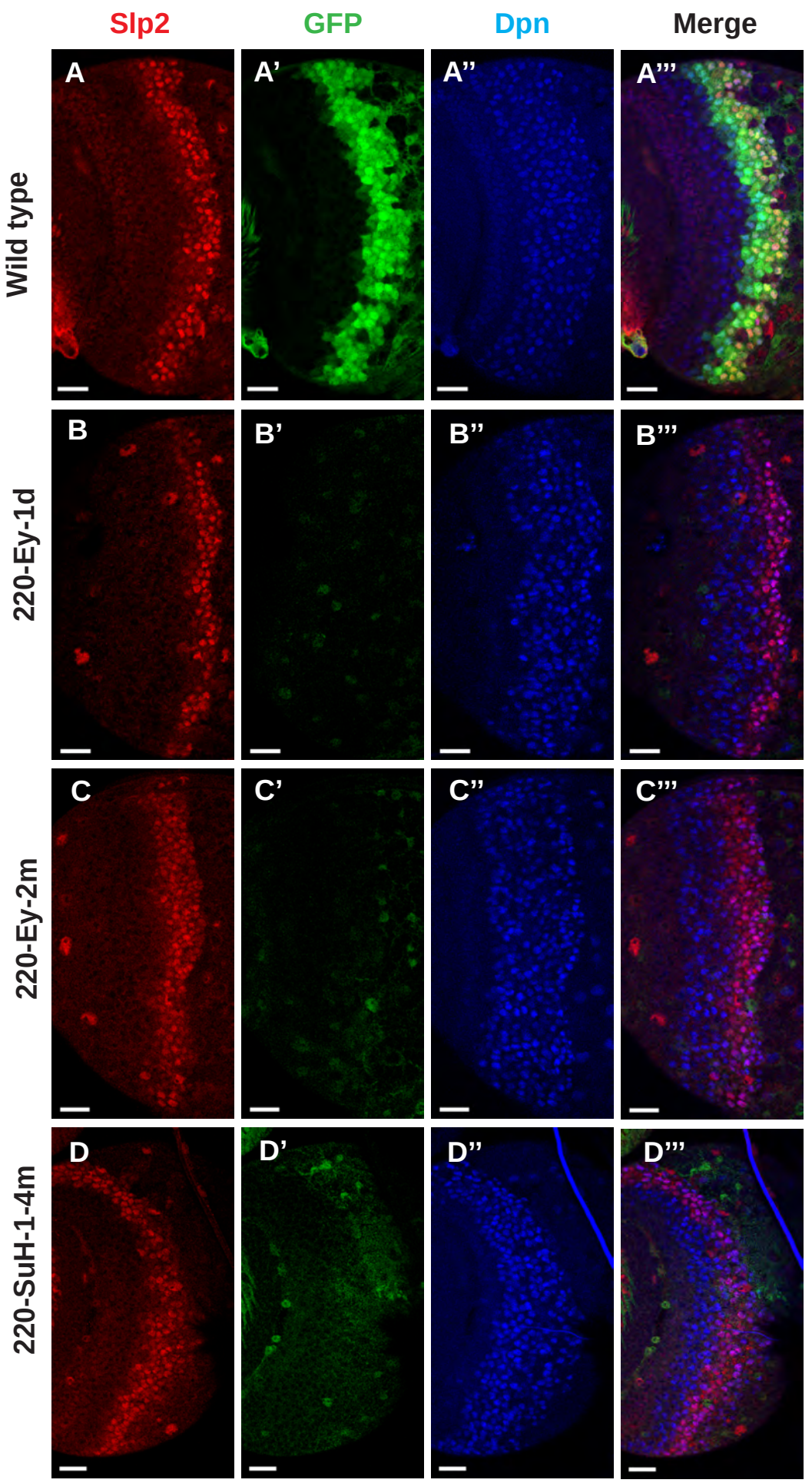
Slp2
GFP
Dpn
Merge
Wild type
220-Ey-1d
220-Ey-2m
220-SuH-1-4m
A
A'
A''
A'''
B
B'
B''
B'''
C
C'
C''
C'''
D
D'
D''
D'''

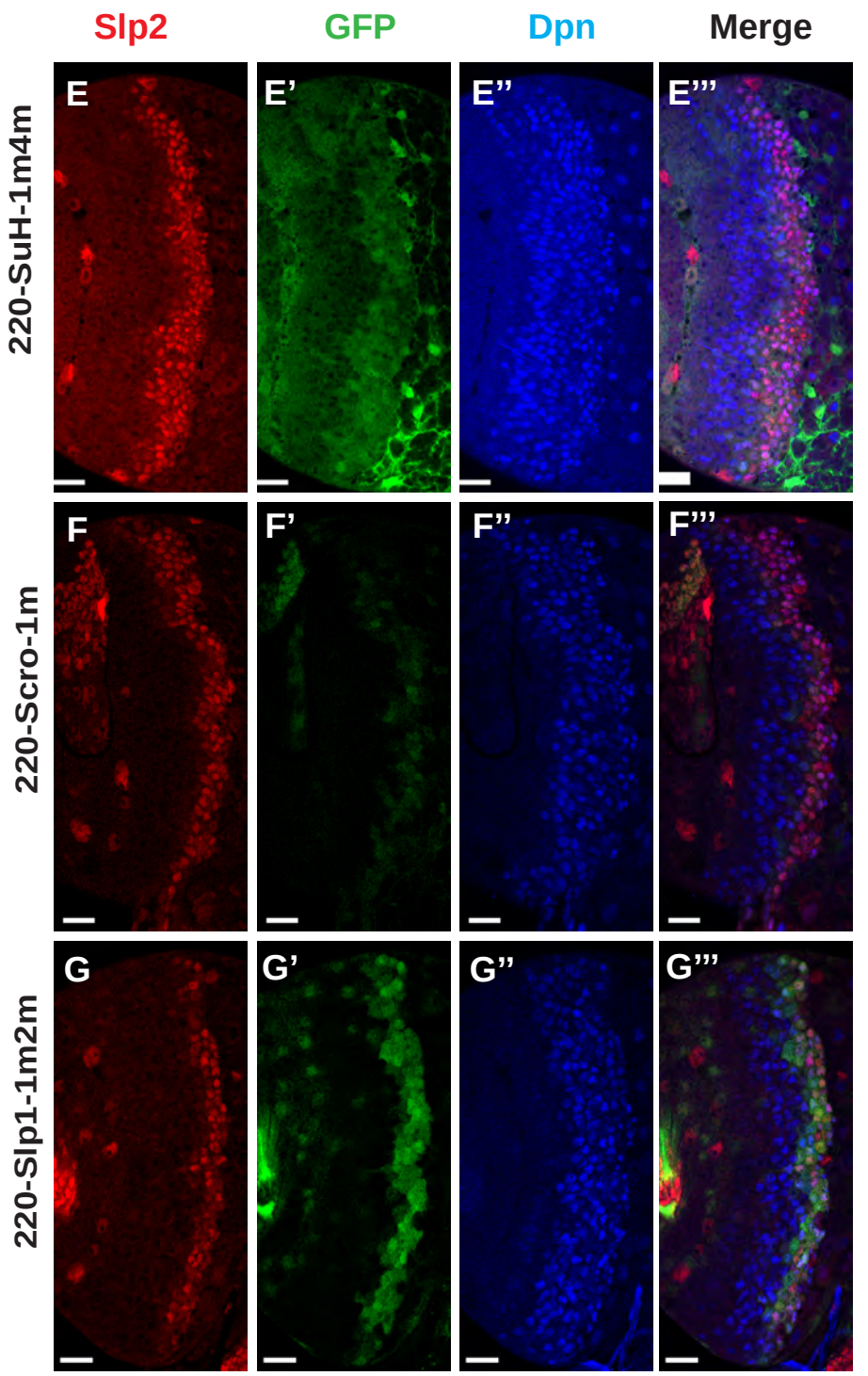
Slp2
GFP
Dpn
Merge
220-SuH-1m4m
220-Scro-1m
220-Slp1-1m2m
E
E'
E''
E'''
F
F'
F''
F'''
G
G'
G''
G'''

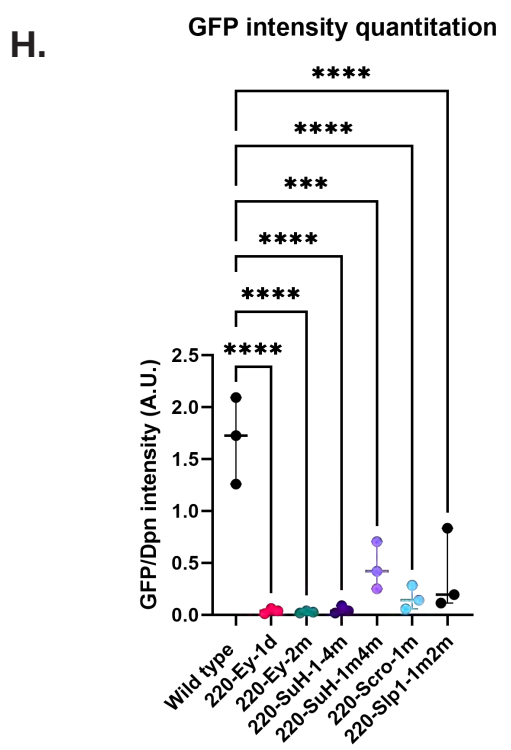
H.
GFP intensity quantitation
GFP/Dpn intensity (A.U.)
2.5
2.0
1.5
1.0
0.5
0.0
****
****
***
****
****
****
Wild type
220-Ey-1d
220-Ey-2m
220-SuH-1-4m
220-SuH-1m4m
220-Scro-1m
220-Slp1-1m2m

Figure7-figure supplement1

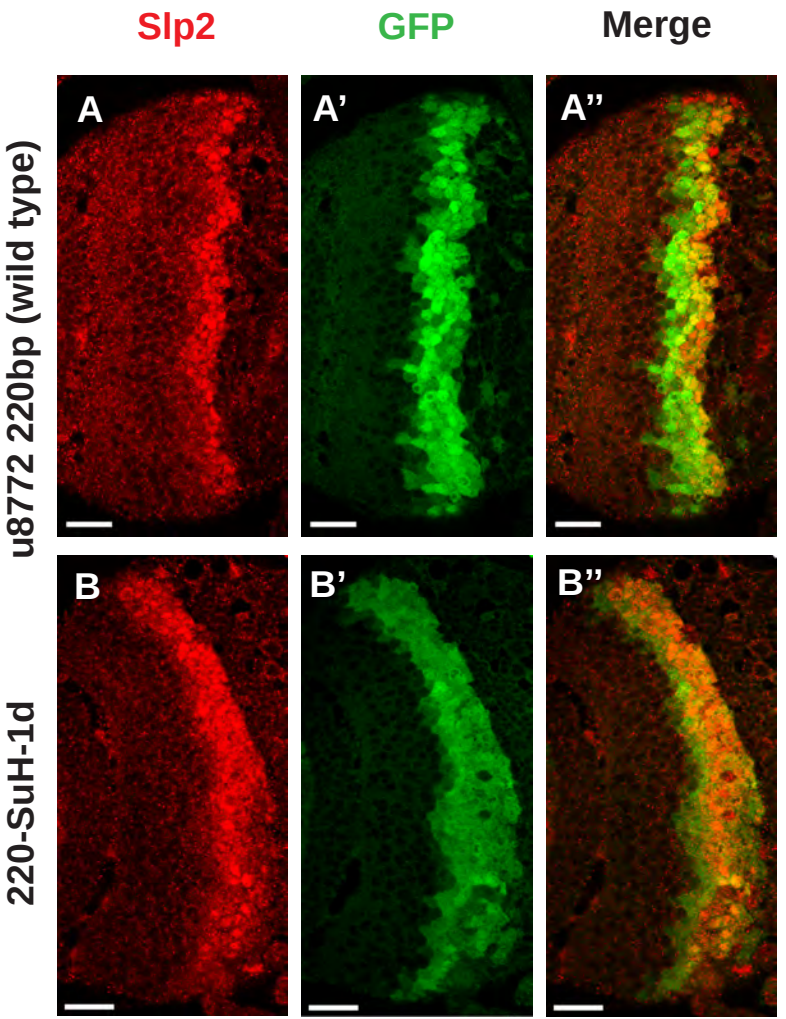

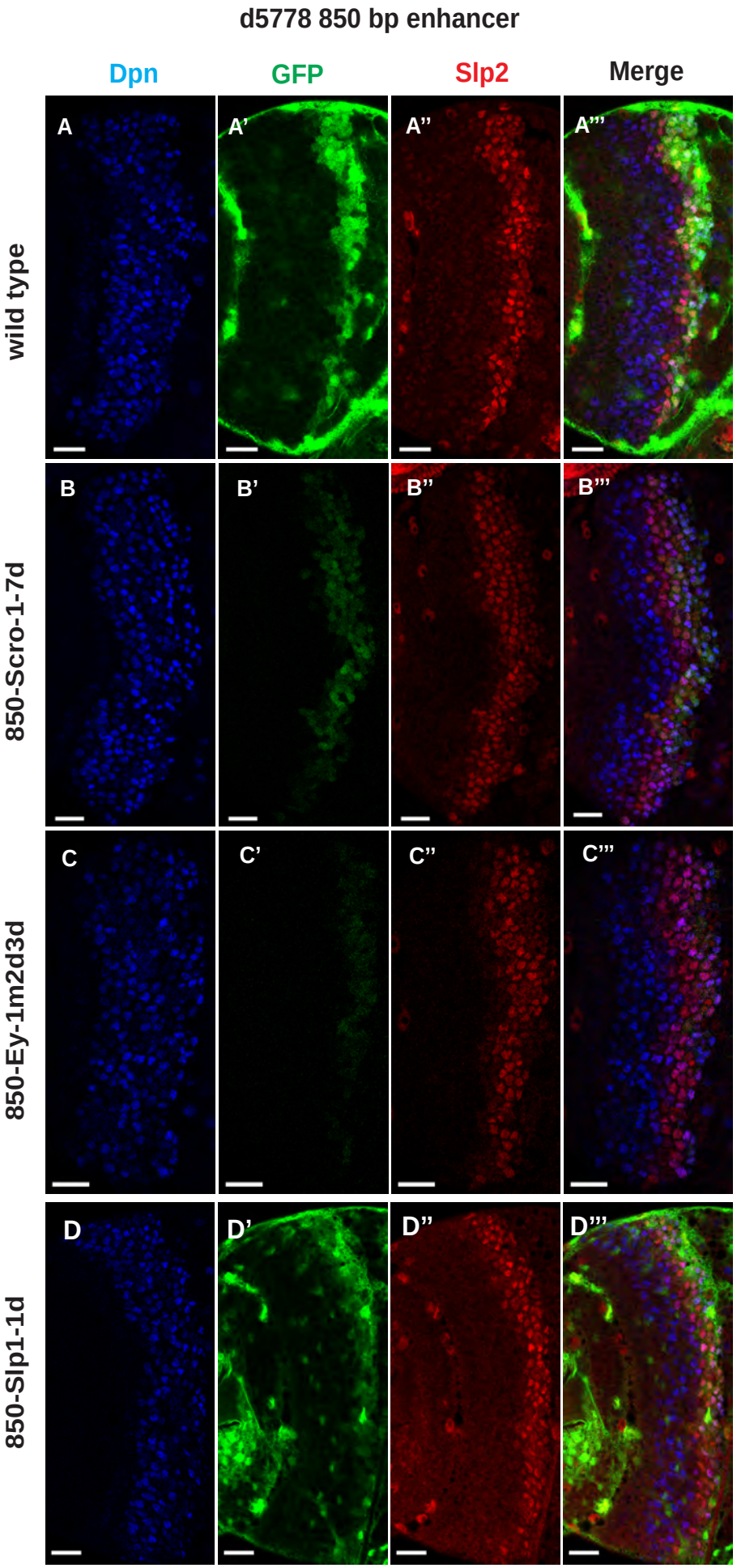
d5778 850 bp enhancer
Dpn
GFP
Slp2
Merge
wild type
850-Scro-1-7d
850-Ey-1m2d3d
850-Slp1-1d
A
A'
A''
A'''
B
B'
B''
B'''
C
C'
C''
C'''
D
D'
D''
D'''

E.

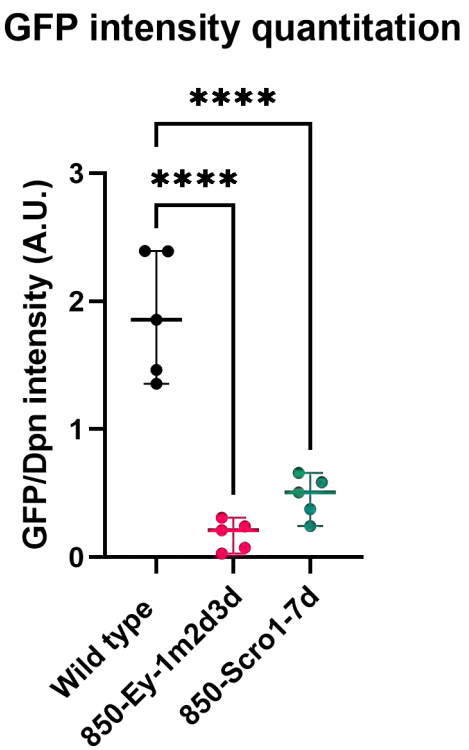
GFP intensity quantitation
****
****
GFP/Dpn intensity (A.U.)
3
2
1
0
Wild type
850-Ey-1m2d3d
850-Scro1-7d

Figure 9

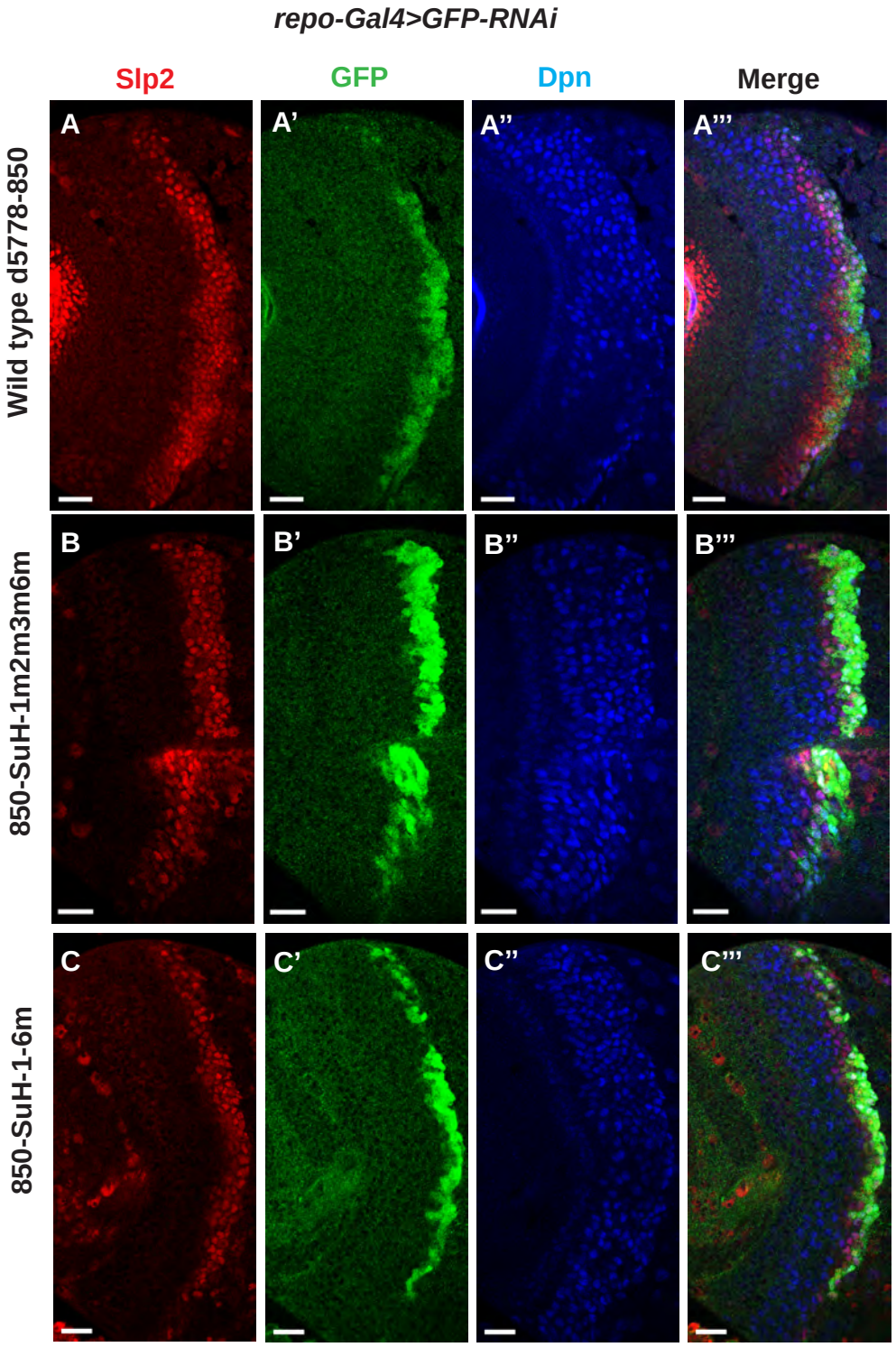
repo-Gal4>GFP-RNAi
Slp2
GFP
Dpn
Merge
Wild type d5778-850
850-SuH-1m2m3m6m
850-SuH-1-6m
A
A'
A''
A'''
B
B'
B''
B'''
C
C'
C''
C'''

D.

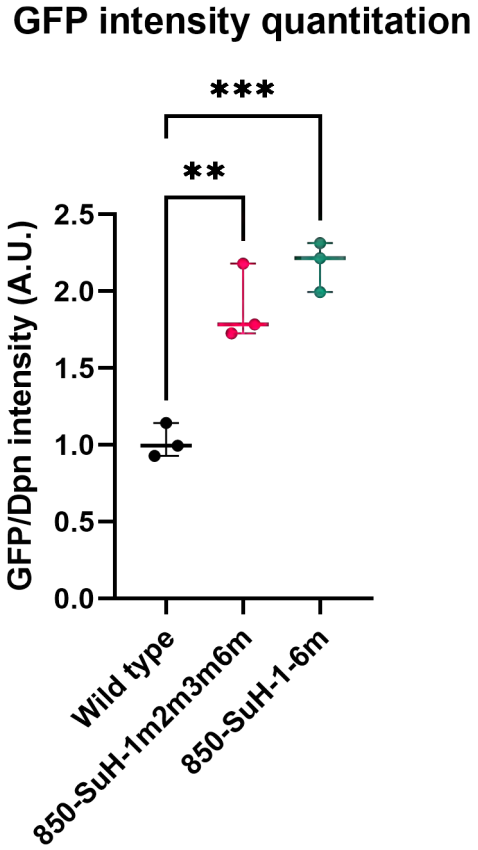
GFP intensity quantitation
***
**
GFP/Dpn intensity (A.U.)
2.5
2.0
1.5
1.0
0.5
0.0
Wild type
850-SuH-1m2m3m6m
850-SuH-1-6m

Figure 9-figure supplement1

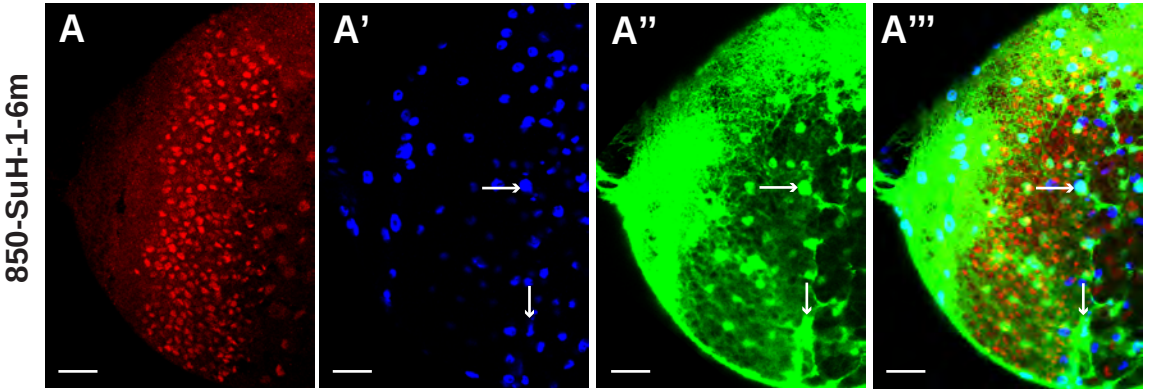

Figure10

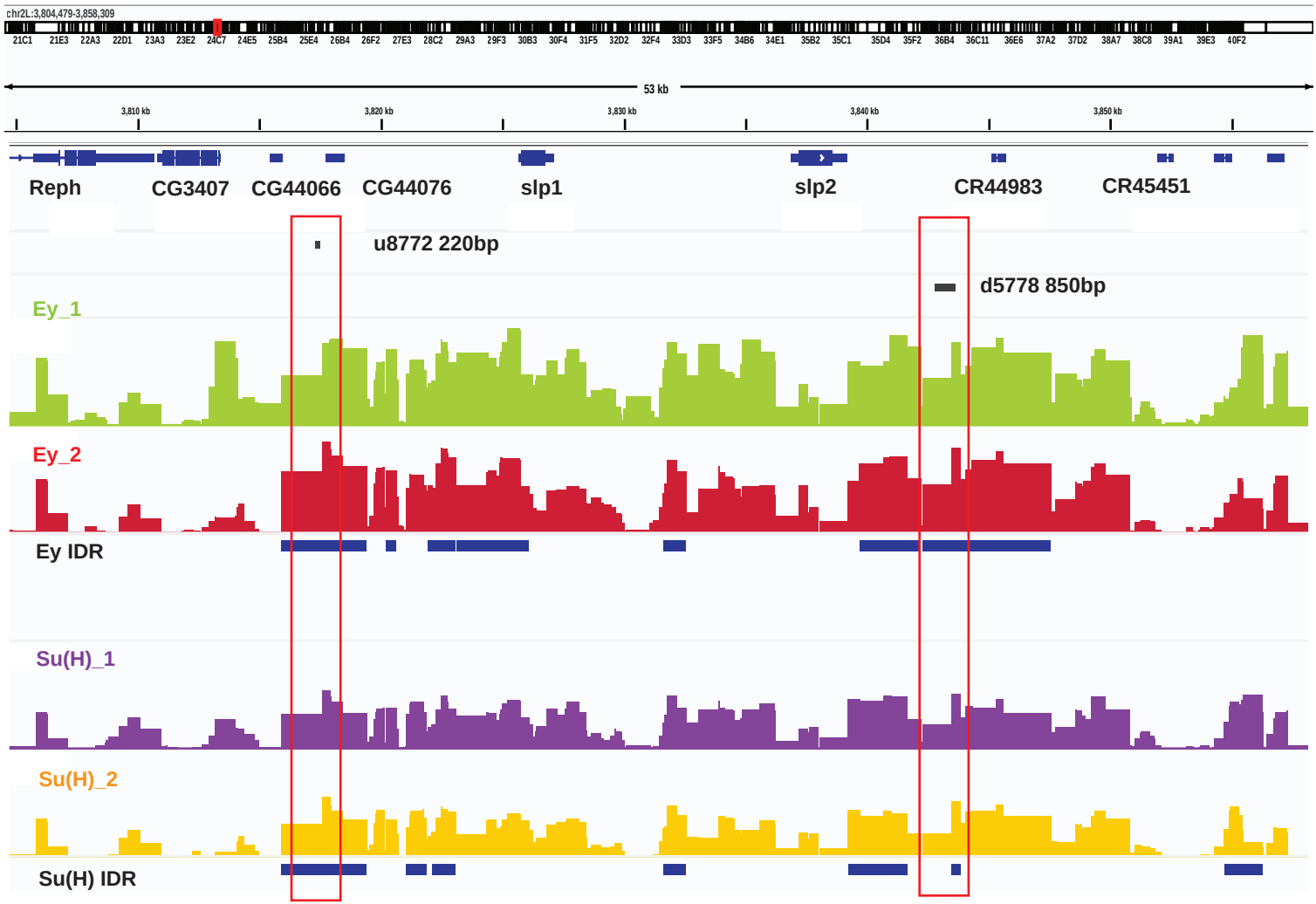
chr2L:3,804,479-3,858,309
21C1 21E3 22A3 22D1 23A3 23E2 24C7 24E5 25B4 25E4 26B4 26F2 27E3 28C2 29A3 29F3 30B3 30F4 31F5 32D2 32F4 33D3 33F5 34B6 34E1 35B2 35C1 35D4 35F2 36B4 36C11 36E6 37A2 37D2 38A7 38C8 39A1 39E3 40F2
53 kb
3,810 kb
3,820 kb
3,830 kb
3,840 kb
3,850 kb
Reph
CG3407
CG44066
CG44076
slp1
slp2
CR44983
CR45451
u8772 220bp
d5778 850bp
Ey_1
Ey_2
Ey IDR
Su(H)_1
Su(H)_2
Su(H) IDR

A.
chr3L:24,720,454-24,758,328
37 kb
24,730 kb
24,740 kb
24,750 kb
Scro
Ey_1
Ey_2
Ey IDR
Su(H)_1
Su(H)_2
Su(H) IDR
B.
chr3R:17,556,930-17,571,097
14 kb
17,558 kb
17,560 kb
17,562 kb
17,564 kb
17,566 kb
17,568 kb
17,570 kb
Hmx
Ey_1
Ey_2
Ey IDR
Su(H)_1
Su(H)_2
Su(H) IDR
C.
chr2R:24,796,266-24,854,155
57 kb
24,800 kb
24,810 kb
24,820 kb
24,830 kb
24,840 kb
24,850 kb
Orc4
CG3611
CG42851
Dll
CG3650
Ey_1
Ey_2
Ey IDR
Su(H)_1
Su(H)_2
Su(H) IDR

Figure 11

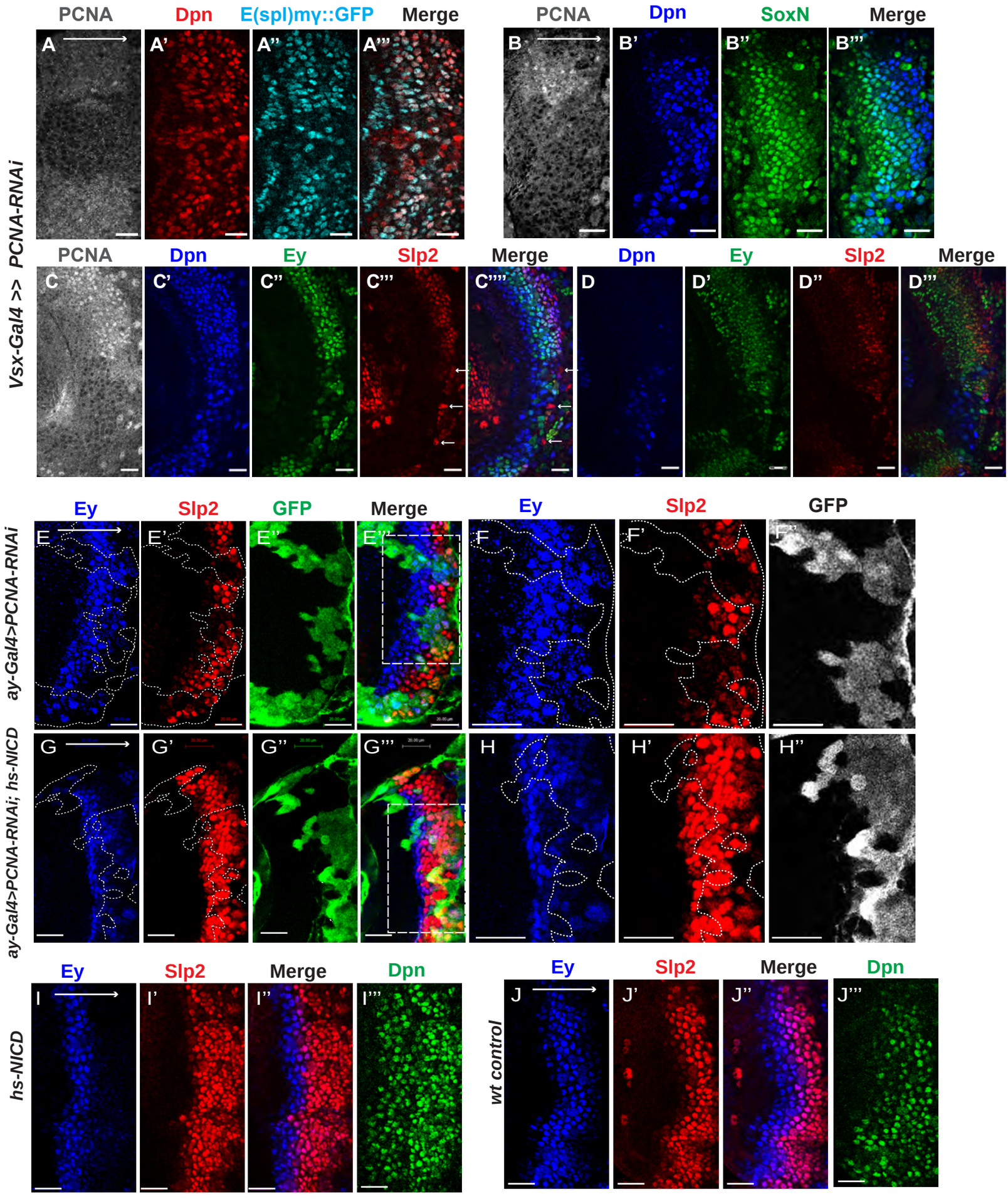
PCNA
Dpn
E(spl)mγ::GFP
Merge
A
A'
A''
A'''
PCNA
Dpn
SoxN
Merge
B
B'
B''
B'''
Vsx-Gal4 >> PCNA-RNAi
PCNA
Dpn
Ey
Slp2
Merge
C
C'
C''
C'''
C''''
Dpn
Ey
Slp2
Merge
D
D'
D''
D'''
ay-Gal4>PCNA-RNAi
Ey
Slp2
GFP
Merge
E
E'
E''
E'''
Ey
Slp2
GFP
F
F'
F''
ay-Gal4>PCNA-RNAi; hs-NICD
G
G'
G''
G'''
H
H'
H''
hs-NICD
Ey
Slp2
Merge
Dpn
I
I'
I''
I'''
wt control
Ey
Slp2
Merge
Dpn
J
J'
J''
J'''

Figure 11- figure supplement1

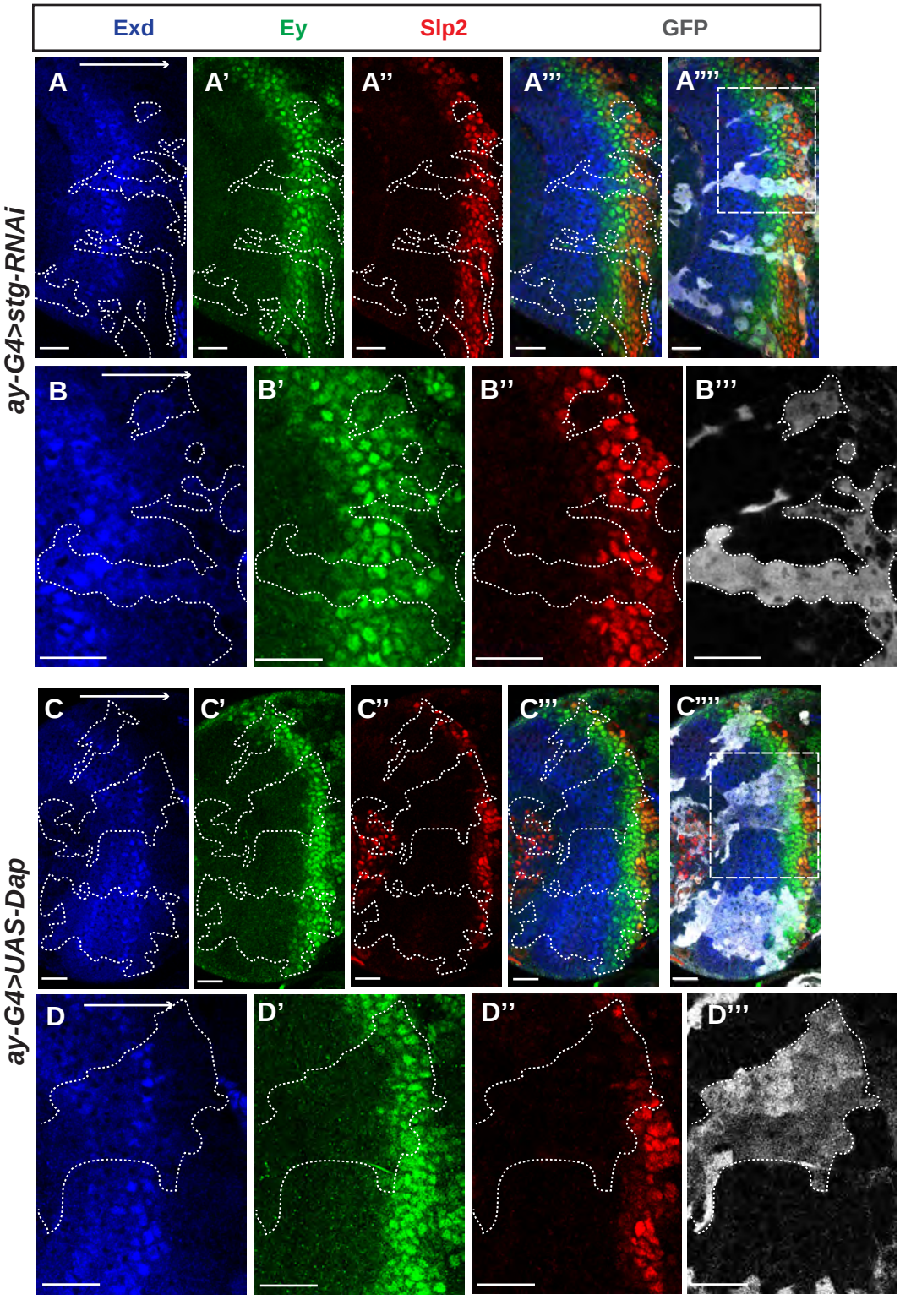

Figure 12

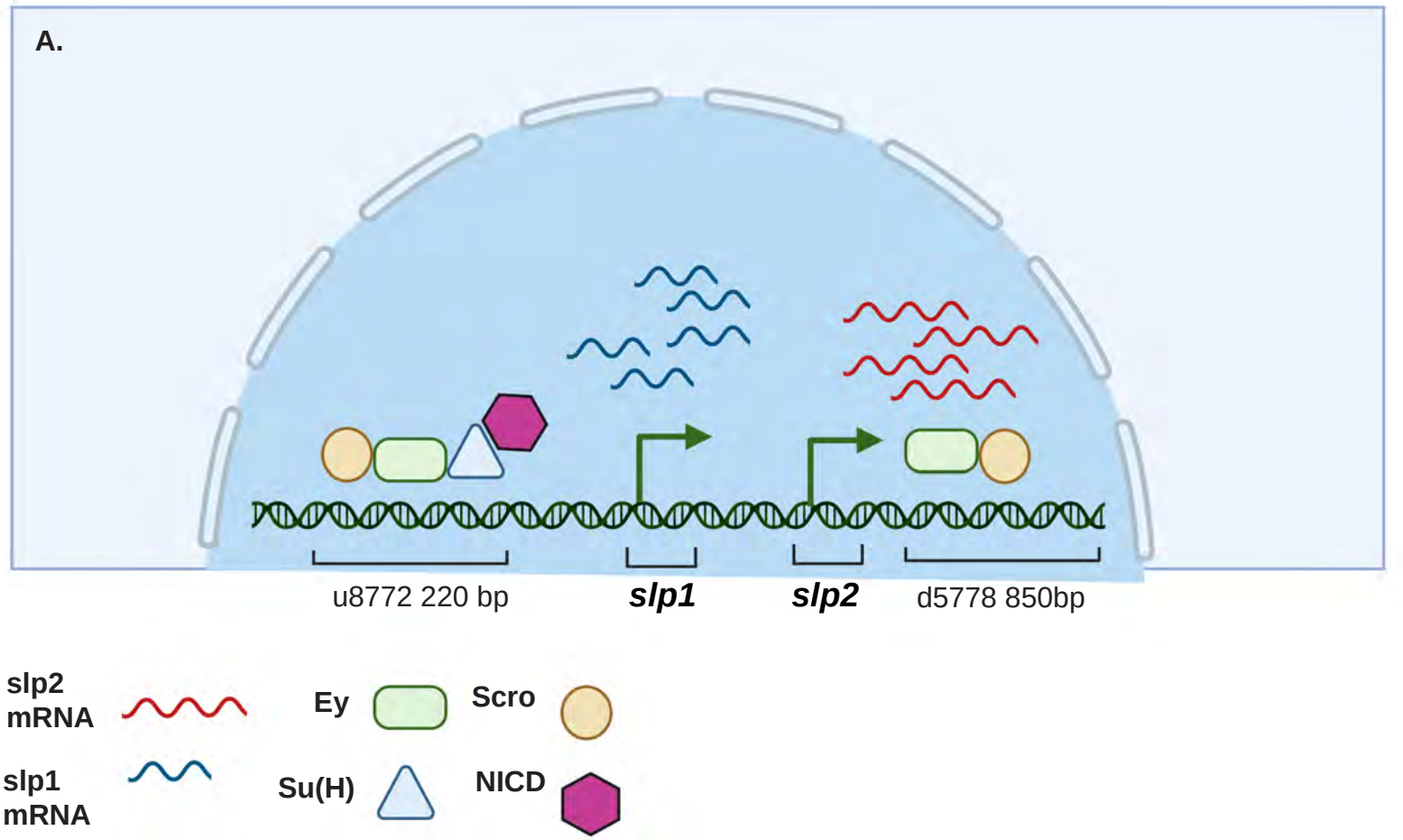
A.
u8772 220 bp
slp1
slp2
d5778 850bp
slp2 mRNA
Ey
Scro
slp1 mRNA
Su(H)
NICD

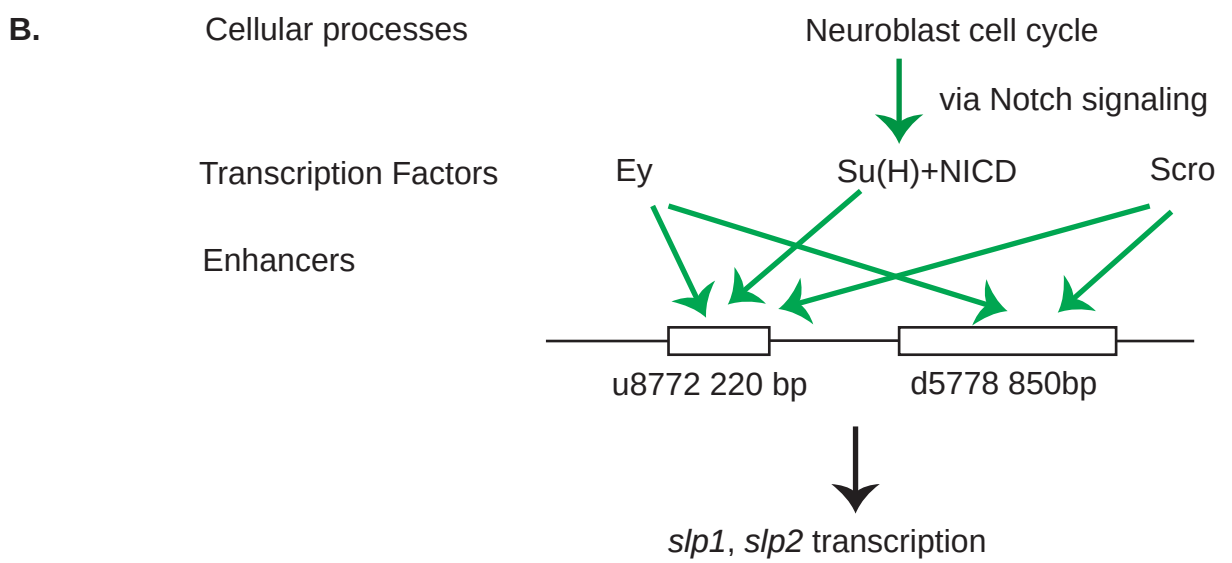
B.
Cellular processes
Neuroblast cell cycle
via Notch signaling
Transcription Factors
Ey
Su(H)+NICD
Scro
Enhancers
u8772 220 bp
d5778 850bp
slp1, slp2 transcription

Key Resources Table				
Reagent Type	**Designation**	**Source**	**Identifiers**	**Additional Information**
Antibody	anti SoxN (Rabbit polyclonal)	Claude Desplan	N/A	IF 1:250
Antibody	anti- Ey (Rabbit polyclonal)	Claude Desplan	N/A	IF 1:500
Antibody	anti-Slp1 (Rabbit polyclonal)	Claude Desplan	N/A	IF 1:500
Antibody	anti-Slp2 (Guinea-pig polyclonal)	Claude Desplan	N/A	IF 1:500
Antibody	anti-Scro (Guinea-pig polyclonal)	Claude Desplan	N/A	IF 1:100
Antibody	Anti-D (Rabbit polyclonal)	Claude Desplan	N/A	IF 1:500
Antibody	Anti-Dpn (Guinea pig polyclonal)	Chris Doe	N/A	IF 1:500
Antibody	Anti-Dpn (Rat monoclonal)	Abcam	Antibody#: Ab195173	IF 1:500
Antibody	Anti-B-H1 (Rat polyclonal)	Tiffany Cook	N/A	IF 1:200; Tiffany Cook
Antibody	Anti-GFP (Sheep polyclonal)	AbD Serotec	4745-1051	IF 1:500
Antibody	Anti-Repo (mouse monoclonal)	Developmental Studies Hybridoma Bank	8D12 anti-Repo	IF 1:50
Antibody	Anti-PCNA (mouse monoclonal)	Abcam	ab29	IF 1:10
Antibody	Anti-betaGalactosidase (Chicken polyclonal)	Abcam	Antibody#: Ab9361	IF 1:500
Antibody	Cy5 AffiniPure Anti-RatIgG (Donkey polyclonal)	Jackson ImmunoResearch Laboratories Inc.	Catalog_#: 712-175-153	IF !:500
Antibody	Cy3 AffiniPure Anti-RatIgG (Donkey polyclonal)	Jackson ImmunoResearch Laboratories Inc.	Catalog_#: 712-165-153	IF 1:500
Antibody	Cy3 AffiniPure Anti-Guinea Pig IgG (Donkey polyclonal)	Jackson ImmunoResearch Laboratories Inc.	Catalog_#: 706-165-148	IF 1:500
Antibody	Alexa Fluor® 647 AffiniPure Anti-Guinea Pig	Jackson ImmunoResearch Laboratories Inc.	Catalog_#: 706-605-148	IF 1:500

	(Donkey polyclonal)			
Antibody	Alexa Fluor® 488 AffiniPure Anti-Guinea Pig IgG (Donkey polyclonal)	Jackson ImmunoResearch Laboratories Inc.	Catalog_#: 706-545-148	IF 1:500
Antibody	Alexa Fluor® 647 AffiniPure Anti-Goat IgG (Donkey polyclonal)	Jackson ImmunoResearch Laboratories Inc.	Catalog_#: 705-605-147	IF 1:500
Antibody	DyLight 405 AffiniPure Anti-Mouse IgG (Donkey polyclonal)	Jackson ImmunoResearch Laboratories Inc.	Catalog_#: 715-475-151	IF 1:500
Antibody	Alexa Fluor® 647 AffiniPure Anti-Rabbit IgG (Donkey polyclonal)	Jackson ImmunoResearch Laboratories Inc.	Catalog_#: 711-605-152	IF 1:500
Antibody	Cy5 AffiniPure Anti-Mouse IgG (Donkey polyclonal)	Jackson ImmunoResearch Laboratories Inc.	Catalog_#: 715-175-151	IF 1:500
Antibody	Alexa Fluor® 647 AffiniPure Anti-Chicken IgY (IgG) (Donkey polyclonal)	Jackson ImmunoResearch Laboratories Inc.	Catalog_#: 703-605-155	IF 1:500
Antibody	Alexa Fluor® 488 AffiniPureDonkey Anti-Mouse IgG (Donkey polyclonal)	Jackson ImmunoResearch Laboratories Inc.	Catalog_#: 715-545-151	IF 1:500
Antibody	Alexa Fluor® 488 AffiniPure Anti-Sheep (Donkey polyclonal)	Jackson ImmunoResearch Laboratories Inc.	Catalog_#: 713-545-147	IF 1:500
Antibody	DyLight 405 AffiniPure Anti-Rat IgG (Donkey polyclonal)	Jackson ImmunoResearch Laboratories Inc.	Catalog_#: 712-475-153	IF 1:500
Antibody	DyLight 405 AffiniPure Anti-Rabbit IgG (Donkey polyclonal)	Jackson ImmunoResearch Laboratories Inc.	Catalog_#: 711-475-152	IF 1:500
Antibody	anti-Rabbit IgG, Alexa Fluor Â® 555 conjugate (Donkey polyclonal)	Life Technologies	Catalog_#: A-31572	IF 1:500

Antibody	Anti-Opa (Rabbit polyclonal)	J. Peter Gergen	N/A	IF 1:100; J. Peter Gergen
Antibody	Anti-Erm (Rat polyclonal)	Claude Desplan	N/A	1:100
Recombinant DNA Reagent	pJR12 plasmid	Rister, J. et al. (2015). PMID: 26785491 DOI: 10.1126/science.aab3417	N/A	Jens Rister
Recombinant DNA Reagent	pCFD5 plasmid	Addgene	Addgene Plasmid #73914	Fillip Port
Recombinant DNA Reagent	UAS-LT3-Dam plasmid	Andrea Brand	N/A	
Recombinant DNA Reagent	pJR12-hsNICD plasmid	This paper	N/A	See section on 'Plasmid constructs' in 'Materials and Methods'
Recombinant DNA Reagent	UAS-LT3-DamEy	This paper	N/A	See section on 'Plasmid constructs' in 'Materials and Methods'
Recombinant DNA Reagent	UAS-LT3-DamSu(H)	This paper	N/A	See section on 'Plasmid constructs' in 'Materials and Methods'
Recombinant DNA Reagent	CoinFlp plasmid	Addgene	Addgene Plasmid #52889	Iswar Hariharan
Recombinant DNA Reagent	GMR35H02 BAC	BACPAC resources	CH321-94O18	
Recombinant DNA Reagent	Su(H) cDNA.	Drosophila Genomics Resource Center	GH10914	
Recombinant DNA Reagent	Notch cDNA	Drosophila Genomics Resource Center	LD34134	
Recombinant DNA Reagent	CH321-86A18 (BAC)	BACPAC resources		BAC encoding *dpn* enhancer
Sequence-based reagent	220-Ey-1d gBlock	This study	N/A	See Supplementary Table 3 for sequence
Sequence-based reagent	220-Ey-2m gBlock	This study	N/A	See Supplementary Table 3 for sequence
Sequence-based reagent	220-SuH-1-4m	This study	N/A	See Supplementary Table 3 for sequence
Sequence-based reagent	220-SuH-1m4m	This study	N/A	See Supplementary Table 3 for sequence
Sequence-based reagent	220-Scro-1m	This study	N/A	See Supplementary Table 3 for sequence
Sequence-based reagent	220-Slp1-1m2m	This study	N/A	See Supplementary Table 3 for sequence
Sequence-based reagent	850-Ey-1m2d3d	This study	N/A	See Supplementary Table 3 for sequence
Sequence-based reagent	850-SuH-1m2m3m6m	This study	N/A	See Supplementary Table 3 for sequence

Sequence-based reagent	850-SuH-1-6m	This study	N/A	See Supplementary Table 3 for sequence
Sequence-based reagent	850-Scro-1-7d	This study	N/A	See Supplementary Table 3 for sequence
Sequence-based reagent	850-Slp1-1d	This study	N/A	See Supplementary Table 3 for sequence
Sequence-based reagent	Ey gene block	This study	N/A	See Supplementary Table 3 for sequence
Sequence-based reagent	SlpR2-2FP	This study	N/A	5'TTAGGCGCGCCAGTGCGTGTCTGCCCTTTCATTTTG 3'
Sequence-based reagent	SlpR2-2RP	This study	N/A	5' ATATATGCGGCCGCCCCAGCTAGCTCCCTTCACTCTTCT 3'
Sequence-based reagent	SlpL1-5FP	This study	N/A	5' TTAGGCGCGCCGAATCGAAATGCTTCCCCGCCTCG 3'
Sequence-based reagent	SlpL1-5RP	This study	N/A	5' ATATATGCGGCCGCTGAACGTGCAACATCAAAGGCCGC 3'
Sequence-based reagent	SlpM1-FP	This study	N/A	5' TTAGGCGCGCCGCGGCCTTTGATGTTGCACGTTCA 3'
Sequence-based reagent	SlpM1-RP	This study	N/A	5' ATATATGCGGCCGCGGACAGTTCGGAATGTGCCTCGA 3'
Sequence-based reagent	Slpf1-FP	This study	N/A	5' TTAGGCGCGCCGAATCGAGTGGTGAGCGATAG 3'
Sequence-based reagent	Slpf1-RP	This study	N/A	5' ATATATGCGGCCGCTCTGATATTTTTCACGGCTCA 3'
Sequence-based reagent	Slpf2-FP	This study	N/A	5' TTAGGCGCGCCTTCGACCTTGTAGTGGCAAG 3'
Sequence-based reagent	Slpf2-RP	This study	N/A	5' ATATATGCGGCCGCCGGAGATCGGAAGGTTAGTG 3'
Sequence-based reagent	Slpf3-FP	This study	N/A	5' TTAGGCGCGCCTCTCCTTGTTGCTCCTCACA 3'
Sequence-based reagent	Slpf3-RP	This study	N/A	5' ATATATGCGGCCGCTGAACGTGCAACATCAAAGG 3'
Sequence-based reagent	d5778FP	This study	N/A	5' TTAGGCGCGCCTGGTCTT

				TTACGTTAATCTGGGCAGCT 3’
Sequence-based reagent	d5778RP	This study	N/A	5’ ATATATGCGGCCGCACATTACGCATTGCATTCCTCCTCCTT 3’
Sequence-based reagent	d5778-850FP	This study	N/A	5’ TTAGGCGCGCCCATTAACTCGAGTCTGGTTTCCGAT 3’
Sequence-based reagent	d5778-850RP	This study	N/A	5’ ATATATGCGGCCGCCGTACATATTCTCCAGGAGTTCGGTC 3’
Sequence-based reagent	pJRLPseq3	This study	N/A	5’ AGATGGGTGAGGTGGAGTACG 3’
Sequence-based reagent	pJR12-TATA-seq	This study	N/A	5’ AGCTGCGCTTGTTTATTTGCTTAG 3’
Sequence-based reagent	SuHDamFP	This study	N/A	5’ ATATATGCGGCCGCAAATGAAGAGCTACAGCCAATTTAATTTAAACGCCGCC 3’
Sequence-based reagent	SuHDamRP	This study	N/A	5’ AAAATACTCGAGTCAGGATAAGCCGCTACCATGACTATTCCATTGC 3’
Sequence-based reagent	DamseqFP1	This study	N/A	5’ TGAGGGGAGACATAGTACTGGT 3’
Sequence-based reagent	DamseqFP2	This study	N/A	5’ GAAGGTCTGGTTGAGCGCCATA 3’
Sequence-based reagent	pCFD5-u8772-gRFP1	This study	N/A	5’ GCGGCCCGGGTTCGATTCCCGGCCGATGCATCGAAATTTCCTGGTATTCGGTTTTAGAGCTAGAAATAGCAAG 3’
Sequence-based reagent	pCFD5-u8772-gRRP1	This study	N/A	5’ CGCCTCGCCCAAATGCATTTTGCACCAGCCGGGAATCGAACCC 3’
Sequence-based reagent	pCFD5-u8772-gRFP2	This study	N/A	5’ AAATGCATTTGGGCGAGGCGGTTTTAGAGCTAGAAATAGCAAG 3’
Sequence-based reagent	pCFD5-u8772-gRRP2	This study	N/A	5’ TTAGTTTGATTGTTTCGA

				AGTGCACCAGCCGGGAATCGAACCC 3’
Sequence-based reagent	pCFD5-u8772-gRFP3	This study	N/A	5’ CTTCGAAACAATCAAACTAAGTTTTAGAGCTAGAAATAGCAAG 3’
Sequence-based reagent	pCFD5-u8772-gRRP3	This study	N/A	5’ ATTTTAACTTGCTATTTCTAGCTCTAAAACAAACTGGAAGTCATTGACCCTGCACCAGCCGGGAATCGAACCC 3’
Sequence-based reagent	pCFD5-d5778-gRFP1	This study	N/A	5’ GCGGCCCGGGTTCGATTCCCGGCCGATGCAATAAGTCCTTGGGTAATACGGTTTTAGAGCTAGAAATAGCAAG 3’
Sequence-based reagent	pCFD5-d5778-gRRP1	This study	N/A	5’ AACATTTATCTAGGACATCTTGCACCAGCCGGGAATCGAACCC 3’
Sequence-based reagent	pCFD5-d5778-gRFP2	This study	N/A	5’ AGATGTCCTAGATAAATGTTGTTTTAGAGCTAGAAATAGCAAG 3’
Sequence-based reagent	pCFD5-d5778-gRRP2	This study	N/A	5’ TGTTGGCAAGCGGCGCTTCATGCACCAGCCGGGAATCGAACCC 3’
Sequence-based reagent	pCFD5-d5778-gRFP3	This study	N/A	5’ TGAAGCGCCGCTTGCCAACAGTTTTAGAGCTAGAAATAGCAAG 3’
Sequence-based reagent	pCFD5-d5778-gRRP3	This study	N/A	5’ ATTTTAACTTGCTATTTCTAGCTCTAAAACTTTCGATATCCCAGCTCCTTTGCACCAGCCGGGAATCGAACCC 3’
Sequence-based reagent	u8772crdelFP	This study	N/A	5’ TTGCAAATACTTTTTATTCAAGGAATCGAC 3’
Sequence-based reagent	u8772crdelRP	This study	N/A	5’ AATCTCAAGTTTGGTGTTTGTAATTTTTGG 3’
Sequence-based reagent	d5778crdelFP	This study	N/A	5’ CTATTGAAGGGCGGACATATTAGACAACAATTGGATCGCTTG 3’
Sequence-based reagent	d5778crdelRP	This study	N/A	5’ CTGCATTCCATCCCGTCG

				CATCCTTGTC 3’
Sequence-based reagent	pJRGFPdelFP1	This study	N/A	5’ TTAGAGATGCATCTCAAA AAAATGGTGGGCATAAT AGTGTTGTTTATATATAT CAAAAATAACAAC 3’
Sequence-based reagent	pJRGFPdelRP1	This study	N/A	5’ CCACCGGTCGCCACCGAC GTCAGC GGCCGGCCGC 3’
Sequence-based reagent	pJRGFPdelFP2	This study	N/A	5’ GTCGCGGCCGGCCGCTG ACGTCGGTGGCGACCGG TGGATCGTTTAAACAGGC C 3’
Sequence-based reagent	pJRGFPdelRP2	This study	N/A	5’ CAATAACTCGAGGAGCG CCGGAGT ATAAATAGAGGCGCTTC GTCTACG 3’
Sequence-based reagent	pJRGFPdelseqFP	This study	N/A	5’ CCATTATAAGCTGCAATA AACAAGTTAACAAC 3’
Sequence-based reagent	pJRGFPdelseqRP	This study	N/A	5’ GTCGCTAAGCGAAAGCT AAGC 3’
Sequence-based reagent	U63seqfwd	This study	N/A	5’ ACGTTTTATAACTTATGC CCCTAAG 3’
Sequence-based reagent	pCFD5seqrev	This study	N/A	5’ GCACAATTGTCTAGAATG CATAC 3’
Sequence-based reagent	dpnenFP	This study	N/A	5’ TTAGGCGCGCCCTTCGCT TTTGCCTG GTCGGCTCATCGG 3’
Sequence-based reagent	dpnenRP	This study	N/A	5’ ATATATGCGGCCGCACGC CTCGTCCTGGCACCCTC 3’
Sequence-based reagent	NICDFP	This study	N/A	5’ TATTTAACCGGTTATTATC AAATGTAGATGGCCTCG GAACCCTTG 3’
Sequence-based	NICDRP	This study	N/A	5’

reagent				ATAATAGTTTAAACATGAGTACGCAAAGAAAGCGGGCAC 3’
Sequence-based reagent	hscFP1	This study	N/A	5’ TATTTAACCGGTTATTATCAAATGTAGATGGCCTCGGAACCCTTG 3’
Sequence-based reagent	hscRP1	This study	N/A	5’ GGAAGTTCCTATTCTCTAGAAAGTATAGGAACTTCGAATTCCAAAATGAGTACGCAAAGAAAGCGGGCAC 3’
Sequence-based reagent	hscFP2	This study	N/A	5’ GTGCCCGCTTTCTTTGCGTACTCATTTTGGAATTCGAAGTTCCTATACTTTCTAGAGAATAGGAACTTCC 3’
Sequence-based reagent	hscRP2	This study	N/A	5’ ATAATAGTTTAAACGAAGTTCCTATTCTCTAGAAAGTATAGGAACTTCCCCGC 3’
Genetic reagent (*D. melanogaster*)	*UAS-ey -RNAi*	Bloomington Drosophila Stock Centre	BDSC 32486; Symbol: CG1464; Flybase ID:FBgn0005558	
Genetic reagent (*D. melanogaster*)	*UAS-Su(H)-RNAi*	Vienna Drosophila Stock Centre	VDRC 103597 Symbol: CG3497; Flybase ID: FBgn0004837	
Genetic reagent (*D. melanogaster*)	*UAS-N-RNAi*	Bloomington Drosophila Stock Centre	BDSC 7078; Symbol: CG3936; Flybase ID: FBgn0004647	
Genetic reagent (*D. melanogaster*)	*UAS-Dl-RNAi*	Vienna Drosophila Stock Centre	VDRC 32788; Symbol: CG3619; Flybase ID: FBgn0000463	
Genetic reagent (*D. melanogaster*)	*UAS-PCNA-RNAi*	Vienna Drosophila Stock Centre	VDRC 51253; Symbol: CG9193; Flybase ID: FBgn0005655	
Genetic reagent (*D. melanogaster*)	*UAS-mam-DN*	Justin Kumar	Symbol: CG8118; Flybase ID: FBgn0002643	Justin Kumar

Genetic reagent (*D. melanogaster*)	*UAS-stg-RNAi*	Vienna Drosophila Stock Centre	VDRC 17760; Symbol: CG1395 Flybase ID: FBgn0003525	
Genetic reagent (*D. melanogaster*)	*UAS-dap*	Bloomington Drosophila Stock Centre	BDSC 83338; Symbol: CG1772 Flybase ID: FBgn0010316	
Genetic reagent (*D. melanogaster*)	*UAS-scro-RNAi*	Bloomington Drosophila Stock Centre	BDSC 33890; Symbol: CG17594 Flybase ID: FBgn0287186	
Genetic reagent (*D. melanogaster*)	*UAS-Ey*	Bloomington Drosophila Stock Centre	BDSC56560	
Genetic reagent (*D. melanogaster*)	*UAS-Scro*	FlyORF	F000666	
Genetic reagent (*D. melanogaster*)	*GMR35H02*-Gal4	Bloomington Drosophila Stock Centre (Pfeiffer et. al. 2008)	BDSC 49923	
Genetic reagent (*D. melanogaster*)	*GMR41H10*-Gal4 (*SoxN*-Gal4)	Bloomington Drosophila Stock Centre (Pfeiffer et. al. 2008)	N/A	No longer available from BDSC
Genetic reagent (*D. melanogaster*)	*UAS-GFP-nls*	Bloomington Drosophila Stock Centre	BDSC 4776	
Genetic reagent (*D. melanogaster*)	*UAS-EGFP-RNAi*	Bloomington Drosophila Stock Centre	BDSC 9931	
Genetic reagent (*D. melanogaster*)	*ayGal4 "y w hsFLP; act>y+>Gal4 UAS-GFP / CyO"*	Ito, K. et al (1997) PMID: 9043058 DOI: 10.1242/dev.124.4.761	N/A	
Genetic reagent (*D. melanogaster*)	*"y w hs FLP; act>y+>Gal4 UAS GFP / CyO; UASDCR2/TM6B"*	Zhu, H. et al. (2022) PMID: 35273186 DOI: 10.1038/s41467-022-28915-3	N/A	
Genetic reagent (*D. melanogaster*)	*ayGal4 UASlacZ*	Bloomington Drosophila Stock Centre	BDSC 4410	
Genetic reagent (*D. melanogaster*)	*"y,w, hsFLP, UASCD8GFP; FRT40A tubGal80; tubGal4/TM6B"*	Liqun Luo	N/A	

Genetic reagent (*D. melanogaster*)	*"y,w,; UbiRFPnls FRT40A/CyO"*	Bloomington Drosophila Stock Centre	BDSC 34500	
Genetic reagent (*D. melanogaster*)	*FRT40A slp^{S37A} /SM6-TM6B*	Sato, M. and Tomlinson, A. (2007) PMID: 17215299 DOI: 10.1242/dev.02786	N/A	Andrew Tomlinson
Genetic reagent (*D. melanogaster*)	*E(spl)mγGFP*	Almeida, M.S. and Bray, S. J. (2005) PMID: 16275038 DOI: 10.1016/j.mod.2005.08.004	N/A	
Genetic reagent (*D. melanogaster*)	*"VsxGal4;Dpn-LacZ/CyO; UAS-Dcr2/TM6B"*	Erclik, T. et al (2017) PMID: 28077877 DOI: 10.1038/nature20794	N/A	
Genetic reagent (*D. melanogaster*)	*dpn*-Gal4 (GMR13C02)	Bloomington Drosophila Stock Centre	BDSC47859	
Genetic reagent (*D. melanogaster*)	*repo*-Gal4	Bloomington Drosophila Stock Centre	BDSC7415	
Genetic reagent (*D. melanogaster*)	*"y,w,hsFlp; Sp/CyO; u8772 220 GFP/Tm6B"*	This study	N/A	See section on 'Fly stocks and genetics' in 'Materials and Methods'
Genetic reagent (*D. melanogaster*)	*"y,w,hsFlp; Sp/CyO; d5778 850 GFP/Tm6B"*	This study	N/A	See section on 'Fly stocks and genetics' in 'Materials and Methods'
Genetic reagent (*D. melanogaster*)	*"y,w, hsFlp; Sp/CyO; 220-Ey-1d/Tm6B"*	This study	N/A	See section on 'Fly stocks and genetics' in 'Materials and Methods'
Genetic reagent (*D. melanogaster*)	*"y,w, hsFlp; Sp/CyO; 220-Ey-2m/Tm6B"*	This study	N/A	See section on 'Fly stocks and genetics' in 'Materials and Methods'
Genetic reagent (*D. melanogaster*)	*"y,w, hsFlp; Sp/CyO; 220-SuH-1-4m/Tm6B"*	This study	N/A	See section on 'Fly stocks and genetics' in 'Materials and Methods'
Genetic reagent (*D. melanogaster*)	*"y,w, hsFlp; Sp/CyO; 220-SuH-1m4m/Tm6B"*	This study	N/A	See section on 'Fly stocks and genetics' in 'Materials and Methods'
Genetic reagent (*D. melanogaster*)	*"y,w, hsFlp; Sp/CyO; 220-Scro-*	This study	N/A	See section on 'Fly stocks and genetics' in

	1m/Tm6B"			'Materials and Methods'
Genetic reagent (*D. melanogaster*)	*"y,w, hsFlp; Sp/CyO; 220-Slp1-1m2m/Tm6B"*	This study	N/A	See section on 'Fly stocks and genetics' in 'Materials and Methods'
Genetic reagent (*D. melanogaster*)	*"y,w, hsFlp; Sp/CyO; 850-Ey-1m2d3d/Tm6B"*	This study	N/A	See section on 'Fly stocks and genetics' in 'Materials and Methods'
Genetic reagent (*D. melanogaster*)	*"y,w, hsFlp; Sp/CyO; 850-SuH-1m3m6m/Tm6B"*	This study	N/A	See section on 'Fly stocks and genetics' in 'Materials and Methods'
Genetic reagent (*D. melanogaster*)	*"y,w, hsFlp; Sp/CyO; 850-SuH-1m2m3m6m/Tm6B"*	This study	N/A	See section on 'Fly stocks and genetics' in 'Materials and Methods'
Genetic reagent (*D. melanogaster*)	*"y,w, hsFlp; Sp/CyO; 850-SuH-1-6m/Tm6B"*	This study	N/A	See section on 'Fly stocks and genetics' in 'Materials and Methods'
Genetic reagent (*D. melanogaster*)	*"y,w, hsFlp; Sp/CyO; 850-Scro-1-7d/Tm6B"*	This study	N/A	See section on 'Fly stocks and genetics' in 'Materials and Methods'
Genetic reagent (*D. melanogaster*)	*"y,w, hsFlp; Sp/CyO; 850-Slp1-1d/Tm6B"*	This study	N/A	See section on 'Fly stocks and genetics' in 'Materials and Methods'
Genetic reagent (*D. melanogaster*)	*"y,w, hsFlp; Sp/CyO; UAS-DamEy/Tm6B"*	This study	N/A	See section on 'Fly stocks and genetics' in 'Materials and Methods'
Genetic reagent (*D. melanogaster*)	*"y,w, hsFlp; Sp/CyO; UAS-SuHDam/Tm6B"*	This study	N/A	See section on 'Fly stocks and genetics' in 'Materials and Methods'
Genetic reagent (*D. melanogaster*)	*"y,w,hsFlp; Sp/CyO; UAS-Dam/Tm6B"*	This study	N/A	See section on 'Fly stocks and genetics' in 'Materials and Methods'
Genetic reagent (*D. melanogaster*)	*"Dcr2; tubG80ts; SoxNG4"*	This study	N/A	See section on 'Fly stocks and genetics' in 'Materials and Methods'
Genetic reagent (*D. melanogaster*)	*"Dcr2; Su(H)RNAi/CyO; u8772-220-GFP/Tm6B"*	This study	N/A	See section on 'Fly stocks and genetics' in 'Materials and Methods'
Genetic reagent (*D. melanogaster*)	*"Dcr2; Su(H)RNAi/CyO; d5778-850-GFP/Tm6B"*	This study	N/A	See section on 'Fly stocks and genetics' in 'Materials and Methods'
Genetic reagent (*D. melanogaster*)	*"y,w,hsFlp; Sp/CyO; UAS-eyRNAi/Tm6B"*	This study	N/A	See section on 'Fly stocks and genetics' in 'Materials and Methods'
Genetic reagent (*D. melanogaster*)	*"y,w,hsFlp; Sp/CyO; UAS-eyRNAi/Tm6B"*	This study	N/A	See section on 'Fly stocks and genetics' in 'Materials and Methods'
Genetic reagent (*D. melanogaster*)	*"y,w,hsFlp; ayGal4 UASlacZ/CyO; UAS-eyRNAi/Tm6B"*	This study	N/A	See section on 'Fly stocks and genetics' in 'Materials and Methods'

Genetic reagent (*D. melanogaster*)	*"y,w,hsFlp; ayGal4 UASlacZ/CyO; hsNICD/Tm6B"*	This study	N/A	See section on 'Fly stocks and genetics' in 'Materials and Methods'
Genetic reagent (*D. melanogaster*)	*"y,w,hsFlp; Ubi RFPnls FRT40A; u8772-220-GFP/Sm6-Tm6B "*	This study	N/A	See section on 'Fly stocks and genetics' in 'Materials and Methods'
Genetic reagent (*D. melanogaster*)	*"y,w,hsFlp; Ubi RFPnls FRT40A; d5778-850-GFP/Sm6-Tm6B"*	This study	N/A	See section on 'Fly stocks and genetics' in 'Materials and Methods'
Genetic reagent (*D. melanogaster*)	*"y,w,hsFlp; UAS Dc2; dpn-Gal4 /Sm6-Tm6B"*	This study	N/A	See section on 'Fly stocks and genetics' in 'Materials and Methods'
Genetic reagent (*D. melanogaster*)	*"y,w,hsFlp; UAS Dc2; repo-Gal4 /Sm6-Tm6B"*	This study	N/A	See section on 'Fly stocks and genetics' in 'Materials and Methods'
Genetic reagent (*D. melanogaster*)	*"y,w,hsFlp; UAS GFP RNAi; d5778-850-GFP /Sm6-Tm6B"*	This study	N/A	See section on 'Fly stocks' and 'Making of transgenic fly stocks' in 'Materials and Methods'
Genetic reagent (*D. melanogaster*)	*"y,w,hsFlp; UAS GFP RNAi; 850-SuH-1m3m6m/Sm6-Tm6B"*	This study	N/A	See section on 'Fly stocks' and 'Making of transgenic fly stocks' in 'Materials and Methods'
Genetic reagent (*D. melanogaster*)	*"y,w,hsFlp; UAS GFP RNAi; 850-SuH-1m2m3m6m/Sm6-Tm6B"*	This study	N/A	See section on 'Fly stocks' and 'Making of transgenic fly stocks' in 'Materials and Methods'
Genetic reagent (*D. melanogaster*)	*"y,w,hsFlp; UAS GFP RNAi; 850-SuH-1-6m/Sm6-Tm6B"*	This study	N/A	See section on 'Fly stocks' and 'Making of transgenic fly stocks' in 'Materials and Methods'
Genetic reagent (*D. melanogaster*)	*"y,w,hsFlp; ayGal4 UAS PCNA RNAi; hsNICD/ Sm6-Tm6B"*	This study	N/A	See section on 'Fly stocks and genetics' and 'Making of transgenic fly stocks' in 'Materials and Methods'
Genetic reagent (*D. melanogaster*)	*"VsxGal4; E(spl) mγGFP/ CyO; UAS Dc2/ Tm6B"*	This study	N/A	See section on 'Fly stocks and genetics' in 'Materials and Methods'
Genetic reagent (*D. melanogaster*)	*y, w, nos-Cas9*	Bloomington Drosophila Stock Centre	BL54591	See section on 'Fly stocks' and 'Making of transgenic fly stocks' in 'Materials and Methods'
Genetic reagent (*D. melanogaster*)	*"y, w; PBAC{y[+]-attP-9A}VK00027"*	Bloomington Drosophila Stock Centre	BL9744	See section on 'Fly stocks' and 'Making of transgenic fly stocks' in 'Materials and Methods'
Sequence-based	Stellaris-Quasar	This study	Symbol: CG2939-	See section

reagent	570-conjugated *slp2* mRNA probes		RA; Flybase ID: FBtr0077500	'Fluorescence in situ hybridization' in 'Materials and Methods'
Sequence-based reagent	Stellaris-Quasar 670- conjugated *slp1* mRNA probes	This study	Symbol: CG16738-RA; Flybase ID: FBtr0077499	See section 'Fluorescence in situ hybridization' in 'Materials and Methods'
peptide, recombinant protein	AscI	New England Biolabs	Catalog_#: R0558S	See section 'Plasmid constructs 'in 'Materials and Methods'
peptide, recombinant protein	NotI-HF	New England Biolabs	Catalog_#: R3189S	See section 'Plasmid constructs 'in 'Materials and Methods'
peptide, recombinant protein	XhoI	New England Biolabs	Catalog_#: R0146S	See section 'Plasmid constructs 'in 'Materials and Methods'
peptide, recombinant protein	AgeI-HF	New England Biolabs	Catalog_#: R3552S	See section 'Plasmid constructs 'in 'Materials and Methods'
peptide, recombinant protein	PmeI	New England Biolabs	Catalog_#: R0560S	See section 'Plasmid constructs 'in 'Materials and Methods'
peptide, recombinant protein	ZraI	New England Biolabs	Catalog_#: R0659S	See section 'Plasmid constructs 'in 'Materials and Methods'
commercial assay or kit	NEB Builder HiFi DNA Assembly kit	New England Biolabs	E2621L	See section 'Plasmid constructs 'in 'Materials and Methods'
commercial assay or kit	Expand High Fidelity PCR System, dNTPack	Roche	04738268001	See section 'Plasmid constructs 'in 'Materials and Methods'
commercial assay or kit	Platinum SuperFi II PCR mastermix	Invitrogen	12368010	See section 'Plasmid constructs 'in 'Materials and Methods'
commercial assay or kit	REDExtract-N-Amp™ PCR ReadyMix	Sigma-Aldrich	R4775-1.2ML	See section 'Plasmid constructs 'in 'Materials and Methods'
commercial assay or kit	DNeasy Blood and Tissue Kit	Qiagen	69504	See section 'Plasmid constructs 'in 'Materials and Methods'
peptide, recombinant protein	DpnI	New England Biolabs	Catalog_#: R0176S	See section 'DamID-seq' in 'Materials and Methods'
peptide, recombinant protein	DpnII	New England Biolabs	Catalog_#: R0543S	See section 'DamID-seq' in 'Materials and Methods'
peptide, recombinant protein	AlwI	New England Biolabs	Catalog_#: R0513S	See section 'DamID-seq' in 'Materials and Methods'
peptide, recombinant protein	Quick Ligation kit	New England Biolabs	Catalog_#: M2200S	See section 'DamID-seq' in 'Materials and Methods'

peptide, recombinant protein	T4 DNA ligase	New England Biolabs	Catalog_#: M0202S	See section 'DamID-seq' in 'Materials and Methods'
peptide, recombinant protein	T4 DNA polymerase	New England Biolabs	Catalog_#: M0203S	See section 'DamID-seq' in 'Materials and Methods'
peptide, recombinant protein	Klenow fragment	New England Biolabs	Catalog_#: M0210S	See section 'DamID-seq' in 'Materials and Methods'
peptide, recombinant protein	Klenow 3'->5' exo-enzyme	New England Biolabs	Catalog_#: M0201S	See section 'DamID-seq' in 'Materials and Methods'
peptide, recombinant protein	NEBNext High-Fidelity 2X PCR master mix	New England Biolabs	Catalog_#: M0541S	See section 'DamID-seq' in 'Materials and Methods'
peptide, recombinant protein	Advantage 2 cDNA polymerase	Clontech	Catalog_#: A63880	See section 'DamID-seq' in 'Materials and Methods'
peptide, recombinant protein	RNase A	Roche	Catalog_#: 11119915001	See section 'DamID-seq' in 'Materials and Methods'
commercial assay or kit	Qubit dsDNA HS assay kit	Invitrogen	Catalog_#: Q32851	See section 'DamID-seq' in 'Materials and Methods'
commercial assay or kit	Agencourt AMPure XP beads	Beckman-Coulter	Catalog_#: A63880	See section 'DamID-seq' in 'Materials and Methods'
Sequence-based reagent	AdRt oligo	Marshall, O. J., et al (2015) PMID: 27490632 DOI: 10.1038/nprot.2016.084	N/A	5' CTAATACGACTCACTATAGGGCAG CGTGGTCGCGGCCGAGGA 3'
Sequence-based reagent	AdRb oligo	Marshall, O. J., et al (2015) PMID: 27490632 DOI: 10.1038/nprot.2016.084	N/A	5' TCCTCGGCCG 3'
Sequence-based reagent	DamID_PCR oligo	Marshall, O. J., et al (2015) PMID: 27490632 DOI: 10.1038/nprot.2016.084	N/A	5' GGTCGCGGCCGAGGATC 3'
Sequence-based reagent	NGS_PCR1	Marshall, O. J., et al (2015) PMID: 27490632 DOI:	N/A	5' AATGATACGGCGACCACCGA*G 3'

		10.1038/nprot.2016.084		*= phosphorothioate linkage
Sequence-based reagent	NGS_PCR2	Marshall, O. J., et al (2015) PMID: 27490632 DOI: 10.1038/nprot.2016.084	N/A	5' CAAGCAGAAGACGGCATACGA*G 3' *= phosphorothioate linkage
Sequence-based reagent	NGS_adaptors	Marshall, O. J., et al (2015) PMID: 27490632 DOI: 10.1038/nprot.2016.084	N/A	
Software, algorithm	FIMO based web-application	Bart Deplancke	Site: https://biss.epfl.ch	
Software, algorithm	FIMO	Grant, C.E., et al.(2011) PMID: 21330290 DOI: 10.1093/bioinformatics/btr064	Site: https://meme-suite.org/meme Versions 4.11.1 to 5.4.1	Accessed between 2016 to 2022; See section 'Bioinformatic analysis' in 'Materials and Methods'.
Software, algorithm	The MEME suite	Bailey, T.L. et al (2015) PMID: 25953851 DOI: 10.1093/nar/gkv416	Site: https://meme-suite.org/meme Versions 4.11.1 to 5.4.1	Accessed between 2016 to 2022; See section 'Bioinformatic analysis' in 'Materials and Methods'.
Software, algorithm	TOMTOM	Gupta, S. et al (2007) PMID: 17324271 DOI: 10.1186/gb-2007-8-2-r24	Site: https://meme-suite.org/meme Versions 4.11.1 to 5.4.1	Accessed between 2016 to 2022; See section 'Bioinformatic analysis' in 'Materials and Methods'.
Software, algorithm	JASPAR	Sandelin, A. et al. (2004) PMID: 14681366 doi: 10.1093/nar/gkh012	Site: https://jaspar.genereg.net/ releases 6, 7, 8,9.	Accessed between 2016 to 2022; See section 'Bioinformatic analysis' in 'Materials and Methods'.
Software, algorithm	Fly Factor Survey	Zhu, L.J. et al (2011) PMID: 21097781 DOI: 10.1093/nar/gkq858	Site: https://mccb.umassmed.edu/ffs	Accessed between 2016 to 2022; See section 'Bioinformatic analysis' in 'Materials and Methods'.
Software, algorithm	Sequence Manipulation Suite Version 2	Stothard, P. (2000) PMID: 10868275 DOI: 10.2144/00286ir01	Site: https://www.bioinformatics.org/sms2	Accessed between 2016 to 2022; See section 'Bioinformatic analysis' in 'Materials and

				Methods'.
Software, algorithm	Primer3web version 4.1.0	Site: https://bioinfo.ut.ee/primer3	Primer3web version 4.1.0	
Software, algorithm	damidseq_pipeline	Marshall, O.J. and Brand, A.H. (2015) PMID : 26112292 DOI: 10.1093/bioinformatics/btv386	Site: http://owenjm.github.io/damidseq_pipeline Version: v1.4.6	See section 'DamID-seq data analysis' in 'Materials and Methods'.
Software, algorithm	Irreproducibility Discover Rate (IDR)	Nathan Boley	Site: https://github.com/nboley/idr Version: 2.0.3	See section 'DamID-seq data analysis' in 'Materials and Methods'.
Software, algorithm	Integrated Genomics Viewer (IGV)	Robinson, J.T., et al. (2012) PMID: 21221095 doi: 10.1038/nbt.1754	IGV_Linux_2.11.0	See section 'DamID-seq data analysis' in 'Materials and Methods'.
Software, algorithm	DAVID	Site: https://david.ncifcrf.gov	Releases 6.8 and Dec 2021	See section 'DamID-seq data analysis' in 'Materials and Methods'.
Software, algorithm	FIJI	Schindelin, J. et al (2012) PMID: 22743772 doi: 10.1038/nmeth.2019	FIJI version 2.3.051	See section 'Image analysis' in 'Materials and Methods'.
Software, algorithm	GraphPad Prism	GraphPad	GraphPad Prism version 9.2.0	See section 'DamID-seq data analysis' in 'Materials and Methods'.
Software, algorithm	Adobe Photoshop	Adobe	Adobe Photoshop 2022 version: 23.4.1	
Software, algorithm	Adobe Illustrator	Adobe	Adobe Illustrator 2022 Version 26.3.1	

1